Characterisation of the reaction of 1,4-phenylenebismaleimide with Ca^{2+} -ATPase and elucidation of the intramolecular crosslink site

Thesis presented for the degree of Master of Science (Med) of the University of Cape Town

by

Tshepo W. Seekoe BSc (Hons) (UCT)
November 1997

Acknowledgements

I am grateful to Prof. D.B. McIntosh, my supervisor, for his invaluable encouragement and inspiration, offering a considerable part of his time to discussions and continuing enthusiasm in creating my better understanding of biochemistry. I wish to extend my gratitude also to Prof. M.C. Berman, for his stimulating discussions and critical evaluation of this work. I also wish to thank Mr D. Woolley and Mrs J. Moulder for their meticulous expert technical assistance, Mr R. Alexander for routine preparation of SR vesicles, and Mr A. Mahomed for analysis of the preparations. My thanks also extends to Katlego and Tshireletso; and especially to my parents Max and Moeda, for their encouragement, interest in my work and support during the course of this study.

The financial assistance offered during this research study by the Medical Research Council (M.R.C) is gratefully acknowledged. This work was carried out in the Department of Chemical Pathology, University of Cape Town.

Abstract

The SR Ca^{2+}-ATPase is an ATP driven pump that removes calcium from the sarcoplasm and myofibrils to allow muscle relaxation. The sulfhydryl crosslinker, 1,4-phenylenebismaleimide, reacts with Ca^{2+}-ATPase (110 kD) to form a species with an apparent molecular weight of 125 kD, as well as dimers and high order oligomers, on SDS-PAGE. During the course of this study we have optimised and characterised the reaction of 1,4-phenylenebismaleimide with SR Ca^{2+}-ATPase to produce the 125 kD species that is reminiscent of an E125 species formed by intramolecular crosslink with glutaraldehyde. The glutaraldehyde crosslink involves the active site Lys 492 and Arg 678, in a zero distance link that overlaps with the ATP binding pocket, since it can be inhibited by nucleotides. It has been previously shown that the putative intramolecular crosslink with 1,4-phenylenebismaleimide is also sensitive to nucleotide binding.

We show that the formation of the putative intramolecular crosslink of SR vesicles (approximately 20 % of ATPase) with 1,4-phenylenebismaleimide is optimum at alkaline pH with micromolar concentrations of the crosslinker. The formation of ATPase dimers and high order oligomers, which were prominent in the reaction with SR vesicles, were eliminated by solubilising in Triton X-100. Under these conditions and in the presence of calcium, two intramolecular crosslinks are formed as seen in the formation of 125 and 130 kD species. The former seems to be in proximity of the γ-phosphate and the latter in the β-phosphate region of the ATP binding site according to nucleotide protection studies. In the presence of detergent (Triton X-100) and absence of calcium, only the 125 kD species is formed and requires stabilisation by thapsigargin, a sesquiterpene lactone that binds the transmembrane α-helices. These conditions yield up to 60 % intramolecularly crosslinked ATPase.

Trypsin digestion altered the apparent molecular weight of the 125 kD species to 135 kD, suggesting, in accordance with the results of glutaraldehyde crosslink, that the putative

intramolecular crosslink is between tryptic fragments A and B. [^{14}C]1,4-phenylenebismaleimide was synthesised to further characterise the reaction and to elucidate crosslinked amino acid residue following protein digestion, radioactive peptide purification, and sequencing.

From filtration studies it was evident that a number of sulfhydryl residues were derivatized in both SR vesicles and solubilised Ca^{2+}-ATPase. The results suggests that there is very fast reacting set of sulfhydryl groups, which could comprise of sulfhydryls from Ca^{2+}-ATPase and/or a minor contaminant protein as previous studies have indicated. Only this fast set was reduced by nucleotide binding. In Triton X-100, the total reactive residues increased two-fold and the biphasic nature of the curve showed that the intramolecular crosslink possibly involves a fast reacting sulfhydryl residue and a slow reacting one. Derivatization with [^{14}C]1,4-phenylenebismaleimide followed by digestion and HPLC analysis revealed radiolabelled peaks. Purification and sequencing of the adducts identified 8 reactive cysteines, namely Cys 12, Cys 344, Cys 364, Cys 471, Cys 498, Cys 636, Cys 670 and Cys 674. The cysteines involved in the putative intramolecular crosslink could not be identified but it is proposed that either Cys 471 or Cys 498 crosslink with Cys 670 or Cys 674.

ABBREVIATIONS

AMPPCP	Adenosine-5'(-ß-methylene) triphosphate
AMPPNP	Adenosine-5'(-ß-imino) triphosphate
AMPS	Ammonium persulphate
CHES	2-[N-cyclohexylamino] ethanesulfonic acid
1,2 DHPC	1,2 Diheptanoyl-sn-glycero-3-phosphocholine
DMSO	Dimethylsulphoxide
EDANS	N-acetyl-N'-(5-sulpho-1-naphthyl) ethylene diamine
EGTA	Ethyleneglycol-bis-(ß-aminoehtyl ether) N,N,N',N'-tetraacetic acid
E-P	Phosphoenzyme
EPPS	[N-(2-hydroxyethyl) piperazine-N'-3-propanesulfonic acid]
FITC	Fluorescein isothiocyanate
GF/F	Glass fibre filtres
HEPES	N-[2-hydroxyethyl] piperazine N'-[ethanesulfonic acid]
HEPPSO	(N-[2-Hydroxyethyl]piperazine-N'-[2-hydroxypropanesulphonic acid])
IAF	6(-iodoacetamido) flourescein
ISL	Iodoacetamide Spin Label
LDH	Lactose dehydrogenase
MES	(2-[N-Morpholino]ethanesulphonic acid
MOPS	3-[N-Morpholino] propane-sulphonic acid

NEM	N-ethylmaleimide
PAGE	Polyacrylamide gel electrophoresis
1,4-PBM	1,4-Phenylenebismaleimide
Pi	Inorganic phosphate
pNPP	para Nitrophenylphosphate
SDS	Sodium dodecyl sulphate
SR	Sarcoplasmic reticulum
TCA	Trichloroacetic acid
TDAB	Tetradecyltrimethyl-ammonium bromide
TMAH	Tetramethylammonium hydroxide
TEMED	N,N,N′,N′-Tetramethylethylenediamine
TES	N-tris[Hydroxymethyl]methyl-2-aminoethanesulphonic acid)
Tris	Tris (Hydromethyl)aminoethane

Page

CONTENTS

1. INTRODUCTION

ATP dependent membrane pumps can be classified into four types depending on the membrane type, catalytic mechanism and transported substrate.

(i) P-type ATPases (60-180 kD): are cation pumps that form a phosphoryl intermediate at a specific aspartate residue during the catalytic cycle. Examples include the bread mould, *Neurospora* H^+-ATPase; mammalian H^+,K^+-ATPase responsible for acidifying the stomach, Na^+,K^+ and Ca^{2+}-ATPases. They can be located in the plasmamembrane and/or intracellular membranes.

(ii) F-type ATPases or ATP synthases (>400 kD): utilize a proton gradient to synthesize ATP. Their catalytic mechanism does not include a phosphoenzyme intermediate. The name was coined by Penefsky et al., 1960, when they isolated a soluble ATP hydrolyzing, coupling factor 1 (or F1) that was required to couple electron transfer to ATP synthesis.

(iii) V-type ATPases(>400 kD): are proton pumps, rather similar in structure and catalytic mechanism to the F-type ATPases, that reside in vacoular membranes of fungi, yeast and endo/exocytic vesicles of eukaryotes. The gradient of protons is used as an energy source for the accumulation of various neurotransmitters and other effectors.

(iv) Multidrug resistance P-glycoprotein (140-170 kD): hydrolyze ATP (Horio et. al., 1988) to translocate a wide range of substrates e.g vinblastine, anthracycline, sulphonylurea (Gottesman and Pastan, 1993; Aguilar-Bryan et al., 1995, Horio et al., 1988).

1.1. The family of P-type ATPases

1.1.1 General features and properties of P-type ATPases

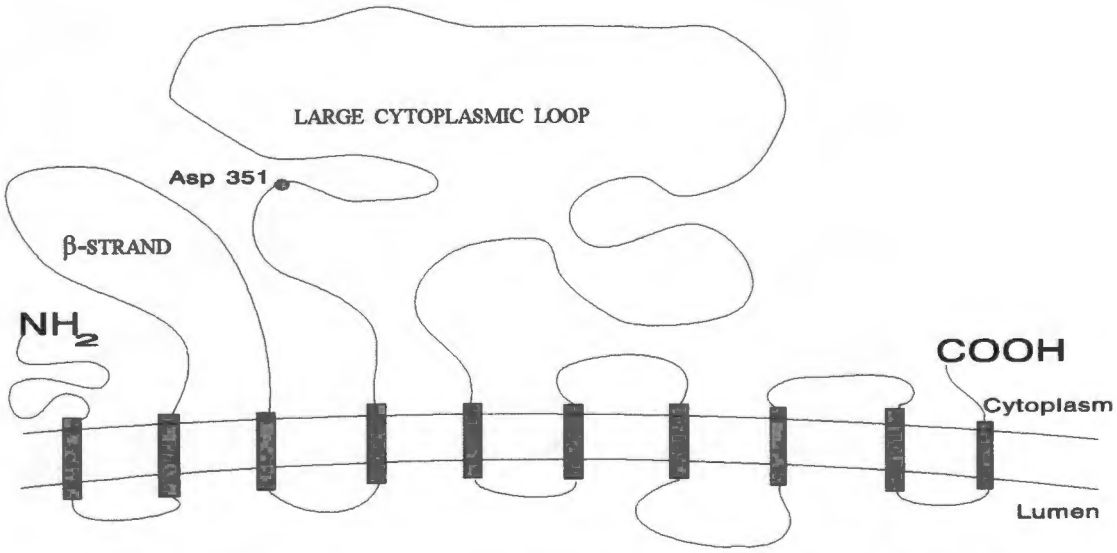

Figure 1.1 A schematic representation of a two dimensional structure of Ca^{2+}-ATPase (Asp 351, phosphorylation site).

P-type ATPases consist of either a single polypeptide, .e.g. Ca^{2+}-ATPase (Dufour et al., 1978) or two polypeptides, α and β e.g Na^+,K^+-ATPase (Vasilets and Schwartz, 1993). In the latter case the larger α subunit is the one similar to that of Ca^{2+}-ATPase and is catalytic. They share (1) minimal mechanism represented by a 4 step Post-Albers scheme i.e. E1→ E1P→ E2P→ E2→ E1, where E1 and E2 refer to outward and inward facing ion binding sites and ion translocation is concomitant with phosphorylation-dephosphorylation; (2) homologous amino acid sequence motifs, and (3) similar transmembrane topology (see Figure 1.1). They all have an N-terminus located in the cytoplasm and two fairly large cytoplasmic loops, one referred to as the ß-strand domain, and the second larger loop containing the phosphorylation and ATP binding domains. There are 6-10 predicted transmembrane helices with the variability in the carboxyl terminal helices. The homologous motifs are

(i) TGES motif located in the small cytoplasmic loop or β-strand domain.

(ii) DKTGT motif, where "D" is the aspartyl residue phosphorylated, and is located in the phosphorylation domain.

(iii) KGAXE motif located upstream of the phosphorylation domain in the large cytoplasmic loop. Fluorescein isothiocyanate reacts specifically with this lysyl residue in the sarcoplasmic reticulum Ca^{2+}-ATPase (Mitchinson et al., 1982) and several other pumps (Kirley et al., 1985; Hicks and Parsons, 1992). Since the fluorescein moiety resembles AMP in size and shape, it is thought that this segment is involved in ATP binding.

(iv) GDGXNDPXP at the junction of the end of the large cytoplasmic loop and the membrane region. This region is generally known as the 'Hinge' because of sequence similarity to the hinge region of phosphokinases (MacLennan et. al., 1985). It is thought to link the ATP binding domain to the phosphorylation domain and the abundance of glycine and proline residues, which are generally involved in bends of secondary protein structure, in the Hinge suggest flexibility and perhaps "sliding" motion (Taylor and Green, 1989, Moller et al., 1996).

1.1.2 Animal P-type ATPases

1.1.2.1 Ca^{2+}-ATPases

Animal Ca^{2+}-ATPases are located in the sarco/endoplasmic reticulum and plasmamembrane. Sarco/endoplasmic reticulum Ca^{2+}-ATPases are encoded by three (SERCA) genes; with SERCA1 encoding fast twitch, SERCA2 slow twitch and SERCA3 muscle and non-muscle Ca^{2+}-ATPases. Within each of these groups there are 3-4 isoenzymes which differ at their carboxyl terminal ends due to alternative splicing

(Zarain-Herzberg et. al., 1990). They have a molecular weight of approximately 110 kD and are specifically inhibited by thapsigargin. The plasmamembrane Ca^{2+}-ATPases are larger (MW ~140 kD) and are modulated by calmodulin and protein kinases (Carafoli et al., 1996).

The Ca^{2+}-ATPase (E.C.36.1.38) is the most abundant protein of the sarcoplasmic reticulum, which pumps Ca^{2+} from the sarcoplasm and myofibrils to allow muscle relaxation. The pump is considered an ideal model system since it consists of a single polypeptide and relatively pure preparations can be obtained. The pump has been cloned and sequenced (MacLennan et al., 1985), and the isolated vesicles are thought to be orientated as in the native muscle reticulum. The characteristics of this ion pump are extensively dealt with in later sections of this dissertation.

1.1.2.2 Na^+,K^+- and H^+,K^+-ATPases

Na^+,K^+-ATPases are located in the plasmamembrane of all animal cells and pump 3 Na^+ extracellularly and 2 K^+ intracellularly per turnover cycle. This pump is specifically inhibited by the cardioactive steroid, ouabain. The first report of Na^+,K^+-ATPase activity was in a homogenate of nerve fibres of the shore crab, *Carcinus maenas* (Skou, 1957). Optimal activity was found with a $Mg^+/Na^+/K^+$ combination and Ca^{2+} was inhibitory. Later , Post et al. (1969) published their seminal paper, which showed that there was co-dependence between potassium ions transported intracellularly and sodium ions transported extracellularly, at a ratio of 2:3 respectively. As with all P-type ATPases a phosphorylation-dephosphorylation cycle involving a ß-aspartyl phosphate intermediate is obligatory for transport (Post et al.,1965, Post and Kume, 1973).

Na^+,K^+-ATPase consists of two subunits, an α-subunit and a β-subunit. The functional unit of Na^+,K^+-ATPase appears to be a (αβ) dimer (for review see Vasilets and

Schwarz, 1993). Electron microscopy of Na^+,K^+-ATPase membrane crystals indicated a structural unit of $(\alpha\beta)_2$ (Skriver et al., 1992). The pump possibly has two central α-subunits with flanking β-subunits. However, the monomer (αβ) is active in detergent solutions (Vilsen et al., 1987) and the association of αβ units into higher oligomers may modulate catalysis and transport.

It is the α-subunit of Na^+,K^+-ATPase which is catalytic and undergoes the major conformational change between the two forms, E1 and E2 (Post et al., 1972). The conformation is determined by ATP (Shani et al., 1987) and K^+ or Na^+ binding (Norby and Jensen, 1971). There may be two ATP binding sites, one with high affinity and the other with low affinity, representing catalytic and regulatory sites (Thoenges and Schoner, 1997). ATP at high concentrations accelerates ATPase turnover up to 20-fold, due to an ATP-activation of K^+ deocclusion (Post et al., 1972; Forbush III, 1987)

Na^+,K^+-ATPase resides in the E2 conformation in the absence of cations (Norby and Jensen, 1971). Addition of Na^+ rapidly converts the enzyme into an E1 state. Preincubation with K^+ slows the transition (Skou and Esmann, 1983). In the reverse direction the K^+-induced transition (E1 → E2) is equally fast and slowed by Na^+. The $E1{\cdot}Na^+$ species has a high affinity for nucleotide and $E2{\cdot}K^+$ species a low affinity as shown by eosin binding (Esmann,1994).

Mammalian stomach lumen acidification by parietal cells, which is vital to digestion, is performed by a proton pump, the H^+,K^+-ATPase. This pump is responsible for translocation of protons extracellularly and potassium ions intracellularly. It is highly homologous to Na^+,K^+-ATPase and is also composed of an α (100 kD) and a ß (80 kD) subunit. It is specifically inhibited by Sch-28080 and omeprazole, agents used in the treatment of stomach ulcers (Wingo and Smolka, 1995). The number of transmembrane helices has been investigated using trypsin digestion, SDS-PAGE and amino acid sequencing, but the results are conflicting. Models of 8 or 10

transmembrane helices (Karlish et. al., 1993; Bamberg and Sachs, 1994) or possibly 12 (Subrahmanyeswara-Rao et. al., 1991) have been proposed.

The gastric pump also appears to be a ($\alpha\beta$) dimer. The n-dodecyl β-maltoside solubilised protein migrates as a 360 kD complex on Blue Native PAGE, a PAGE system that utilize a mixture of Triton X-100, Na-Taurodeoxycholate and Coomasie Blue G to minimize membrane protein aggregation while retaining native like structure (Shin and Sachs, 1996, Schagger and Jagow, 1991). Cu-Phenanthroline crosslinking followed by SDS-PAGE revealed that the α-subunits, and not the β-subunits interact in the dimers (Shin and Sachs, 1996), very similarly to the Na^+,K^+-ATPase structure mentioned above.

1.1.2.3 Cu^{2+}-ATPases

Cu^+-ATPase maintains copper ions below toxic levels (Haywood et al., 1985). It is predicted to possess 8 transmembrane helices and has a cysteine and histidine rich N-terminus that is thought to be the initial copper binding site before translocation (Lutsenko and Kaplan, 1995). This motif in the N-terminus is conserved among metal ATPases, and even in cyanobacteria, suggesting an ancient lineage (Soloiz et al., 1994; Phung et al., 1994). Specific mutations of the Cu^+-ATPase are responsible for the human Wilson (autosomal recessive) and Menkes (X-linked) diseases. These copper transport disorders are, in case of the former, due to excess copper in hepatocytes because of poor copper exportation, and, in case of the latter, insufficient copper in most tissues because of entrapment in kidney and intestinal parietal cells.

1.1.3 Bacterial P-type ATPases

Bacterial P-type ATPases can be broadly divided into those that confer resistance to (toxic) heavy metal ions (e.g. CadA-ATPase, cadmium pump of *Staphylococcus*

aureus Soloiz and Vulpe, 1996) and those that translocate essential ions to effect homeostasis (e.g. Ca^{2+}-ATPase and K^+-ATPase). The heavy metal ion ATPases are characterized by a cysteine and histidine rich N-terminus, an intramembranous CPx motif and an HP doublet after the phosphorylation domain (Soloiz and Vulpe, 1996).

Two Cu^{2+} ATPases have been described in *Enterococcus hirae*, namely CopA and CopB to effect import and export copper respectively (Odermatt et al., 1993). The evidence for a difference in function is based on the observation that mutagenesis of CopA induced a significantly higher tolerance to high medium concentration(6 mM $CuSO_4$) of copper than altered CopB. They are homologous with the human Cu^{2+} ATPases.

Gram negative bacteria P-type Ca^{2+}-ATPase (60 kD) activity has been described in *Flavobacteruim odoratum* (Gambel et. al., 1992). Micromolar concentrations of orthovanadate, a fairly specific P-type ATPase inhibitor, inhibited calcium dependent phosphoenzyme formation. The phosphoenzyme, like all acyl phosphates, is alkaline sensitive.

Another bacterial P-type ATPase is the K^+ transport system of *Eschericha coli* (Heese et. al., 1984). The pump appears to comprise a 59 kD (KdpA) subunit, a 72 kD (KdpB) subunit and a 21 kD (KdpC) subunit (Epstein et. al., 1990). KdpA forms the transmembrane segment of the pump and is involved in K^+ binding and translocation in concert with KdpB. The latter is possibly responsible for ATP dependent conformational changes. The functional significance of KdpC is uncertain but predicted structural similarity to the β-subunit of Na^+,K^+-ATPase suggests possible functional similarity.

1.1.4 Yeast , fungal, and plant, P-type ATPases

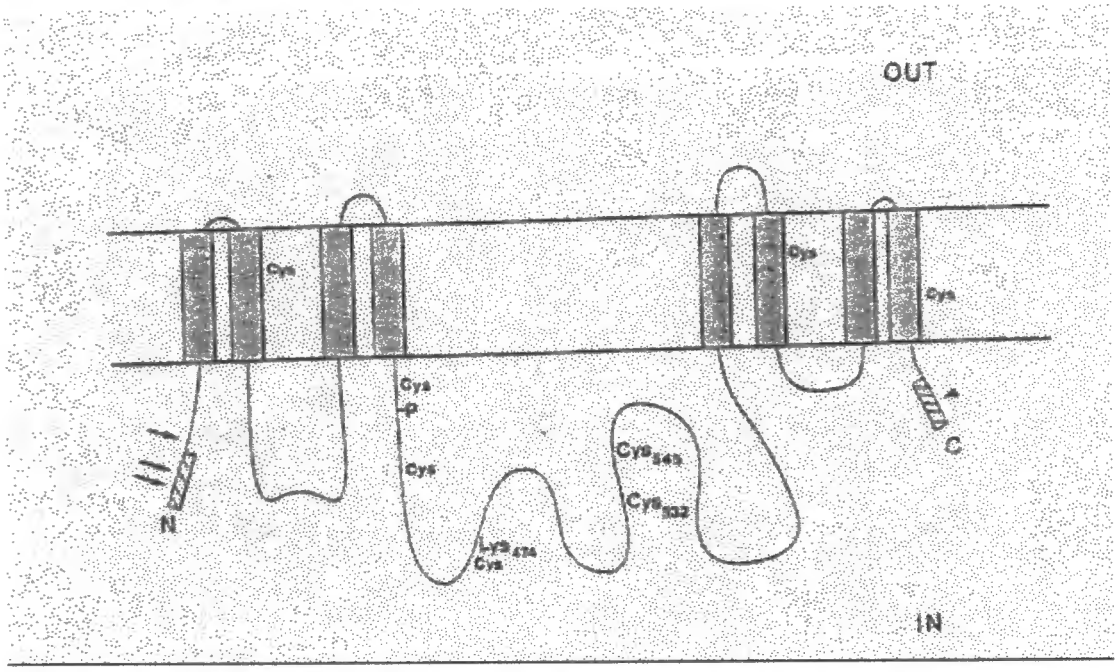

Figure 1. 2 Model of Plasma membrane H^+-ATPase of *Neurospora crassa* showing cysteine dispositioning. P, phosphorylation site; Lys 474, site of FITC labelling; Cys 532 and Cys 545, are sites of reaction with NEM; *arrows*, sites of trypsin digestion in the absence of ligands; *arrowhead*, site of trypsin digestion in the presence of Mg^{2+} and vanadate; *hatched areas*, antigenic sites (Pardo and Slayman, 1989, Chang and Slayman, 1990)

The plasma membranes of yeast, fungal and plant cells contain an H^+-ATPase that serves to generate a proton motive force for use as an energy source for a number of secondary transport systems. The proton pumps are very similar to the aforementioned ATPases, forming a β-aspartyl phosphoenzyme intermediate (Dame and Scarborough, 1981) and reacting with fluorescein isothiocyanate (Pardo and Slayman, 1988), see Figure 1.2. The monomeric species (105 kD) appears to be the functional unit (Goormaghtigh, 1986).

These pumps are interesting from the point of view of the role of sulfhydryl groups as they possess only 8 (compared to 24 in sarcoplasmic reticulum Ca^{2+}-ATPase) and 3 are predicted to be transmembrane. Of the 5 in the cytoplasmic portion, 2, at least in

Neurospora crassa, are reactive to NEM and one (Cys-532) may be located near/in the active site (Chang and Slayman, 1990).

Ion pumps have also been reported in plants. A germinating pollen grain, predominantly the plasmalemma and a growing pollination tube of *Vicia faba*, shows Ca^{2+}-ATPase activity (Bednarska, 1993) suggesting a significant role in fertilization. *Petunia hybrida* Hort III unpollinated pistil and transmitting tract of the style immediately after pollination has significantly higher plasmalemmal Ca^{2+}-ATPase activity when compared to the same cells later after pollination (Bednarska and Butow, 1995)

1.2 Structure of sarcoplasmic reticulum Ca^{2+}-ATPase

1.2.1 Primary, secondary and tertiary structure

The first Ca^{2+}-ATPase to be cloned and sequenced was the slow twitch (and cardiac) form (MacLennan et al., 1985) and the fast twitch followed (Brandl et al., 1986). The deduced amino acid sequence, shown in Figure 6.1 (page 89), permitted secondary structure predictions to be made and hydropathy plots led to the identification of 10 putative membrane spanning segments. This model was reinforced by the finding that amino acids 870-890, between M7 and M8 were luminal, whereas 657-652 were cytoplasmic (Clarke et. al., 1990) using peptide specific monoclonal antibodies. Although the ten-membrane pass-model has been challenged, especially with respect to related pumps, it is still the preferred model for Ca^{2+}-ATPase (Stokes et al., 1994).

The calcium binding sites were predicted to be in the stalk region, but latter studies pinpointed them in the membrane. The residues now implicated in Ca^{2+} binding through site-directed mutagenesis are E309 [M4]; E771 [M5]; N796, T799 , D800 [M6] and E908 [M8] (Clarke et al., 1989). They observed complete loss of Ca^{2+} binding and

transport activity in pumps mutated in these residues. Ca^{2+} binding was measured indirectly through Ca^{2+} inhibition of Pi phosphorylation. Contrary to what is seen with the wild type, mutants exhibited phosphate-dependent phosphorylation in the presence Ca^{2+}. The same residues were later examined in more detail with respect to their individual involvement in binding each of the two Ca^{2+} (Andersen and Vilsen, 1994, 1995). Site 1 (deeper) was constituted of E771, T799, D800 and site 2 (superficial) of E309, N796 and D800 as shown in Figure 1. 3. Some of the assignments were based on the knowledge that inhibition of Pi phosphorylation occurs with the binding of one Ca^{2+}, whereas phosphorylation by ATP requires both cations. For example, (i) Asn796 probably ligates the second (superficial) calcium as its mutation inhibited phosphorylation by either ATP or inorganic phosphate and prevented calcium occlusion, (ii) Thr799 could bind the first (deeper) calcium as its mutation inhibited phosphorylation by inorganic phosphate and not by ATP and also blocked calcium occlusion. The fact that the latter mutation permitted phosphorylation by ATP which requires binding of both Ca^{2+} suggested that the second site was intact contrary to what was observed with a mutation in N796.

Andersen (1995) demonstrated that the mutation R763G resulted in calcium activated ATP hydrolysis without accumulation of calcium in vesicle, a characteristic feature of ionophore treated pump. This suggests that this residue could act as a gate preventing efflux of accumulated Ca^{2+} through the unphosphorylated pump.

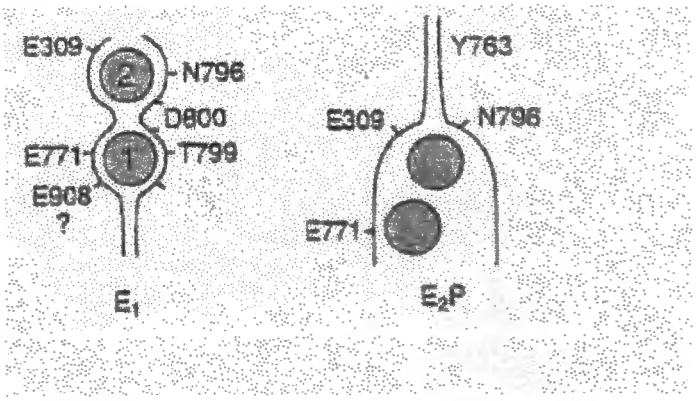

Figure 1.3 Hypothetical structure of the Ca^{2+} occlusion sites and Ca^{2+} binding sites in the E1 and E2P forms, respectively. The cytopalsmic surface is at the top and the question mark indicates that Glu-908 is less significant to occlusion compared with other residues (Andersen and Vilsen, 1995)

Following secondary structure predictions of α helices and β strands (MacLennan et al., 1985), a crude 3-D structure was predicted by comparing highly conserved segments of nucleotide binding sites among ATPases (Taylor and Green, 1989). Using affinity labelling and fluorescence energy transfer (Gutier-Merino et. al., 1987; Bigelow and Inesi, 1991) it was postulated that Lys515 is 53 Å away from Cys670/Cys674, 42 Å and 77 Å from the maleimide sites (Cys344/Cys364) and 60 Å above the membrane surface as shown on Figure 1.4. Combining affinity labelling, 3-D structure predictions, sequence homologies and mutational studies, McIntosh (1998) proposed a speculative structure of the large cytoplasmic loop (Figure 1.5).

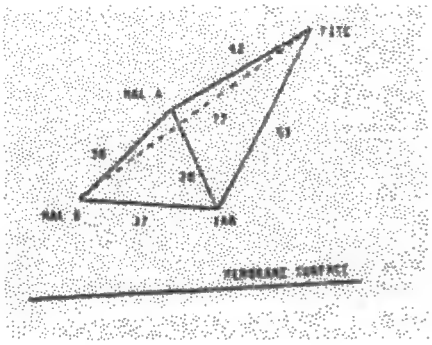

Figure 1.4 Model of spatial relationship of fluorophore sites relative to each other. The panel depicts sites labelled by FITC, iodoacetamide derivatives (IAA), and maleimide derivatives (MAL A and MAL B). The numbers indicate the mean distances in angstroms (Bigelow and Inesi, 1991).

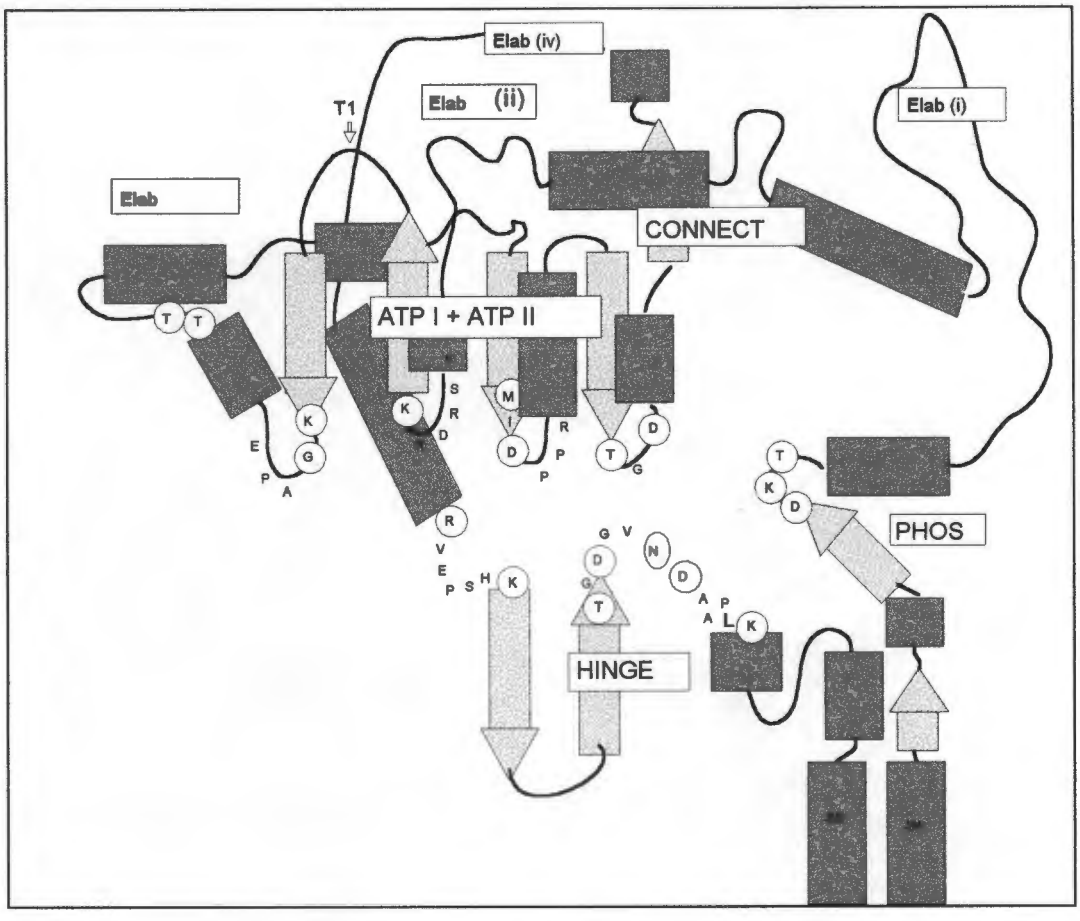

Figure 1.5 Speculative structure of the large cytoplasmic loop showing possible nucleotide binding residues; Phos, phosphorylation site (McIntosh, 1998).

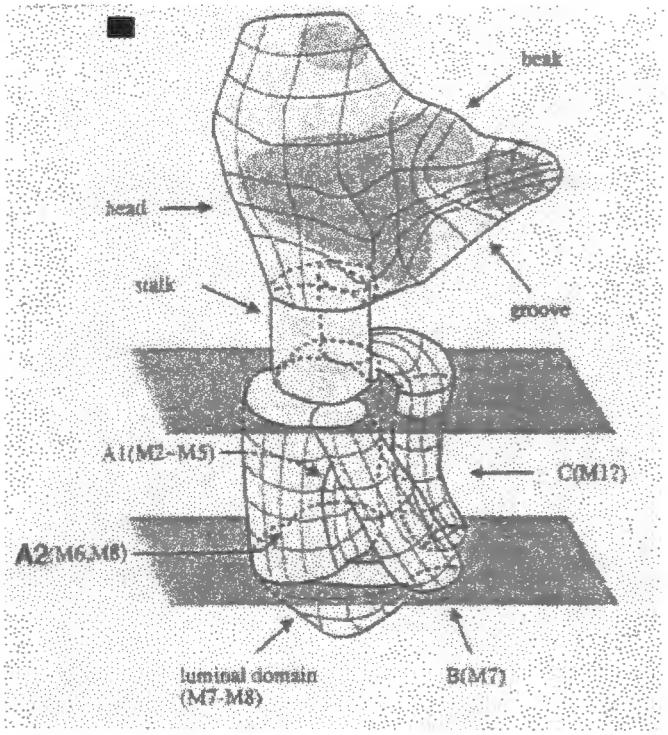

Figure 1.6 Three dimensional structure Ca^{2+}-ATPase at 14 Å showing transmembrane segments M1 to M8; cytoplasmic domain (top) and luminal domain (Toyoshima et. al., 1993)

A 14 Å three-dimensional structure of native SR Ca^{2+} -ATPase has been obtained from cryoelectron microscopy and helical image analysis of two-dimensional vanadate crystals, Figure 1.6 (Toyoshima et al.,1993).The height of the pump is 120 Å with 32 Å in the membrane and a 25 Å stalk. The protein distribution is 70% cytoplasmic and 5% luminal. Three transmembrane masses are seen, one of which is likely to comprise the four transmembrane helices that make up the Ca^{2+} transport channel (M4, M5, M6 and M8, identified by site directed mutagenesis). There are two masses in the stalk section which form a cavity on approaching the head, which could perhaps allow sliding and flexing of the pump during translocation. One cavity in the head region(labelled groove) could possibly be the ATP binding site.

1.2.2 Active site residues

Active site residues have been elucidated by chemical modification, affinity labelling and mutation of conserved residues. The conserved sequences and residues implicated are ^{349}CSDKTGTLT; ^{488}FSRDRKSMS; ^{511}KGAPE; ^{600}DPPR; ^{625}TGD; ^{676}FARVEPSHKS; ^{701}TGDGVND and ^{709}PALK, see Figure 1.7. An intramolecular crosslink between Lys492 and Arg678 with glutaraldehyde (McIntosh, 1992) inhibited by ATP, ADP and AMPPCP (Ross and McIntosh, 1987), suggesting that these residues bind ATP and abut each other. Several probes derivatize Lys492, including TNP-8N$_3$-ATP/AMP (McIntosh et al., 1991), 3-O-(5-Fluoro-2,4-dinitrophenyl)-ATP (Yamasaki et al., 1994), pyridoxal phosphate and pyridoxal ATP (Hinz and Kirley, 1990). In general ,derivitization does not inhibit acetyl phosphate or Pi phosphorylation.

Arg489, Arg505 and Arg678 have been demonstrated to constitute part of the ATP binding site by modification with 1,2-cyclohexanedione (Kawakita et al., 1997). Arg489 and Arg678 were completely protected by MgATP from modification, whereas FITC provided partial protection. Arg505 was slightly protected from modification by the nucleotide, and yet completely blocked by FITC prelabelling. They suggested that these results located Arg489 and Arg678 in the region occupied by the triphosphate moiety of ATP, and Arg505 near the adenosine binding site. ATP-sensitive arginines have been located between residues 506 and 595 by phenylglyoxal labelling (Garcia, 1996). This fits with the labelling of Thr532 and Thr533 with 8-azido ADP in the same region (Lacapere et al., 1993).

Lys515 was demonstrated to be involved in the ATP binding site by labelling with FITC (Mitchinson et al., 1982) in a reaction in which the probe labels about twice (approximately 8.2 nmol/mg of protein) the Ca^{2+}-ATPase molecules that can be phosphorylated (approximately 4.5 nmol/mg of protein) by either ATP or Pi (Nakamura et al., 1997). Mutation of this lysine produced a defective ATP binding site and inhibited activity with either ATP or acetyl phosphate (Maruyama et al., 1989)

Mutation of Lys684 also inhibited phosphorylation by either ATP or Pi, even though nucleotide binding seemed intact, deducing from glutaraldehyde crosslink inhibition by nucleotides (Vilsen et al., 1991).

The conserved segment ^{601}Asp-Pro-Pro-Arg is implicated in binding ATP as alterations D061E or P603G eliminated protection of the glutaraldehyde crosslink by a nucleotide or completely inhibited the actual crosslink respectively (MacLennan et al., 1992). Recent mutational analysis of the conserved segment ^{487}Phe-Ser-Arg-Asp-Arg-Lys^{492} has implicated Phe487, Lys492 and partially Arg489 in the ATP binding site, although this segment does not to participate in either ATP or acetyl phosphate phosphorylation, and translocation activity (McIntosh et al., 1996)

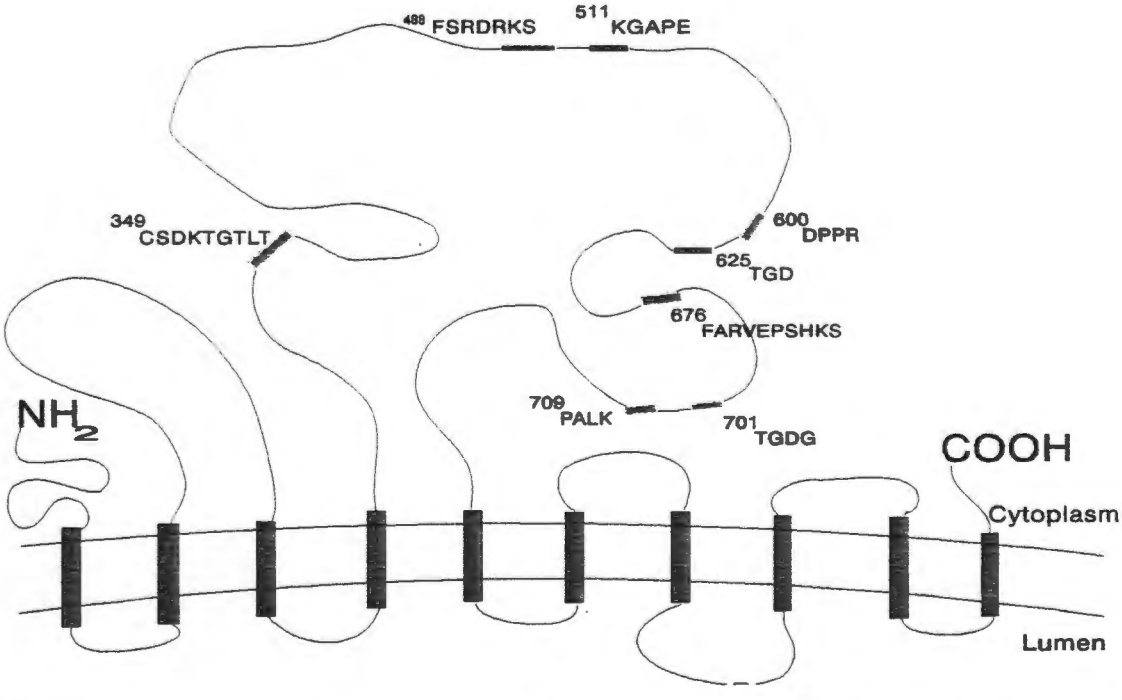

Figure 1.7 A schematic representation of a two dimensional structure of Ca^{2+}-ATPase showing highly conserved sequences.

1.2.3 Reactive sulfhydryl groups and their effect on pump activity

The reactivity and role of sulfhydryls (SH) in sarcoplasmic reticulum Ca^{2+}-ATPase has been analyzed as early as 1976, their dispositioning is shown in Figure 1.8. The reactivity of sulfhydryls with 5,5'-dithiobis(2-nitrobenzoate) allowed classification into fast, moderate and slow groups at pH 7.8 (Murphy, 1976). Out of a total of 25 SH groups (close to the actual number of 24), Murphy found 2.0 fast, 8.5 moderate, 6.6 slow and 8.0. buried. However in the presence of MgATP (MgADP or MgAMPPNP, a non-hydrolysable ATP analogue) the 2 fast -SH groups displayed moderate reactivity, resulting in approximately 10.6 moderate, 7.0 slow and 8.0 buried (Murphy, 1978). In the presence of Ca^{2+} alone or of Ca^{2+} plus nucleotide, all reactive SH groups displayed a single moderate rate constant (Murphy, 1976, 1978). The reactivity changes during the Ca^{2+} translocation cycle as shown in Figure 1.9 . The largest changes being upon the formation or decomposition of E~P, leading to accessibility increasing (17 SH) and decreasing (-24 SH) respectively.

Various other SH directed probes have identified specific residues. Two cysteine residues, Cys670 and Cys674 are selectively reactive to iodoacetamide and iodoacetamide based probes (Baba et. al., 1986; Bishop et. al., 1988; Suzuki et. al., 1994). Cys670 is also reactive with a maleimide based probe, 4-dimethylamino-phenylazophenyl-4'-maleimide (Wawrzynow and Collins, 1993). Covalently bound iodoacetamide and a flourescent derivative, IAEDANS, do not affect the translocation activity of Ca^{2+}-ATPase. IAEDANS reports the conformational change on formation of E1~P·2Ca (Baba et. al., 1986; Suzuki et. al., 1994). The specific reactivity of Cys670 and Cys674 with the polar negatively charged probe, IAEDANS, was suggested to be due to their peripheral location in an α-helix and close to arginine residues 667, 671, 672, 678 whose cationic nature perhaps maintained their reactive anionic thiolate form by lowering their pKa values (Bishop et. al., 1988). They further attributed the non-reactive nature of Cys675 to Glu668 (negatively charged) which might be close in a helical configuration.

Wawrzywnow et al. (1993) used electron paramagnetic resonance (EPR) to show that the high reactivity of Cys 674 to an iodoacetamide spin label (ISL) appears to be due to its hydrophobic location, since the probe was relatively inaccessible to cosolvents. The ISL has also been used to demonstrate that the two motional states of the label observed on Ca^{2+}-ATPase in the presence of a nucleotide and Ca^{2+} correlate to two conformational states of the pump, E1 and E2 (Coan et al., 1972; Coan and Keating, 1982; Lewis and Thomas, 1992). The probe reports a nucleotide-dependent conformational change in the presence of Ca^{2+} (Coan, 1983). The biphasic nature of the fluorescence changes were interpreted in terms of a Ca^{2+}-ATPase oligomer comprising conformationally coupled monomers of slow and fast catalytic kinetics, Mahaney et al. (1995). They also obtained complicated kinetics using ISL attached to Cys-674 and argued for an ATP-dependent phosphorylation regulated by communication within the oligomeric unit.

N-ethylmaleimide (NEM) has been extensively used as a SH reagent. Usually [^{14}C]NEM is used to monitor the reaction but the disappearance of its absorbance at 305 nm upon reacting can also be employed (Riordan and Vallee, 1972). The reaction of NEM with Ca^{2+}-ATPase at pH 7.0 led to the characterization of distinct classes of SH groups, namely SH_F, $SH_{N'}$, SH_D and SH_N, in an increasing order of reactivity (Yamada and Ikemoto, 1980; Kawakita et al. 1980; Kawakita and Yamashita, 1987). SH_F was inhibited by a non-hydrolysable ATP analogue and its modification blocked E-P formation. $SH_{N'}$ was partially inhibited by nucleotide, whereas SH_D and SH_N were not affected by nucleotide. Modification of SH_D blocked E-P decomposition. SH_N, which was the most reactive group, was identified as derivatization of either of two cysteine residues (Cys-344 and Cys-364), which maintained ATPase activity when one residue was modified but inactivated when both were derivatized, SH_D (Kawakita and Yamashita, 1987). The latter is also reactive with Fluorescein 5'-maleimide and 4-dimethylamino-phenylazophenyl-4'-maleimide (Wawrzynow and Collins, 1993). They also showed that cysteines 471, 498, 525, 614 and 636 were modified by these maleimide-based probes. The reactivity of Cys471 with iodoacetamide has been demonstrated to decrease after inactivation of the Ca^{2+}-ATPase with an ATP analogue,

3'(2')-O-biotinyl-thionosine triphosphate suggesting that this residue is near the ATP binding site (Kison et al., 1989). Cys12, Cys525 and Cys670 have been identified to be reactive with NEM (Reithmeyer and MacLennan, 1981). NEM has also been instrumental in identification of reactive cysteine residues and locational significance in yeast H^+-ATPase, identifying Cys221 and Cys532, the latter being near or in the nucleotide binding site (Petrov et al., 1997), neither of which are conserved.

N-(1-pyrene) maleimide, a hydrophobic sulfhydryl probe, reacts with Cys367 of Na^+,K^+-ATPase (Kirby and Peng, 1991). This residue corresponds to Cys349 in the sarcoplasmic reticulum Ca^{2+}-ATPase, a residue conserved in P-type ATPases, which is two amino acids from the phosphorylation residue.

Reduction of two of the three disulphide bonds present per catalytic unit has been implicated in `locking' the pump in ADP reactive phosphoenzyme, suggesting interference with conformational changes of the 3-dimensional protein structure (Daiho and Kanazawa,1994).

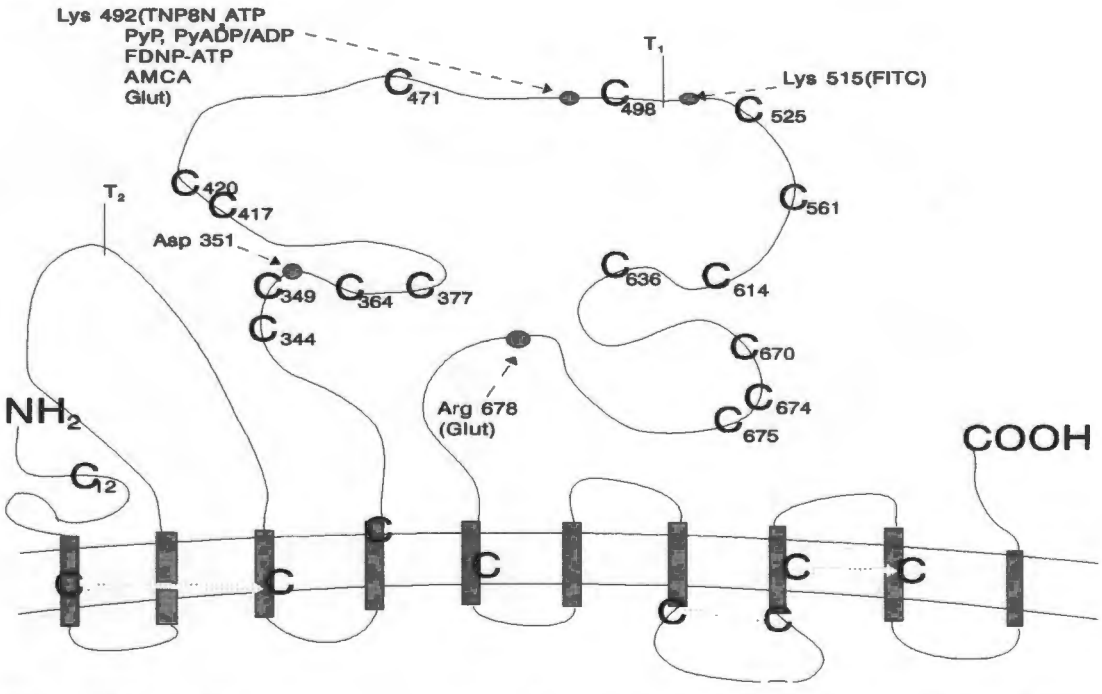

Figure 1.8 A schematic representation of a two dimensional structure of Ca^{2+}-ATPase showing cysteines dispositioning

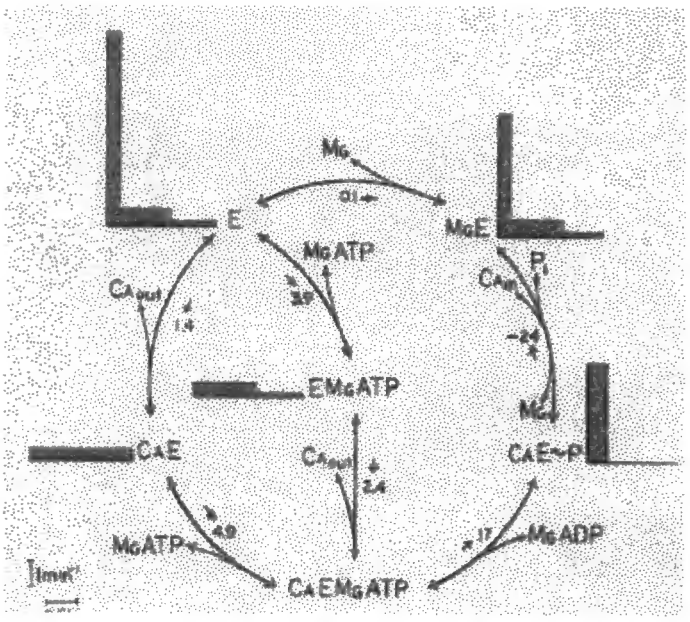

Figure 1.9 Sulfhydryl reactivity profiles of intermediates of the calcium translocation cycle. In the histograms, the height is proportional to the rate constant, and the width to the number of sulfhydryls in a kinetic set (very fast, fast, moderate, slow and unreactive). The numbers between the intermediates are the difference in the total free energies of inactivation for the reaction of the reagent with the sulfhydryls (SH). The horizontal scale represents 5 SH and the vertical 1.min^{-1} (Murphy, 1978).

1.3 Mechanism of SR Ca^{2+}-ATPase

1.3.1 Catalytic cycle and affinities for ions and ligands

The sarcoplasmic reticulum Ca^{2+}-ATPase is a protein pump which utilizes energy from ATP hydrlolysis to translocate Ca^{2+} across the membrane in a series of steps involving conformational changes (Scheme 1). Understanding the mechanism of Ca^{2+}-ATPase active transport will require knowledge of the chemistry, energetics and structural changes coupling ATP hydrolysis to transport.

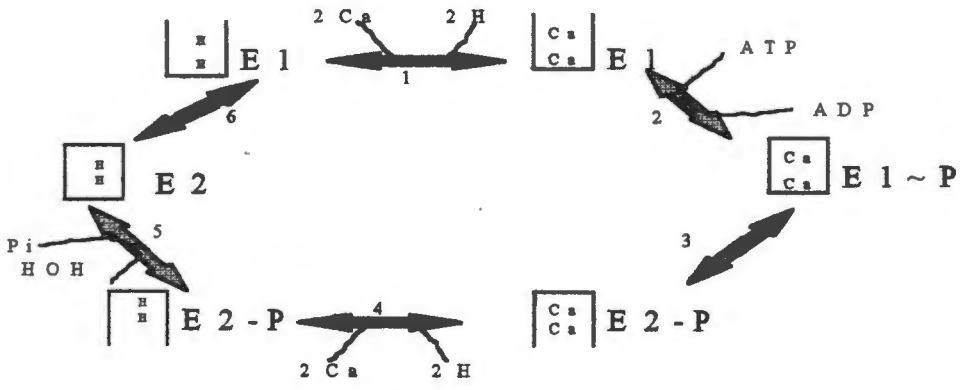

SCHEME 1

In the absence of Ca^{2+} the pump exists as an equilibrium of E1 and E2 species, the latter favoured at low pH (Inesi, 1985; Forge et al., 1993). In the initial step (step 1) two Ca^{2+} sequentially bind the transport sites (Dupont, 1982; Inesi, 1987), suggesting a channel-like model (Inesi, 1987), which is supported by mutational studies (Andersen and Vilsen, 1995). It has also been reported that addition of Mg^{2+} distinguishes two high affinity sites which bind Ca^{2+} in a biphasic reaction (Moutin and Dupont, 1991), thus supporting a channel-like site.

Occupation of the ATP pocket with ATP, ADP or a non-hydrolysable ATP analogue increases the rate of Ca^{2+} binding at pH 6, although they have little effect at pH 8 (Wakabayashi and Shigekawa, 1990; Mintz et al., 1995). The acceleration possibly occurs via an increase in the rate of the deprotonation steps, which are rate limiting in the absence of nucleotides.

Subsequent to the Ca^{2+} binding step is phosphorylation by ATP (or by Pi in the absence of Ca^{2+}, step 6); phosphorylation yielding E1~P species induces Ca^{2+} occlusion (step 2) (Takakuwa and Kanazawa, 1979; Dupont, 1980; Takisawa and Makinose, 1981). The forward phosphorylation step in the presence of Ca^{2+} seems to be associated with ATP induced conformational change (Petithory and Jencks, 1986; Kubo et al., 1990; Coan and Keating, 1982; Lewis and Thomas, 1992).

Step 3, 2Ca.E1~P→2 Ca.E2-P, has been reported to induce conformational change-linked reduction of Ca^{2+} affinity (Froehlich and Heller, 1985) followed by sequential lumenal dissociation from the E2-P species, step 4 (Inesi, 1987; Forge et al., 1995), in a relatively slow step (Orlowski and Champeil, 1991) which can be accelerated by K^+ addition (Moutin and Dupont, 1991). Ultimately follows rapid dephosphorylation of E2-P to regenerate E1 concomitant with translocation of protons towards the lumen, step 6 (Forge et al., 1993; Mintz et al., 1995).

1.4 Use of crosslinking agents as structural and mechanistic probes of Ca^{2+}-ATPase

Crosslinking of amino acid residues can provide information on the protein topology as well as mechanism, especially in so far as essential conformational changes or domain flexing may be inhibited. Treatment of Ca^{2+}-ATPase with crosslinking agents usually results in extensive intermolecular crosslinking because of the high concentration of pumps in the sarcoplasmic reticulum membrane (Chyn and Martonosi, 1977; Louis and Holroyd, 1978). The presence of ATP in the medium can help prevent inactivation of activity (Kurobe et al., 1983). In the latter study using dithiobissuccinimidyl propionate, intermolecular crosslinking was implicated in a Ca^{2+} induced conformational change as the inhibitor could be reversed by cleaving the S-S bond of the crosslinker.

More recently, under mild controlled conditions that result in very little intermolecular crosslinking, glutaraldehyde has been shown to crosslink the Ca^{2+}-ATPase intramolecularly via residues Lys 492 and Arg 678 (McIntosh, 1992). The intramolecular crosslink alters the hydrodynamic properties of the protein in SDS-PAGE such that it migrates with an apparent molecular weight of 125 kD instead of

the usual 110 kD (Ross and McIntosh, 1987a). This intralink is inhibited by ATP, ADP and other nucleotide analogues and by phosphorylation to E2P in either direction of catalysis (Ross et al., 1991). The intralink completely prevents Ca^{2+} release to the vesicle lumen and hydrolysis of E2P occurs via an uncoupled pathway with Ca^{2+} release to the vesicle exterior (McIntosh et al., 1991). Another putative intramolecular crosslink of the protein, as well as dimers and high order oligomers, has been reported with cupric phenanthroline after incubation with melittin, a basic 26 residues amphiphilic peptide presumed to inhibit the pump by either binding the nucleotide binding site or binding to the membrane bilayer and restricting conformational flexibility (Shorina et al., 1997).

The 125 kD species is produced by reaction with many other crosslinkers including glyoxal, formaldehyde, ethylene glycol bis(succinimidyl succinate), p-phenyldiglyoxal (Ross and McIntosh, 1987a) and 1,4-phenylenebismaleimide (Yamasaki and Yamamoto, 1989). Since these crosslinkers are of variable length and specificity, there must be several residues in the vicinity of Lys 492 and Arg 678 that can be crosslinked to form a species of approximate apparent molecular weight of 125 kD.

Reaction of ATP-imidozolidate with Ca^{2+}-ATPase results in the formation of a 130 kD species on SDS-PAGE(Gutowski-Eckel et al., 1993), and reaction of a carbodiimide adduct of ATP yield a 175 kD species. Gutowski-Eckel et al. located the crosslink between Asp 351 and a residue within Lys 684 and Met 700. The carbodiimide-ATP crosslink has not been identified but appears to also involve Asp 351. The large change in apparent molecular weight suggests the crosslink creates a very large polypeptide loop.

The intermolecular crosslink with 1,4-phenylenebismaleimide has been demonstrated to at least involve one cysteine in the nucleotide binding pocket (Cys614) and another near the phosphorylation domain , Cys377 (Yamasaki and Yamamoto, 1989), which is completely inhibited by the formation of E2-VO_4 conformation, an analogue of E2-P,

the phosphoenzyme. A protein band migrating similarly to the 125 kD species formed with glutaraldehyde was observed by the above authors when reacting Ca^{2+}-ATPase with 1,4-phenylenebismaleimide is the subject of this thesis.

2. EXPERIMENTAL PROCEDURES

2.1 Materials

Maleic anhydride, tetrahydrofuran, phenylenediamine, anhydrous sodium acetate, β-mercaptoethanol, dimethyl sulphoxide, trichloroacetic acid and bisacrylamide were from Merck. [^{14}C]maleic anhydride, 1,4-phenylenebismaleimide, Triton X-100, EGTA, Coomasie Brilliant Blue, bromophenol blue, trypsin, ATP, ADP, AMP, CHES, MOPS, MES, HEPES, HEPPSO, TES were from Sigma. TMAH was from Fluka. TDAB was from Aldrich. Glass fibre filters were from Whatman. Quicksafe A scintillant was from Zinsser. Thapsigargin was from LC Services Corporation. Acetonitrile was from Burdick and Jackson. PD-10 columns were from Pharmacia. C18 SepPak cartridges were from Waters-Millipore. Malachite green was from Gurr's. L-ascorbic acid was from Lasechem. Phosphoric acid, silica gel and ferrous sulphate were from Hopkins and Williams. C4 and C18 HPLC columns were from Vydac. Acetic anhydride, KCl, glycerol, glycine, KH_2PO_4, NH_4HCO_3, sodium dodecyl sulphate, Tris, HCl, urea, methanol, ethanol, acetic acid, sucrose, $CaCl_2$ and ammonium persulphate were from BDH Chemicals.

2.2 Synthesis, purification and quantitation of [^{14}C]1,4-phenylenebismaleimide

The synthesis of [^{14}C]1,4-phenylenebismaleimide was modified from the method of Wells and Yount (1982). Commercial non-radioactive maleic anhydride was purified by cold finger sublimation from 100 °C to -80 °C. The next stages were performed in a dry nitrogen box. The purified product (24.5 mg) was dissolved in 1.1 ml tetrahydrofuran in a 5 ml reaction vial with a conical magnetic stirrer. This solution (600 µl) was added into the 2,3 [^{14}C] maleic anhydride vial (19.6 mg, 250 µCi, specific activity 125 mCi/mmol), the contents mixed and returned to the reaction vial. This transfer was repeated once. Phenylenediamine was added and the vial was capped and

removed from the nitrogen box. The orange precipitate was stirred for 24 h at 4 °C. The reaction vial was then centrifuged at 3000 rpm for 5 min to pellet the precipitated [^{14}C]1,4-phenylenebismaleic acid. The precipitate was resuspended in 0.5 ml tetrahydrofuran, followed by a mixture of 0.5 ml acetic anhydride and 25 mg anhydrous sodium acetate. The reactants were magnetically stirred for 1 min at room temperature before gradually heating to 100 °C in an oven. In the first 10 min of oven heating, the reaction vial pressure was released through a mininert valve every 2 min. The reaction was then continued for 22 h in a 100 °C oven, after which the mixture had turned brown-black. The dark solution was allowed to cool to room temperature before incubating on ice for 10 min. Cold water (2 ml) was added to the reaction mixture on ice before stirring for 10 min at 4 °C to hydrolyse any unreacted acetic anhydride. The reaction vial was centrifuged for 5 min at 3000 rpm and the supernatant discarded. The precipitate was resuspended in 1 ml cold water, centrifuged and the supernatant discarded. This wash step was repeated twice more. The precipitate was dissolved in 2 ml acetonitrile. The solution was centrifuged and the harvested supernatant was protected from light. This was repeated and the supernatants pooled. The acetonitrile soluble product(s) was stored at -20 °C and protected from ambient light. Purification of the crude synthesized 1,4-phenylenebismaleimide was carried out using silica gel column chromatography, 20 mm long and 6 mm diameter, in acetonitrile. The dark material, and not the phenylenebismaleimide, was retained on the column. Eluates were analysed and quantified using a Beckman System Gold HPLC, Hewlett-Packard 8450A diode array spectrophotometer and Beckman LS 6000 SE series (liquid scintillation system). An extinction coefficient at 313 nm of 940 $cm^{-1}.M^{-1}$ in acetonitrile was used in the quantification (Wells and Yount, 1982).

2.3 Reaction of sarcoplasmic reticulum Ca^{2+}-ATPase with 1,4-phenylenebismaleimide

The reaction of 1,4-phenylenebismaleimide with sarcoplasmic reticulum Ca^{2+}-ATPase (0.4-1.0 mg of protein/ml) was carried out at 25 °C for various time intervals and in different media as indicated in the legends to the figures.

2.3.1 Measurement of 1,4-phenylenebismaleimide reaction by filtration

The reaction rate of 1,4-phenylenebismaleimide with sarcoplasmic reticulum vesicles and with solubilized Ca^{2+}-ATPase was measured by filtration on glass fibre filters (GF/F). Sarcoplasmic reticulum vesicles (0.4 mg of protein/ml) were reacted with 12.5 μM [^{14}C]1,4-phenylenebismaleimide in 10 mM CHES/TMAH, pH 8.5, 60 mM KCl and 20% (v/v) glycerol. At 5 min intervals, from 5 min to 1 h, aliquots containing 200 μg of protein were mixed with 5 ml of 5% (w/v) TCA, 0.14 M β-mercaptoethanol and incubated for 15 min at 0 °C. The reactants were then filtered through Whatman GF/F filters and washed with 4 x 5 ml water under a mild vacuum for each time interval. The filters were suspended in 10 ml scintillant for an hour before assaying for radioactivity.

In the case of the reaction with solubilized Ca^{2+}-ATPase the medium in addition contained Triton X-100 (0.2% w/v), 5 mM EGTA and 10 μM thapsigargin. Control experiments were conducted to determine [^{14}C]1,4-phenylenebismaleimide binding to filters and non-specific binding of the crosslinker to sarcoplasmic reticulum vesicles and solubilized Ca^{2+}-ATPase. In case of the former, all reactants were added except the protein and in the latter, 12.5 μM [^{14}C] 1,4-phenylenebismaleimide was quenched first with 0.14 M β-mercaptoethanol.

2.3.2 Reaction of 1,4-phenylenebismaleimide with sarcoplasmic reticulum vesicles for digestion and analysis by HPLC

Sarcoplasmic reticulum (0.4-1.0 mg of protein/ml) were reacted for 45 min with 25 μM 1,4-phenylenebismaleimide in 20% (v/v) glycerol, 60 mM KCl, 10 mM CHES/TMAH, pH 8.5, 50 mM EPPS/TMAH, pH 8.1 or 50 mM EPPS/TMAH, pH 7.8, solubilised in 0.2 % (w/v) Triton X-100, 5 mM EGTA, and 10 μM thapsigargin. The crosslink reaction was quenched with 50 μM β-mercaptoethanol and the unattached reagent was removed by gel filtration on PD-10 columns (Pharmacia), equilibrated and eluted with 25 mM NH_4HCO_3. The eluate was digested with 4% (w/w of sarcoplasmic reticulum protein) trypsin for 30 min or 3 h at 35 °C. The peptides were concentrated using a C18 SepPak cartridge (Waters-Millipore). The peptides were eluted with 1.5 ml 10 mM KPi/60% (v/v) acetonitrile. The acetonitrile concentration was then lowered by blowing nitrogen gas over the surface.

2.4 HPLC purification of the peptides

The concentrated digestion mix was initially separated and fractionated using a Vydac C4 column, and significant radioactive peaks were subsequently purified on a C18 column using a Beckman System Gold High Pressure Liquid Chromatograph (Model: Programmable Solvent Module 126) equipped with a diode array detector (Model: Diode Array Detector Module 168). Solvent A was 10 mM KPi/ pH 5.5 and buffer B 10 mM KPi/ 60% (v/v) acetonitrile. The flow rate was 1ml/ min and the absorbance of the effluent was monitored at 210 and 280 nm simultaneously. The solvent gradient is shown in the figures. Fractions (1ml) were collected and a tenth of the volume assayed for radioactivity. Subsequent C18 purifications were achieved with 1/10 of the phosphate concentration each time. Pure [^{14}C] adducts were concentrated by partial lyophilization and then sequenced . Sequence analysis (standard Edman degradation

and PTH derivatization) was performed by Prof. W. Brandt of the Protein Sequence Facility, Department of Biochemistry, University of Cape Town.

2.5 Gel electrophoresis

2.5.1 SDS-PAGE

SDS-PAGE of solubilized sarcoplasmic reticulum vesicles and 1,4-phenylenebismaleimide modified Ca^{2+} -ATPase was performed according to the method of Laemmli (1970). Each slab gel (1.5 mm thick) consisted of 7% (w/v) acrylogel resolving gel and 3% (w/v) acrylogel stacking gel, at pH's 8.6 and 6.8 respectively. The final concentrations of SDS, Tris/HCl, AMPS and Temed were as in Laemmli, unless otherwise specified. Before loading protein samples on gels, they were solubilized with an equal volume of 0.2 M Tris/HCl, pH 6.8, 2% (w/v) SDS, 8 M urea, 1.4 M β-mercaptoethanol and bromophenol blue. Electrophoresis was carried out at 4 °C using 10 mA for approximately 14 h or until the tracking dye was 10-15 mm from the bottom of the resolving gel.

Gels were removed from the supporting plates, fixed for 20 min in 30% (v/v) methanol/10% (v/v) acetic acid; then stained with Coomasie Brilliant Blue in 30% (v/v) methanol/10% (w/v) trichloroacetic acid for at least 8 h before destaining with 30% (v/v) ethanol/10% (v/v) acetic acid. Further clearing of the background stain was achieved by washing overnight in 7% (v/v) acetic acid and stored in water for at least 24 h before heat/vacuum drying.

2.5.2 Acidic gel system

Electrophoresis, designed for resolving Ca^{2+}-ATPase phosphoprotein was carried out using a positively charged detergent, tetradecyltrimethyl-ammonium bromide (TDAB),

with a 7% (w/v) acrylamide resolving gel and a 4% (w/v) acrylamide stacking gel at pH 2 and 4 respectively according to Amory et. al. (1980). The tank buffer was 0.125% (w/v) TDAB/0.56% (w/v) glycine/H_3PO_4, pH 3. Bisacrylamide concentration of the stacking gel was increased to 2.5% (w/v) and for the resolving gel it remained at 0.35% (w/v), a concentration present in BDH Chemicals Acrylogel 5 Premix. TDAB concentration was 2.3 μM for both gel layers.

Crosslinked protein samples (20 μg of protein) were solubilised in an equal volume of solubilisation buffer (0.25 M sucrose, 0.14 M β-mercaptoethanol, 10 μg/ ml malachite green, 35 mM TDAB and 100 mM KH_2PO_4/H_3PO_4 pH 4) before being loaded onto a gel. Each gel was electrophoresed with 15 mA at 4 °C for 18 h before staining with Coomasie Brilliant Blue in 30% (v/v) methanol/10% (w/v) TCA for approximately 4 h. Destaining proceeded overnight in 30% (v/v) ethanol/10% (v/v) acetic acid, with a final wash of water for at 24 h before being photographed and dried.

2.6 Phosphoenzyme formation

Sarcoplasmic reticulum vesicles (0.5 mg of protein/ml) were incubated at 20 °C in 2 ml of 50 mM TES/TMAH, pH 7.5, 500 mM KCl and 5 mM $CaCl_2$. The reaction was started by adding [γ-^{32}P] ATP to a final concentration of 100 μM. After 10, 20 and 30 s, 500 μl aliquots of the reaction mix were quenched into 5 ml ice-cold 4% (w/v) TCA, 4 mM H_3PO_4. These were allowed to stand for 10 min on ice, then filtered on Whatmann GF/F filters under a mild vacuum on a Millipore apparatus. The filters were subsequently washed with 10 ml ice-cold 3.5% (w/v) TCA, 2 mM H_3PO_4 and another 10 ml wash after the resevoir had been removed. The filters were suspended in 5 ml scintillant for 45 min before assaying for radioactivity. Blanks were performed in the absence of $CaCl_2$ and presence of 2 mM EGTA .

3. RESULTS

It has previously been shown that the reaction of sarcoplasmic reticulum vesicles with glutaraldehyde produces a change in mobility of Ca^{2+}-ATPase on SDS-PAGE such that there is an apparent increase in molecular weight from 110 kD to 125 kD (Ross and McIntosh, 1987). The altered hydrodynamic properties of the protein is the result of an intramolecular crosslink between Lys-492 and Arg-678 (McIntosh, 1992).

The reaction of 1,4-phenylenebismaleimide with sarcoplasmic reticulum vesicles produces a similar change in apparent molecular weight following SDS-PAGE, as well as the formation of dimers (Yamasaki and Yamamoto, 1989). Verification of the results obtained by these researchers using their same conditions are shown in Figure 3.1. In lane 1 of the gel the protein content of sarcoplasmic reticulum vesicles preparation is shown. The major protein is the Ca^{2+}-ATPase (MW 110 kD), followed by calsequestrin (53 kD). Increasing time of incubation with 1,4-phenylenebismaleimide (lanes 2-8) results in the disappearance of the 110 kD Ca^{2+}-ATPase band and the formation of the 125 kD species as well as higher molecular weight forms that are near the top of the resolving gel. The maximum level of the 125 kD species is reached in 30 min and corresponds to approximately 20% of the total ATPase. Thereafter the level remains constant presumably because of intermolecular crosslinking. These results are similar to what was described by Yamasaki and Yamamoto.

We then set out to characterize and optimize the formation of the 125 kD species, which we presumed was also an intramolecular crosslink. In particular we hoped to increase the specificity of the reaction by lowering the concentration of the crosslinker. Parameters that were varied were concentration of the crosslinker, salt, cosolvents like glycerol and dimethylsulphoxide, Triton X-100, thapsigargin (a tight binding inhibitor

of Ca^{2+}-ATPase), as well as pH, temperature and time. Salt, cosolvents and temperature were found to have minimal effects (data not shown). It was found that the concentration of the crosslinker could be lowered substantially with if the pH was raised.

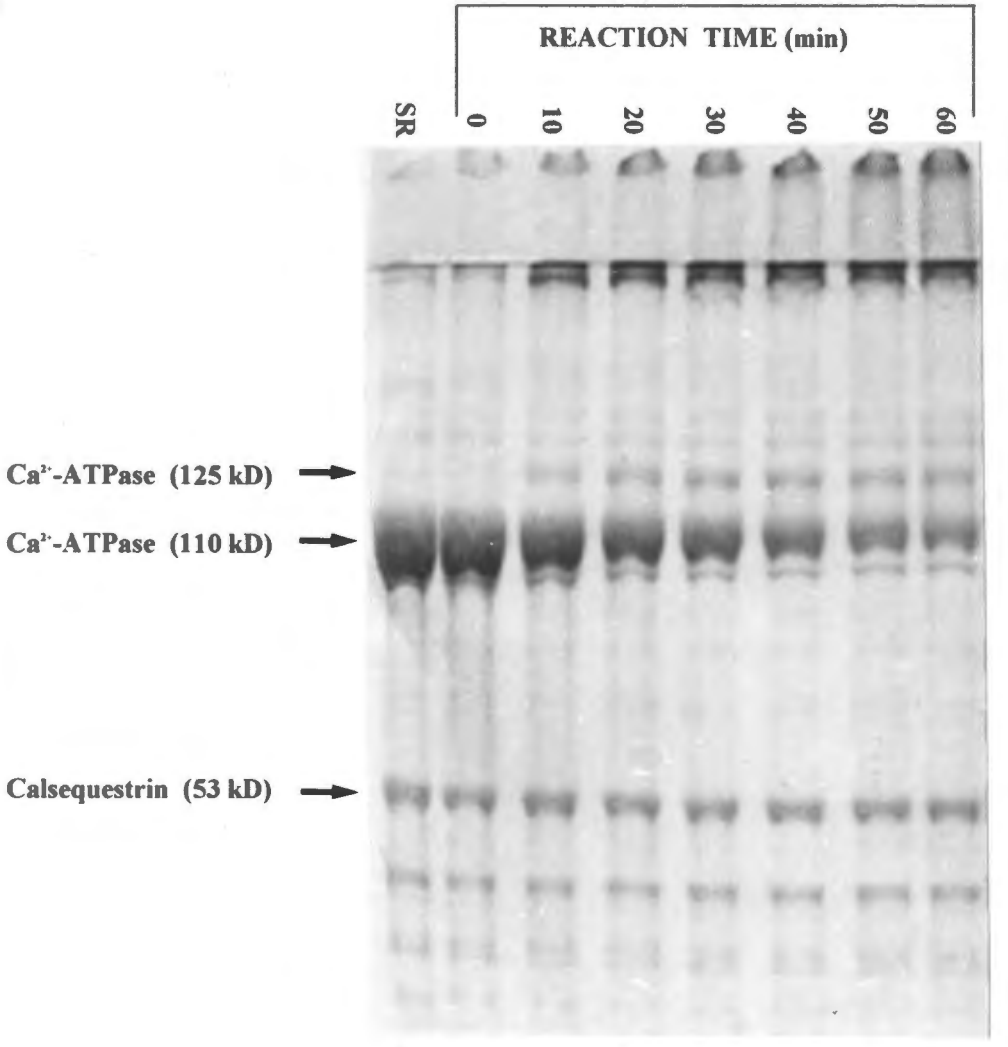

Figure 3.1 SDS-PAGE of the sarcoplasmic reticulum vesicles showing time dependent reaction with 1,4-phenylenebismaleimide. Sarcoplasmic reticulum vesicles (2.5 mg of protein/ml) were reacted with 1 mM 1,4-phenylenebismaleimide in 10 mM Tris/maleate, pH 7, 20% (v/v) glycerol, 60 mM KCl at 25 °C for up to 60 min. Native sarcoplasmic reticulum is shown in the lane labelled SR.

3.1 Optimal pH for the intramolecular crosslink (125 kD species)

The crosslinking reaction was characterized on SDS-PAGE with a reduction of the crosslinker concentration from 1 mM (Yamasaki and Yamamoto, 1989) to 25 μM in the pH range of 6-9.5 at 25 °C. The results following reaction for 10 min and 30 min are shown in Figure 3.2. Increasing pH from 7 to 8.5 resulted in the appearance of the 125 kD species as well as intermolecular crosslinking to dimers and higher molecular weight oligomers. The optimum pH for the intramolecular crosslinking reaction was 8.5 and 8.0 for 10 min and 30 min respectively. It will be shown later that for solubilised Ca^{2+}-ATPase, maximum yield of the intramolecular crosslink was obtained at pH 8.5 and therefore most subsequent experiments have been performed at this pH.

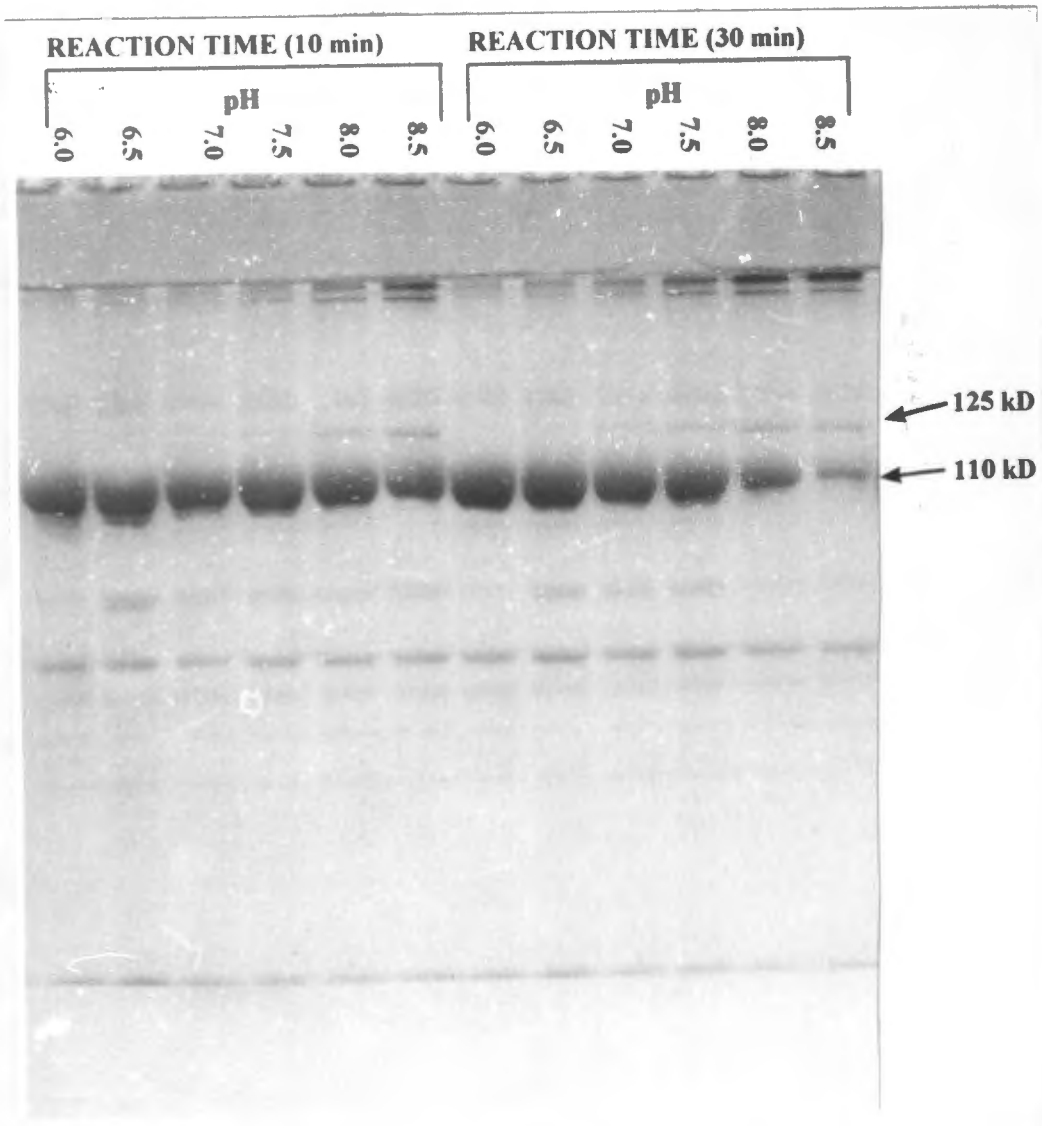

Figure 3.2 The pH dependence of the reaction of 1,4-phenylenebismaleimide with sarcoplasmic reticulum Ca^{2+}-ATPase. Sarcoplasmic reticulum vesicles (0.5 mg of protein/ml) were preincubated at 25 °C for 5 min in 60 mM KCl, 20% (v/v) glycerol, 10 mM MES/TES/MOPS/HEPPSO/HEPES/CHES, pH 6.0/6.5/7.0/7.5/8.0/8.5 prior to reaction with 25 μM 1,4-phenylenebismaleimide for 10 and 30 min. The samples were then subjected to SDS-PAGE.

3.2 Effect of AMPPCP, a non-hydrolysable ATP analogue

The formation of the 125 kD band with 1,4-phenylenebismaleimide was investigated for nucleotide sensitivity, a characteristic of the glutaraldehyde E125 species, using AMPPCP. The sarcoplasmic reticulum vesicles' reaction with the crosslinker in the presence of AMPPCP is shown in Figure 3.3. Formation of the 125 kD band is completely inhibited by 1 mM AMPPCP, as was found by Yamasaki and Yamamoto, 1989. However, contrary to their results in which dimerisation (but not oligomerisation) was enhanced by AMPPNP, another non-hydrolysable ATP analogue, we found that AMPPCP inhibited dimerisation and oligomerisation (Figure 3.3, lanes 7-11). It perhaps suggest that different cysteines are involved in dimer formation at pH 7.0 and pH 8.5 or else nucleotide binding has different effects at these two pHs.

3.3 Effect of iodoacetamide, a sulfhydryl modifying reagent

Iodoacetamide and its flourescent derivative, IEDANS, have been previously used to identify reactive cysteine residues in Ca^{2+}-ATPase (Bishop et al., 1988, Suzuki et al., 1994). The effect of preincubating SR Ca^{2+}-ATPase with iodoacetamide prior to the crosslink reaction with 1,4-phenylenebismaleimide is shown in Figure 3.4. Formation of the 125 kD band and higher molecular weight species is reduced by approximately 50% by prior reaction with iodoacetamide, lanes 7-11, compared with 2-6. Incomplete inhibition by iodoacetamide can be attributed to either (i) slow hydrolysis of iodoacetamide under alkaline conditions (Means and Feeny, 1971) or (ii) partial derivatization of the cysteine residues involved in the crosslink.

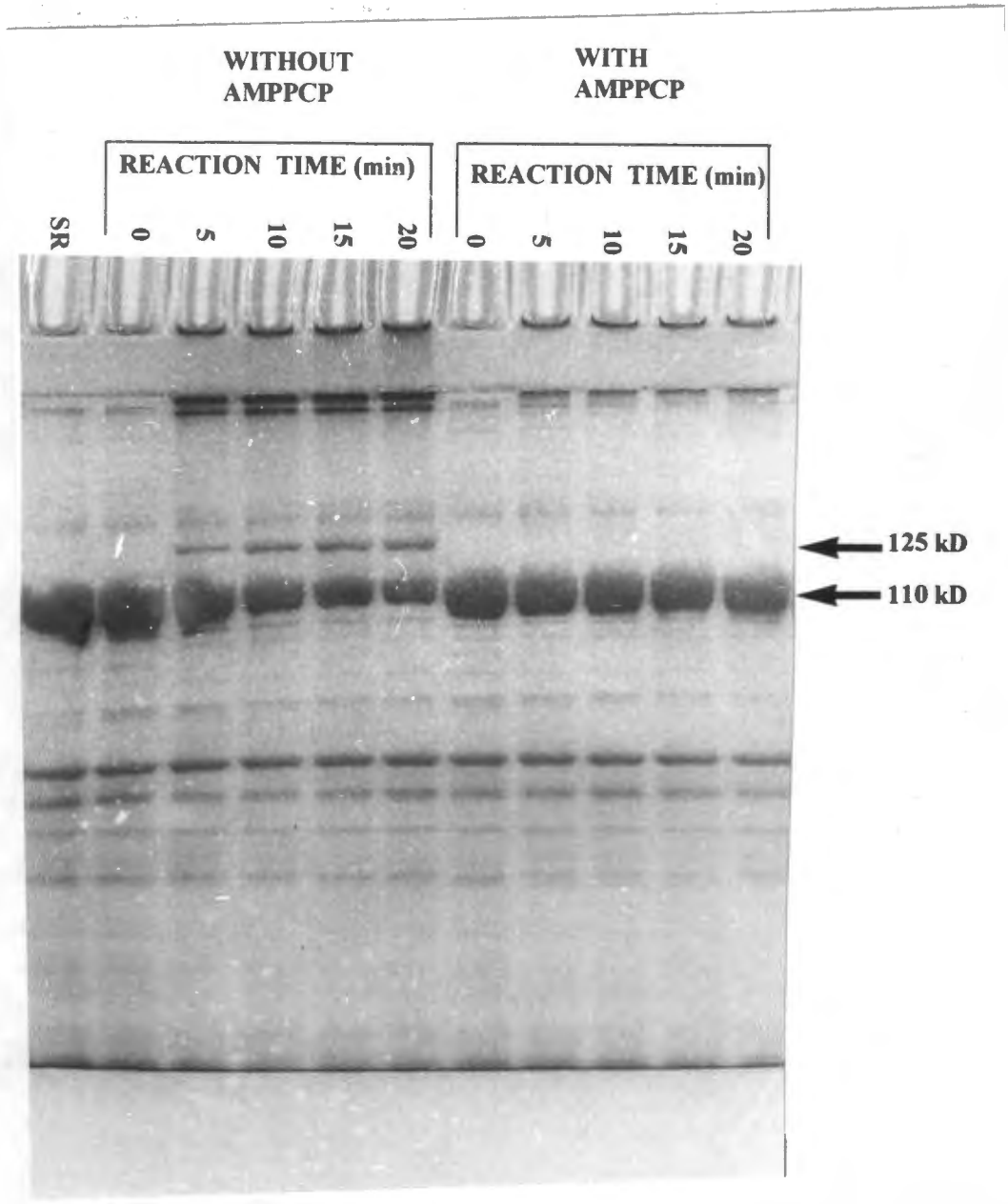

Figure 3.3 Effect of AMPPCP on the formation of the intramolecular crosslink (125 kD species) with 1,4-phenylenebismaleimide. Sarcoplasmic reticulum vesicles (0.5 mg of protein/ml) were preincubated with or without 1mM AMPPCP in 60 mM KCl, 20% (v/v) glycerol, 10 mM CHES/TMAH, pH 8.5 for 5 min at 25 °C. The reaction with 25 μM 1,4-phenylenebismaleimide was stopped at the times indicated. Native sarcoplasmic reticulum preparation is shown in the lane labelled SR.

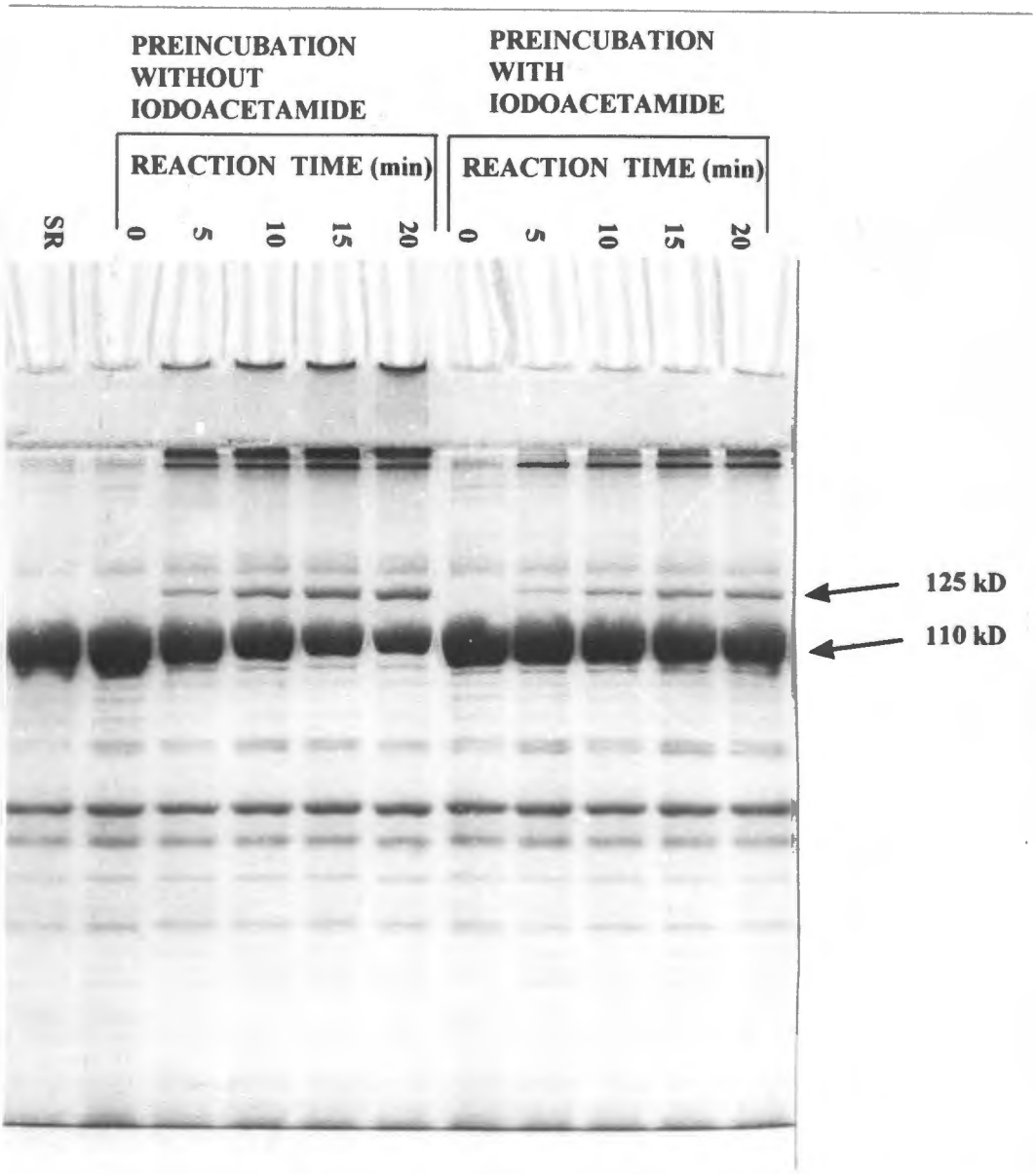

Figure 3.4 Effect of prior chemical reaction of sarcoplasmic reticulum vesicles with iodoacetamide on the crosslink reaction with 1,4-phenylenebismaleimide. Sarcoplasmic reticulum vesicles (0.5 mg of protein/ml) were preincubated without and with 1 mM iodoacetamide in 60 mM KCl, 20% (v/v) glycerol, 10 mM CHES/TMAH, pH 8.5 for 1 h at 25 °C. The crosslink reaction with 25 μM 1,4-Phenylenebismaleimide was then started and stopped at the times indicated for SDS-PAGE. Native Sarcoplasmic Reticulum preparation is shown in the lane labelled SR.

3.4 Effect of a nonionic detergent and thapsigargin on the intramolecular crosslink yield

The effect of sarcoplasmic reticulum vesicles solubilisation with a nonionic detergent was assessed with the aim of minimizing intermolecular crosslink reactions which result in the formation of dimers and higher molecular weight oligomers. In the absence of EGTA (i.e. presence of contaminating calcium, solubilising sarcoplasmic reticulum vesicles with 0.2% (w/v) Triton X-100 reduces intermolecular reactions substantially and an increase of the intramolecular crosslinked specie, 125 kD (figure 3.5, lane B) when compared to without Triton X-100 solubilised sarcoplasmic reticulum vesicles (lane A). Solubilisation also resulted in the formation of a protein band migrating with an apparent molecular weight of 130 kD (lane B). This could be another intramolecular crosslink.

In the presence of EGTA and Triton X-100, the reaction with 1,4-phenylenebismaleimide is much more pronounced (110 kD band completely disappears) and results in the formation of dimers and oligomers (lane 4). This is compatible with the denaturation/aggregation and known instability of the Ca^{2+}-ATPase in nonionic detergent in the absence Ca^{2+} (Møller et. al., 1980; Kosk-Kosicka et.al., 1983; McIntosh and Ross, 1985; McIntosh and Ross, 1988). Thapsigargin has been previously shown to exhibit a stabilizing effect on sarcoplasmic reticulum Ca^{2+}-ATPase under mild denaturing conditions (Davidson and Varhol, 1995). Increasing concentrations of thapsigargin were added to the crosslinking medium in detergent and EGTA and resulted in greatly enhanced levels of 125 kD specie and diminished intermolecular crosslinking (lanes 5-9). The maximum level of 125 kD species and hence stabilization was reached with 10 μM thapsigargin, lane 7, and thereafter the level remained constant. The concentration of Ca^{2+}-ATPase was approximately 2 μM and it appears that a stoichiometry of more than 1:1 thapsigargin:ATPase was required. We estimate that the amount of intramolecular crosslinking approached 50% of the total Ca^{2+}-ATPase. The effects of increasing pH from 7-9.5 on the crosslink reaction was analyzed without and with thapsigargin (Figure 3.6). In the absence of

thapsigargin the dominant reaction at all pH values was dimers and oligomers formation. In the presence of thapsigargin there was a pH dependent increase in the amount of 125 kD species up to pH 8.5 and thereafter oligomer formation dominated, lanes 12 and 13.

3.5 Effects of ATP, ADP and AMP on the intramolecular crosslinks

It has been shown above that the formation the 125 kD species is inhibited by AMPPCP, suggesting active site location. It was of interest to determine whether this also applies to the new intramolecular crosslink of 130 kD form in the presence of Triton X-100 and absence of EGTA (contaminating Ca^{2+})The effects of ATP, ADP and AMP were assessed and the results are shown Figure 3.7. The gel shows that the ATP inhibited both of the intramolecular crosslinks (lane 2), and ADP only on the 125 kD species (lane 3) and AMP neither. This suggests that the new intramolecular crosslink (130 kD species) is in the proximity of the γ-phosphoryl group of ATP and the other crosslink (125 kD species) close to the β-phosphoryl group. However the lack of inhibition by AMP may be due to its poor affinity.

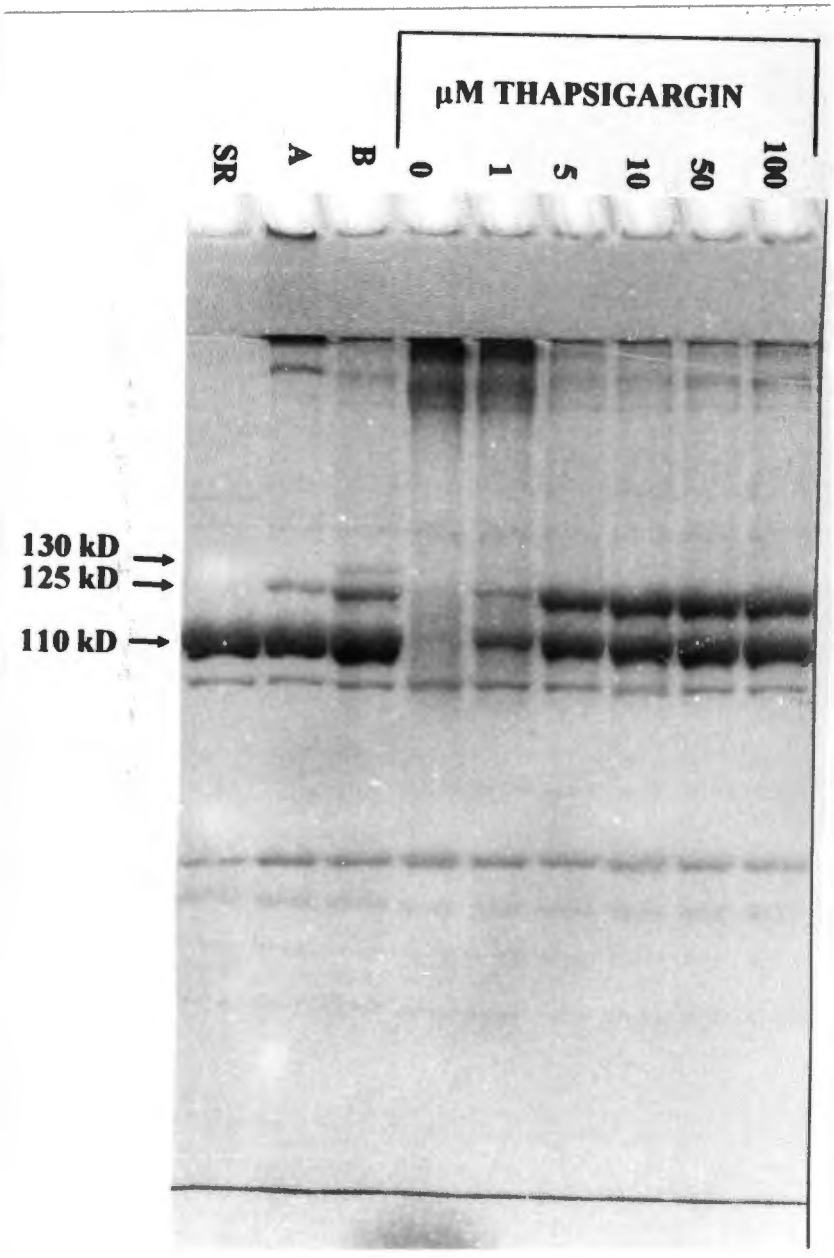

Figure 3.5 Effect of Triton X-100 and thapsigargin on the formation of the intramolecular crosslink and oligomers. Sarcoplasmic reticulum vesicles (0.4 mg of protein/ml) were reacted with 25 μM 1,4-phenylenebismaleimide for 30 min at 25 °C in 60 mM KCl, 20% (v/v) glycerol, 10 mM CHES/TMAH, pH 8.5 (lane A) plus 0.2% (w/v) Triton X-100 (lane B) plus 5 mM EGTA with increasing thapsigargin concentrations, as shown.

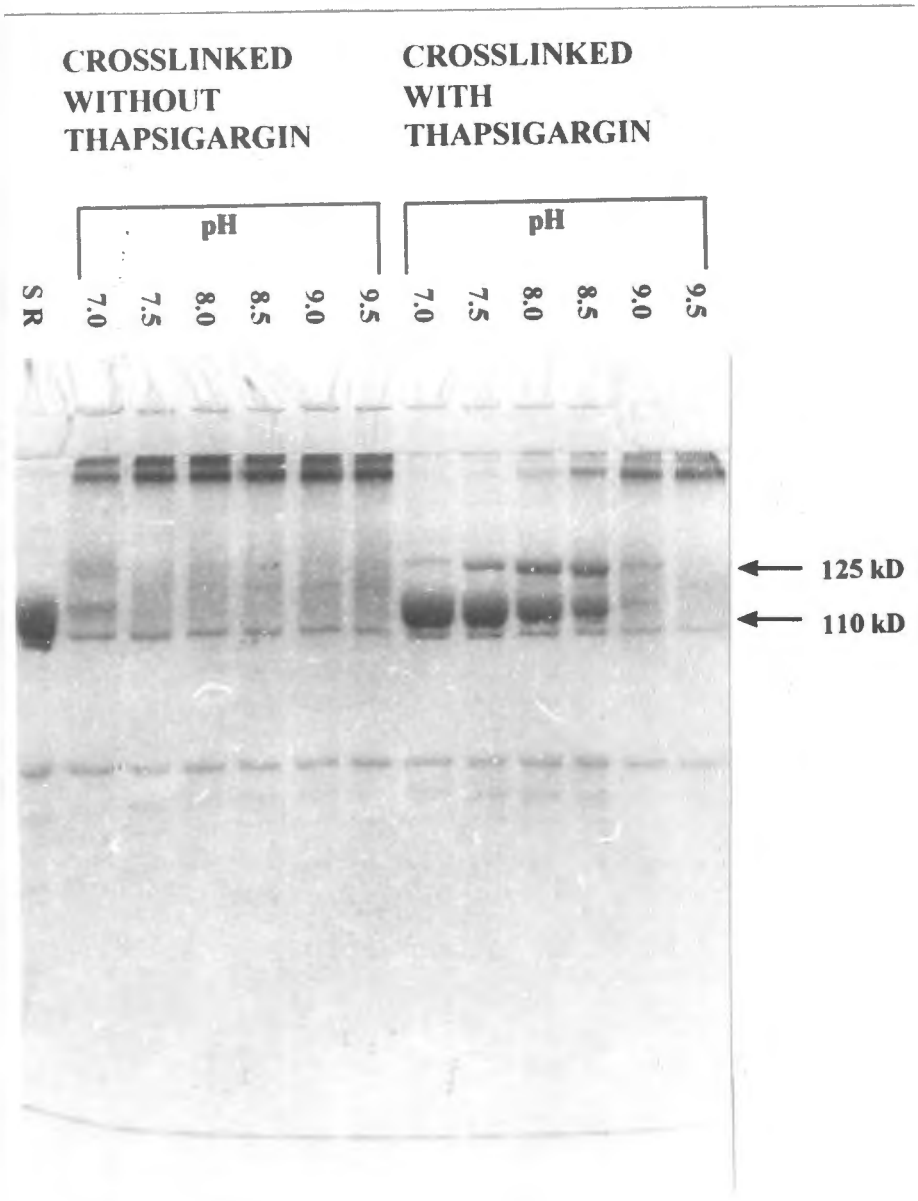

Figure 3.6 The pH dependence of the reaction of 1,4-phenylenebismaleimide with Triton X-100 solubilised Ca^{2+}-ATPase. Sarcoplasmic reticulum vesicles (0.4 mg of protein/ml) were preincubated at 25 °C for 5 min with 0.2% (w/v) Triton X-100, 5 mM EGTA, 60 mM KCl, 20% (v/v) glycerol, 10 mM MOPS/HEPPSO/HEPES/CHES/CHES/CHES, pH 7.0, 7.5, 8.0, 8.5, 9.0, 9.5 without and with 10μM thapsigargin. The reaction with 25 μM 1,4-Phenylenebismaleimide was quenched after 30 min for analysis by SDS-PAGE.

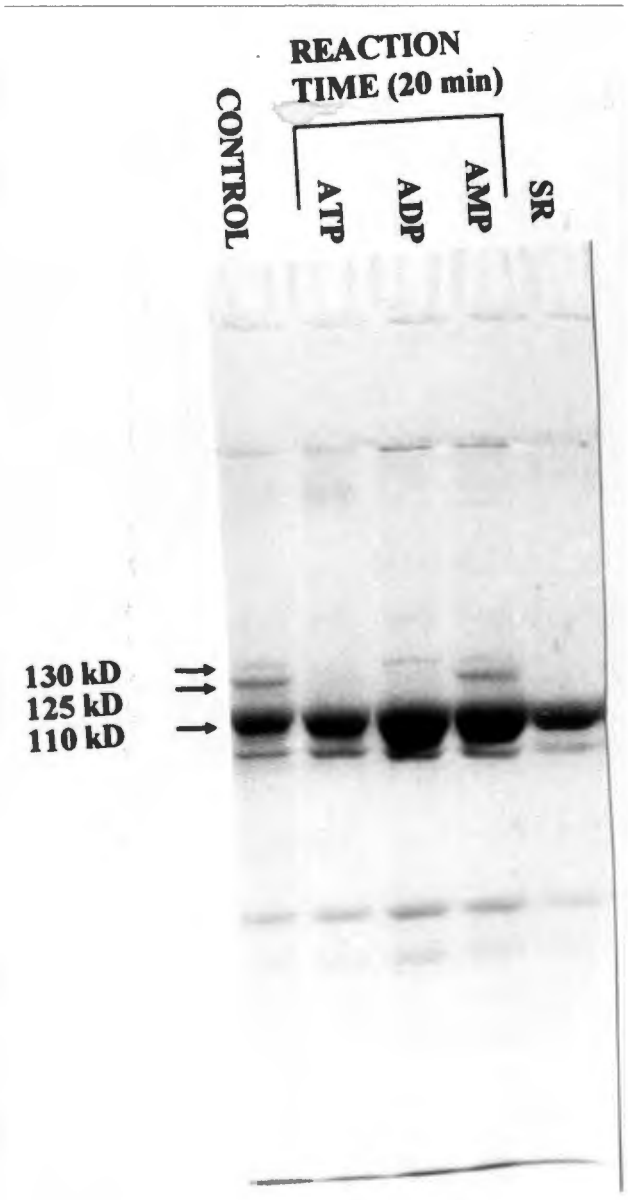

Figure 3.7 Effect of various nucleotides on the formation of the two Triton X-100 associated intramolecular crosslinks with 1,4-phenylenebismaleimide. Sarcoplasmic reticulum vesicles (0.4 mg/ml) were solubilised in 0.2% (w/v) Triton X-100, 60 mM KCl, 20% (v/v) glycerol, 10 mM CHES/TMAH, pH 8.5 with either 1mM of ATP, ADP, AMP or no nucleotide (control). After 5 min preincubation at 25 °C the crosslink reaction with 1,4-phenylenebismaleimide was allowed to proceed for 20 min for SDS-PAGE. Untreated sarcoplasmic reticulum preparation is shown in the lane labelled SR.

3.7 Synthesis, purification and quantitation of [^{14}C]1,4-phenylenebismaleimide

Quantitation of the crosslinking reaction and identification of crosslinked amino acid residues require a radiolabelled reagent as the extinction coefficient of the adduct at 313 nm is too low to be usefully followed by absorbance. The synthesis of [^{14}C]1,4-phenylenebismaleimide was achieved as described in 'Experimental Procedures'. The crude product was brown/black in colour and its HPLC elution profile is shown in Figure 3.8. Essentially a single peak was evident in the 210 nm trace but a few extra smaller peaks appeared at 280 nm. Most of the radioactivity was in the main peak (eluting time, 37 min), which was identified as [^{14}C]1,4-phenylenebismaleimide on the basis of the retention time of cold commercial authentic crosslinker and its spectrum.

Commercial crosslinker is pale brown in colour and we were concerned that the much darker synthesized material contained a significant contaminant that was not apparent in the HPLC trace (none of the peaks appeared to be the black/brown contaminant). It was also desirable to lower the smaller contaminating peaks apparent in the 280 nm trace. Purification was achieved using silica gel chromatography and the black/brown material remained on the column during elution of [^{14}C]1,4-phenylenebismaleimide with acetonitrile. An HPLC elution profile of the purified material is shown in Figure 3.9. The contaminant peaks eluting at around 20 and 60 min on the 280 nm trace were reduced together with the radioactivity associated with them. The calculated concentrations of both the crude and purified [^{14}C]1,4-phenylenebismaleimide using a published extinction coefficient by Wells and Yount as explained in 'Experimental Procedures' were confirmed by comparison of the rate of formation of the 125 kD band with the synthesized crosslinker to that obtained with the commercial reagent. The yield of [^{14}C]1,4-phenylenebismaleimide was 68.4% based on the radioactivity, and 76.8% based on the phenylene content, and the specific activity was 2295 cpm/nmol.

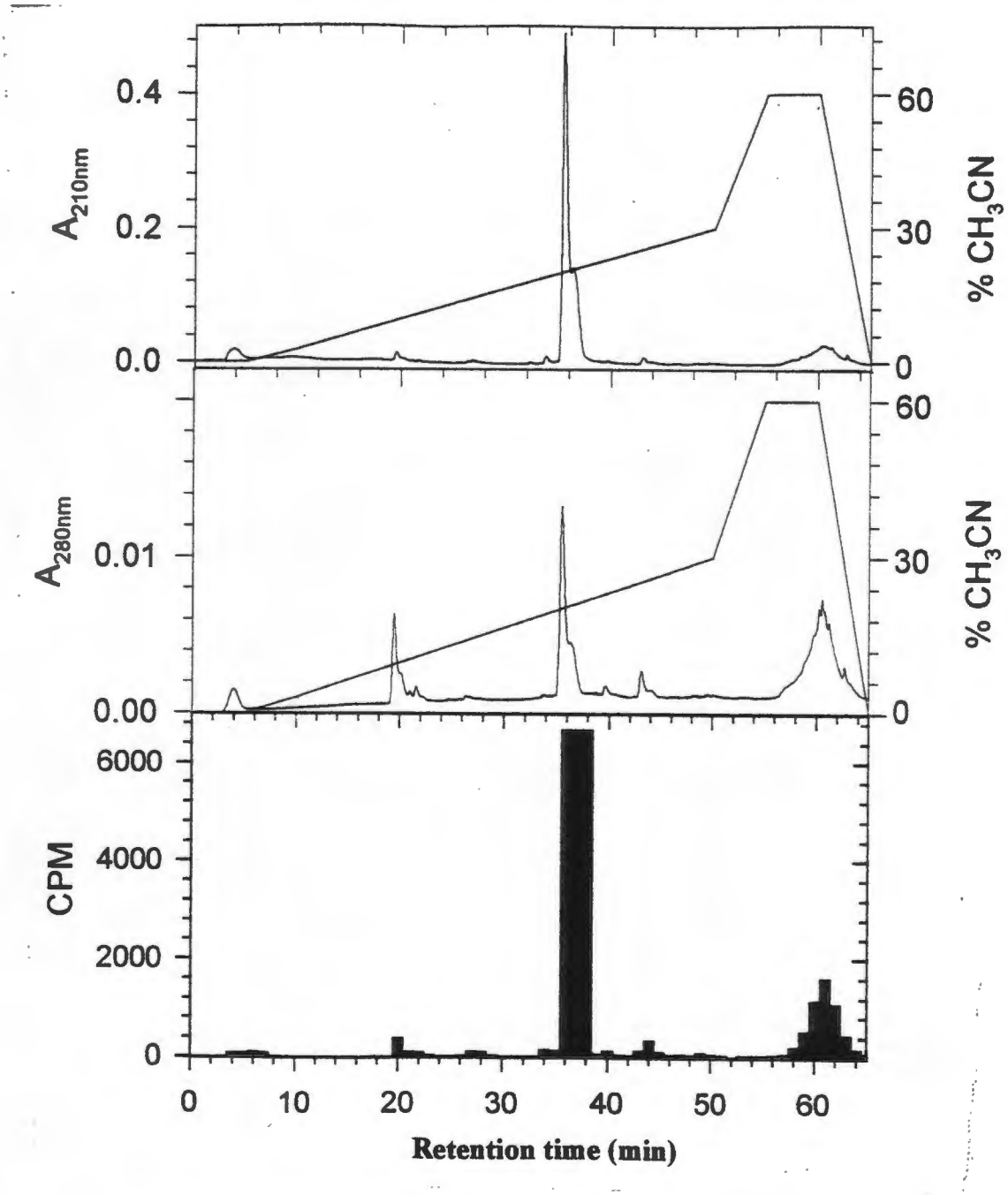

Figure 3.8 HPLC of crude synthesized [^{14}C]1,4-phenylenebismaleimide. The crosslinker was subjected to HPLC on a vydac C18 column with solvent A as 10 mM KPi, pH 5.5 and solvent B 10 mM KPi/60% (v/v) acetonitrile. The elution was monitored at 210 and 280 nm. Fractions were collected at 1 min intervals and assayed for radioactivity.

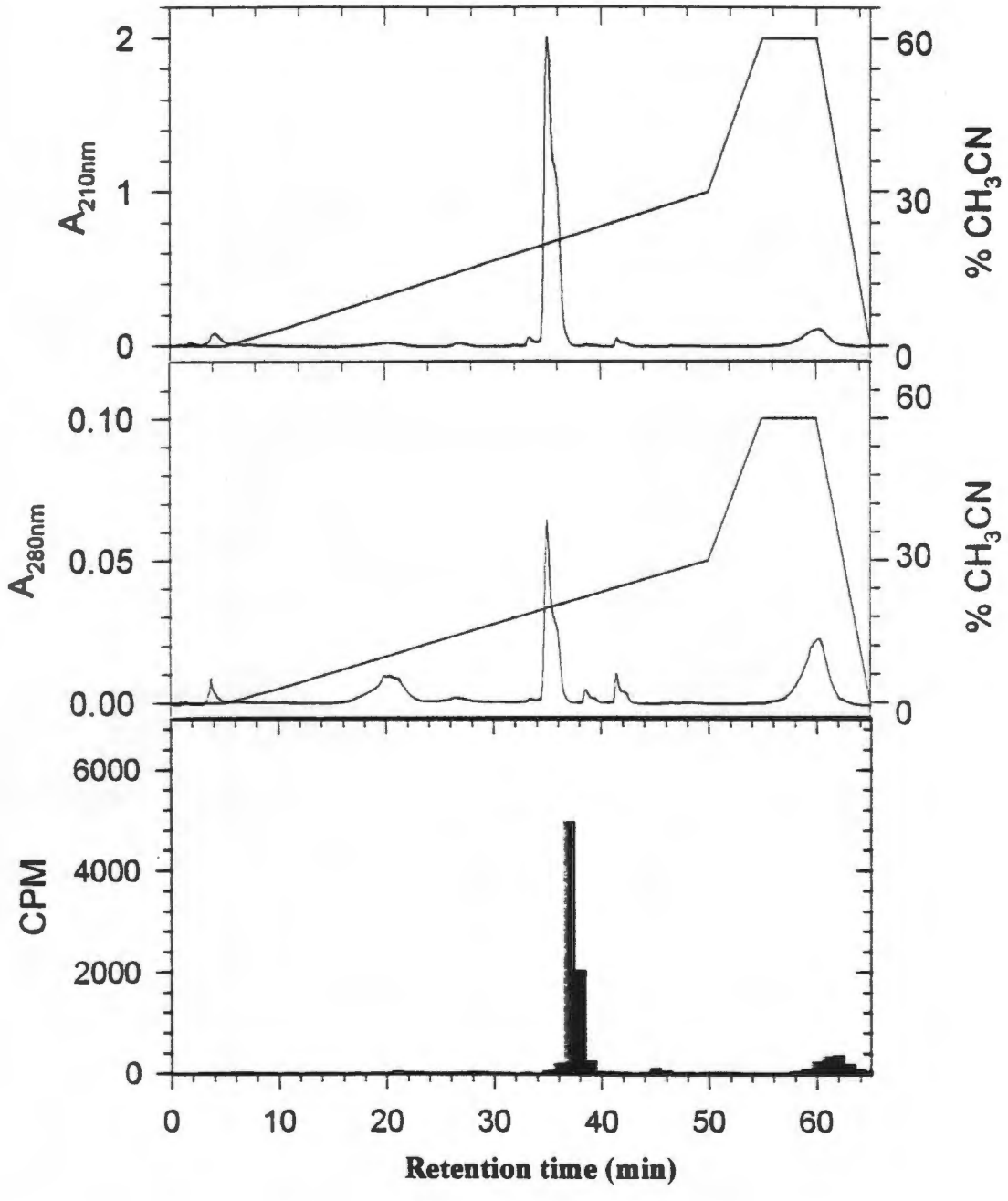

Figure 3.9 HPLC of silica gel column purified [^{14}C]1,4-phenylenebismaleimide. The purified crosslinker was subjected to HPLC on a vydac C18 column with solvent A as 10 mM KPi, pH 5.5 and solvent B 10 mM KPi/60% (v/v) acetonitrile. The elution was monitored at 210 and 280 nm. Fractions were collected at 1 min intervals and assayed for radioactivity.

3.8 Filtration assays

The extent of derivatisation of sarcoplasmic reticulum vesicles by 1,4-phenylenebismaleimide under optimal conditions determined in the preceding sections was measured using the radiolabelled crosslinker and a filtration procedure (Figure 3.10). In panel A, the reaction was performed with sarcoplasmic reticulum vesicles in the absence of detergent, conditions under which intermolecular crosslinking dominate and the intramolecular crosslink is about 10% of the total protein (see Figure 3.4, lanes 2-6 for SDS-PAGE, note the crosslinker concentration is double). The reaction is biphasic, there is a fast reaction (< 30 sec) to the extent of 5 nmol/mg of protein (i.e. approximately 1 mol crosslink/mol ATPase) followed by a slower phase of 5-7 nmol/mg protein over 1h. The presence of AMPPCP lowered the extent of the fast reacting component but made little impact on the slow component.

In panel B, the reaction is measured under optimal conditions for the formation of the intramolecular crosslink and minimal amount of intermolecular crosslinking. Again, in the absence of AMPPCP, the reaction is biphasic with a rapid phase up to 2 nmol/mg of protein and a large slower phase of 10 nmol/mg of protein over 30 min. In the presence of the nucleotide the rapid phase disappeared and the slower phase was similar to that in its absence.

The amount of Ca^{2+}-ATPase in these preparations is approximately 4 nmol/mg of protein (based on maximum phosphoenzyme levels) and thereafter we can expect approximately 2 nmol 1,4-phenylenebismaleimide/mg of protein to be associated with the intramolecular crosslink, since about 50% of the ATPase is 125 kD species (in detergent). The above filtration results suggest that several sulfhydryl groups (up to 4) are being modified. It was surprising that the nucleotide did not alter the kinetics of the slow phase, but rather the fast phase. One possible explanation is that one of the

sulfhydryl groups involved in the crosslink is extremely reactive and the reaction with the second one (to form the crosslink) is much slower.

3.9 Trypsin digestion of crosslinked sarcoplasmic reticulum Ca^{2+}-ATPase

It has been shown previously that low concentrations of trypsin cleave the sarcoplasmic reticulum Ca^{2+}-ATPase (110 kD) at Arg-505 to produce a 55 kD A fragment and a 54 kD B fragment, and to a lesser extent at Arg-798 leading to a 33 kD A1 and 22 kD A2 fragments (MacLennan et.al., 1985). Tryptic digestion of the glutaraldehyde intramolecular crosslinked sarcoplasmic reticulum Ca^{2+}-ATPase produces an apparent increase in the molecular weight from 125 to 135 kD on SDS-PAGE, which is a characteristic of a crosslink between the A (Lys-492) and B (Arg-678) tryptic fragments (Ross and McIntosh, 1986; McIntosh, 1992). We then characterized the intramolecular crosslink of 1,4-phenylenebismaleimide with trypsin digestion on SDS-PAGE as shown in Figure 3.11. Digestion of native sarcoplasmic reticulum vesicles, lanes 2-4, show a single band at 55 kD consistent with the A and B fragments. Reaction of 1,4-phenylenebismaleimide with sarcoplasmic reticulum vesicles under the conditions chosen produced approximately 20 % 125 kD species plus a dimer band and higher oligomers (lane 5). Trypsin digestion produced a band of A+B fragments (from the 110 kD native ATPase) and a 135 kD band (presumably from the 125 kD species) consistent with a crosslink between A and B tryptic fragments, lanes 6-8.

We have shown above (Figure 3.5) that the reaction of 1,4-phenylenebismaleimide with solubilised Ca^{2+}-ATPase in the absence of EGTA (contaminating Ca^{2+}) produces two intramolecularly crosslinked species of 125 kD and 130 kD. This is shown again in lane 9. Digestion of the solubilised Ca^{2+}-ATPase results in the formation of both 135 and 140 kD (as well as 54/55 kD species) consistent with both intramolecular crosslinks connecting residues between fragments A and B.

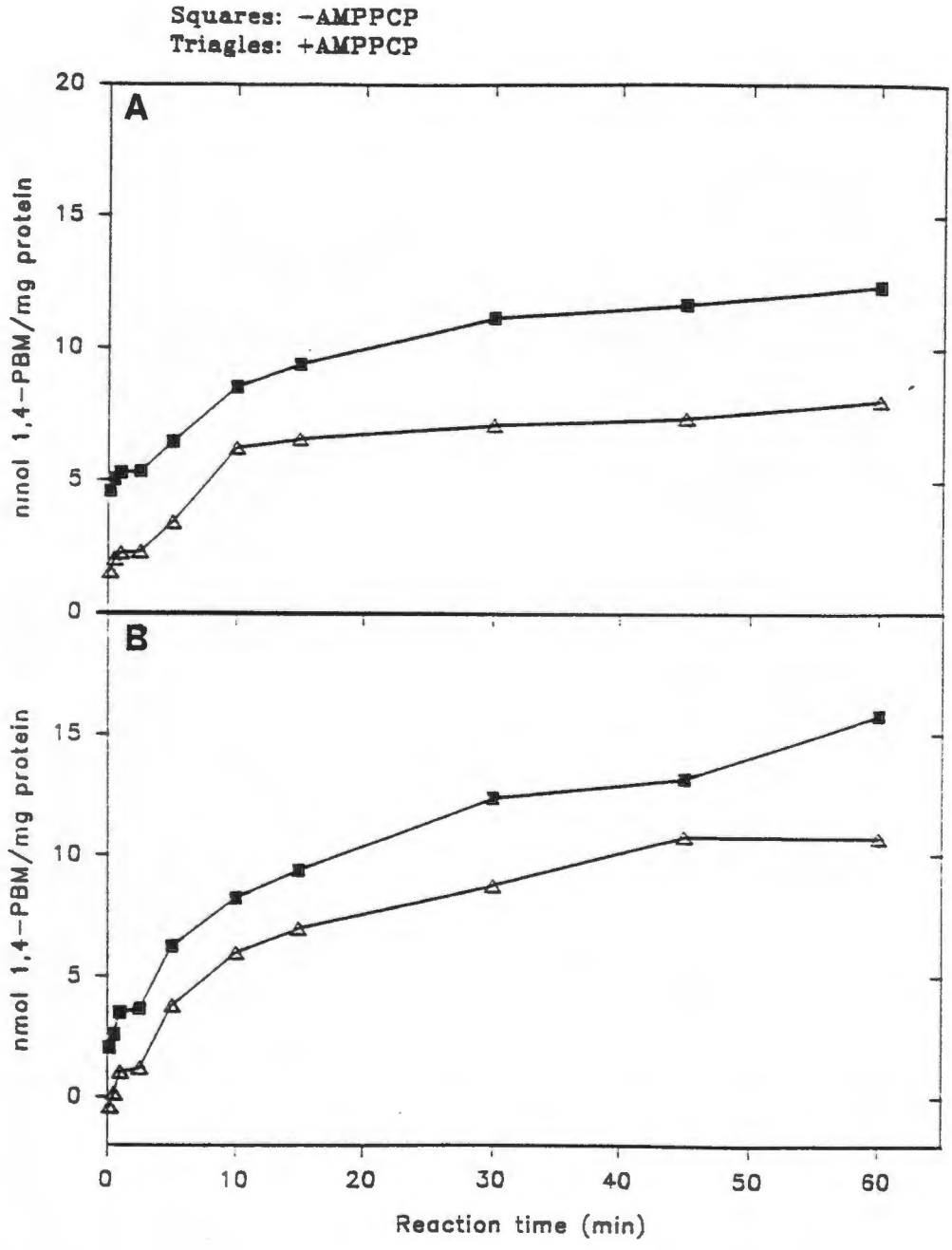

Figure 3.10 Reaction of [^{14}C]1,4-phenylenebismaleimide with sarcoplasmic reticulum vesicles measured by filtration. The reaction of 12.5 μM [^{14}C]1,4-phenylenebismaleimide at 25 °C with sarcoplasmic reticulum vesicles (0.4 mg of protein/ml) in (A) 60 mM KCl, 20% (v/v) glycerol, 10 mM CHES/TMAH, pH 8.5 with or without 1 mM AMPPCP (B) 60 mM KCl, 20% (v/v) glycerol, 10 mM CHES/TMAH, pH 8.5, 0.2% (w/v) Triton X-100, 5 mM EGTA, 10 μM thapsigargin with or without AMPPCP. The reactions were quenched with ice cold 5% (w/v) trichloroacetic acid, 0.14 M β-mercaptoethanol and allowed to stand for 15 min, filtered on GF/F filters (Whatman) and washed with 20 ml H_2O. The filters were suspended in the scintillant for 1 hour prior to assaying for radioactivity. Blanks in which 50 μM β-mercaptoethanol was added prior to the vesicles were subtracted for each of the time points.

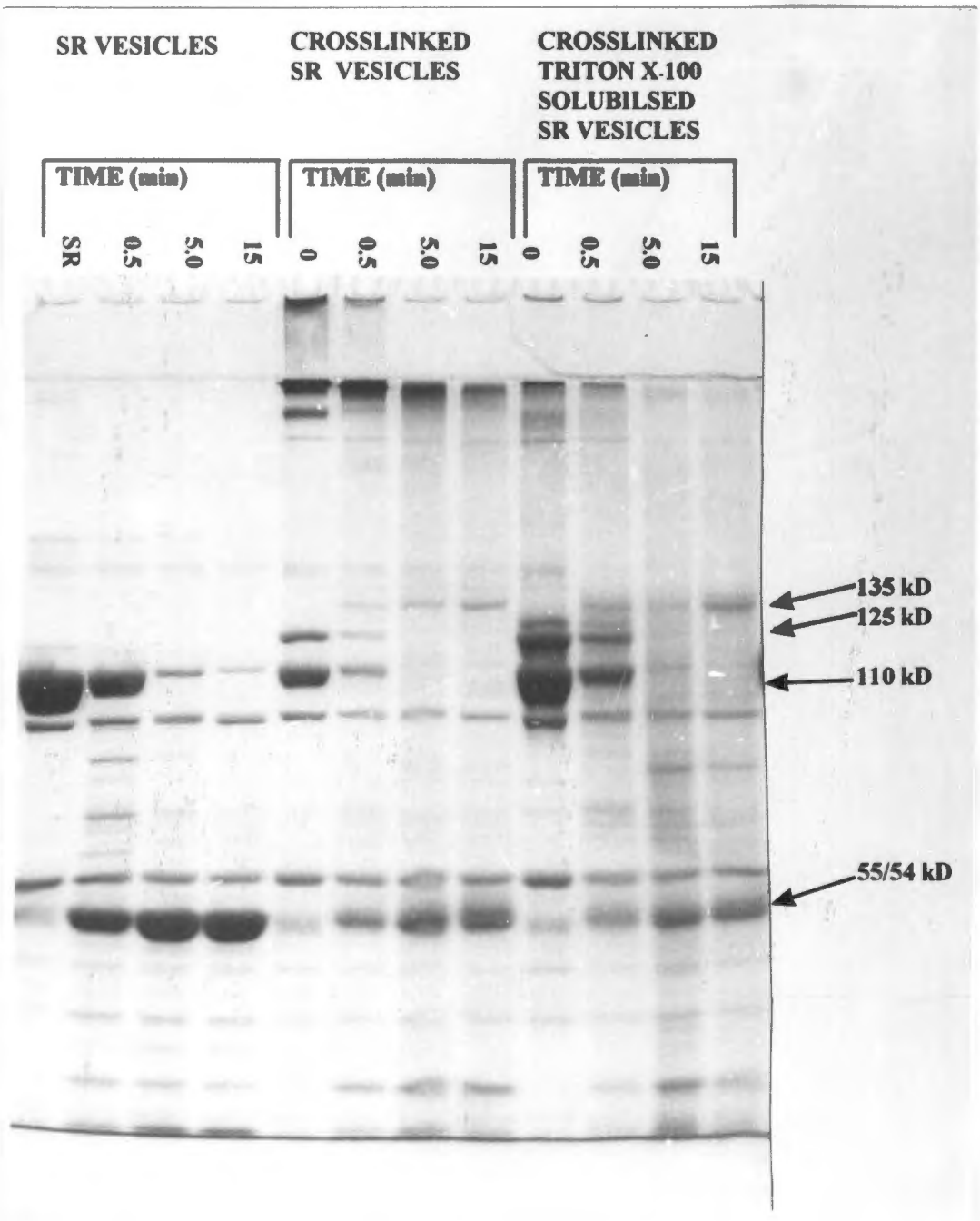

Figure 3.11 Tryptic digestion of native and crosslinked Ca^{2+}-ATPase. Sarcoplasmic reticulum vesicles (0.4 mg of protein/ml) were prereacted with 25 μM 1,4-phenylenebismaleimide at 25 °C for 30 min in 60 mM KCl, 20% (v/v) glycerol, 10 mM CHES/TMAH, pH 8.5 with and without 0.2% (w/v) Triton X-100 as indicated. The reaction was stopped with β-mercaptoethanol and then digested with 1:200 trypsin/SR protein for the times indicated.

3.10 Electrophoresis on an acidic gel system

Crosslinking Lys-492 and Arg-678 with glutaraldehyde stabilizes E1~P with occluded Ca^{2+} (Ross, Davidson and McIntosh, 1991). The protein is readily phosphorylated with small substrates such as acetyl phosphate, but high concentrations of ATP (affinity changes a 1000X) are needed to produce the same level of E1-P. It was of interest to determine whether the 1,4-phenylenebismaleimide crosslinked enzyme similarly stabilized E1-P. The relatively low level of crosslinked species precluded direct activity measurements. We considered that it would be desirable to assess phosphoenzyme levels of the 110 kD and 125 kD species individually. Phosphoenzymes are unstable under conditions usually employed in Laemmli SDS-PAGE (i.e. pH 8.6). We therefore attempted to resolve the two species in acidic gels according to the method of Amory et.al., 1980 (i.e. pH 2.0).

Under the conditions used, the native Ca^{2+}-ATPase band migrated well into the gel. If we look at the glutaraldehyde treated preparation first (Figure 3.12, lanes 8-12), we see that reaction with the crosslinker resulted in the production of a species of slightly lower apparent molecular weight (labelled intralink) as well as other bands which migrated further. Unexpectedly, it appears that the apparent molecular weight of the intramolecularly crosslinked ATPase is reversed compared to pH 8.6. The results obtained with 1,4-phenylenebismaleimide treated Ca^{2+}-ATPase is shown in lanes 2-6. However Ca^{2+}-ATPase intramolecularly crosslinked with 1,4-phenylenebismaleimide was either not distinguishable from the native protein or the intramolecular crosslink with the phenylenebismaleimide was unstable at such low pH values (the resolving gel was at pH 2). Similar to the glutaraldehyde treated protein, the reaction with 1,4-phenylenebismaleimide also induced cleavage of the protein, although to a lesser extent.

3.11 Intramolecular crosslink stability at pH 2.0

In order to determine whether the 1,4-phenylenebismaleimide intramolecularly crosslinked Ca^{2+}-ATPase was due to instability at low pH values, the effect of incubating the 1,4-phenylenebismaleimide reacted sarcoplasmic reticulum Ca^{2+}-ATPase at pH 2.0 over 4h is shown in Figure 3.13. Lane 2, labelled control A is the 1,4-phenylenebismaleimide reacted protein that was kept on ice for 4h after 30 min reaction at 25 °C. There was no marked effect of incubation at pH 2.0 compared with pH 8.5 (compare lanes 6 and 7). In both cases the 110 and 125 kD bands appeared to become a bit more diffuse but the amount of each was not much changed. This result suggest that the crosslink is not particularly unstable at acid pHs.

3.12 Identification of derivatized amino acid residues

In the initial experiments designed to identify labelled amino acid residues crude [^{14}C]1,4-Phenylenebismaleimide was used since a purification method had not been developed. Preliminary experiments indicated that background radioactivity was rather high and resolution of individual peaks required an unusually long elution time. We found that a 4h gradient produced a well spread out peptide profile and reasonable resolution of radioactive peaks. An example of a 3h trypsin digestion of sarcoplasmic reticulum vesicles (10 mg) derivatized under optimal conditions for production of the intramolecular crosslink in Triton X-100 (pH 8.5) is shown in Figure 3.14. The HPLC profile shows a good spread of peptide peaks as well as radioactive peaks but with quite a high background level of radioactivity. The main radioactive peaks are labelled 1-12. The last peak is the result of the steeper gradient after 200 min. Otherwise, no single peak dominated, as might be expected from the results of Figure 3.10, suggesting several reactive sulfhydryls. We selected the larger peaks 3 and 8 for further purification and possible sequencing. The purifications are shown in Figure 3.19. The two radioactive peaks were sequenced. The amino acids sequencing information for all peptides is shown in Table 3.1 (page 64). Peak 3 yielded the sequence ANA(C)NSVIR and peak 8 contained no amino acid residues. The former comes from the native

sequence ^{465}VERANACNSVIRQLMK^{480}. No other sequence was evident that could suggest the crosslink.

Rather than pursuing lesser peaks, it was decided to purify the crude [^{14}C]1,4-phenylenebismaleimide and see if the profile changed. It was also desirable to see which peaks were sensitive to nucleotide binding. An HPLC profile with purified [^{14}C]1,4-phenylenebismaleimide in the absence and presence of 1 mM AMPPCP with 2 mg of protein and at pH 8.5 is shown in Figures 3.15 and 3.16 respectively. The profile in the absence of AMPPCP is fairly different from the one obtained before except for clusters of radioactivity at 60 and 150 min. The main radioactive peaks are labelled 1-5. In the presence of AMPPCP there was much less radioactivity in general and most of this decrease was in the 150 min cluster. Peaks 1, 2 and 4 were purified further (Figure 3.20) and the radioactive peaks were submitted for sequencing. The low level of peptide did not permit definitive conclusions, but peak 1 appeared to be made up of peptides EA(C)R and A(C)(C)FAR from the native sequence ^{660} DLPLAEQREACRRACCFARVEPSHK^{684}. These cysteines are known to be reactive to IEDANS and iodoacetamide (Baba et. al., 1986). Peak 2 yielded the sequence IVETLQS which is just beyond the above sequence and there are no cysteines for 87 residues suggesting that the radioactive peptide, if present, in a smaller amount and not seen. Peak 4, the main peak, yielded two sequences of approximately equal amounts, namely STEE(C)LAY and SLPSV(E)(T)L. The former is very close to the amino terminal end of the protein and has been labelled before by NEM (Reithmeyer and MacLennan, 1981). The latter is from the sequence ^{335}SLPSVETLGCTSVICSD^{351} where the first cysteine, Cys-344, is well labelled with N-ethylmaleimide (Kawakita and Yamashika, 1987)). Both fragments are in the A primary tryptic cleavage product and therefore cannot be the intramolecularly crosslinked residues (shown above to be between primary tryptic fragments A and B. Rather than purify and sequence relatively minor peaks 3 and 5, it was decided to repeat the reaction with more protein.

At this stage we were worried about the stability of the adduct and decided to decrease the digestion time from 3 h to 30 min. The pH of the crosslink medium was lowered to pH 8.5 to 7.8 to try and decrease the level of background radioactivity and

perhaps increase specificity. The results are shown in Figure 3.17. Unexpectedly the HPLC profile was somewhat different from before with major peaks at 70, 90 and 150 min (labelled 2, 3 and 6). Purification of peak 2 (Figure 3.21) resulted in the radioactivity not binding to C18 column. It was decided to sequence this fraction as at least 4 major species had been separated from it. However sequencing revealed several possible peptides, with SMSVY(C)SP as the major species. It was more plentiful than any other sequence and therefore did not appear to be crosslinked. Further purification of this peak resulted in several peptide peaks but none appear to be associated with radioactivity.

Peak 3 yielded two radioactive peaks with most of the radioactivity centered on a peak with a high 280 nm absorbance and sequencing indicated TGTLTTNQ which comes from the native sequence ^{351}DKTGTLTTNQMSVCK^{365} where Cys364 is known to be reactive with N-ethylmaleimide (Kawakita and Yamashika, 1987). Peak 6 purified as a single radioactive peak (Figure 3.21) and yielded two sequences SLPSVETL and GVYEKVGE which derive from ^{330}NAIVRSLPSVETLGCTSVICSD^{351} , as seen above and where Cys344 is known to be N-ethylmaleimide reactive and ^{427}FNETKGVYEKVGEATETALTLVEKMNVFNTEVRNLSKVERANACNS^{473} . These two sequences were present in approximately equal amounts and may be crosslinked. They are both in the A primary tryptic fragment and therefore unlikely to be the intramolecular crosslink seen on gels as the 125 kD species. It seems more likely that the GVYEKVGE peptide is a contaminant, since the fragment would have to be as long as that shown in order for cysteines to be linked and there are several intervening lysines and arginines as tryptic targets.

Minor peak 1(Figure 3.17) has a similar retention time to that sequenced in Figure 3.15, relating to the REACRRACCFAR sequence and was not processed further. Minor peak 4 purified as a single component but yielded no sequence. Minor peak 5 yielded the sequence STEE(C)L, seen before, as is close to the N-terminal amino acid. Minor peak 7, 8 and 9 were purified but separated into several radioactive components and they were not sequenced.

Repeating the above experiment at pH 8.1, rather than pH 7.8, provided the HPLC profile shown in Figure 3.18. The higher pH resulted in enhanced overall labelling, similar to that obtained at pH 8.5 (Figure 3.14). The profile is also similar to the latter experiment, with the most significant peaks in the region 60 to 130 min. Prominent peaks 1 and 4 were purified but yielded no sequence. The latter corresponds to peak 8 of Figure 3.14, which also gave no sequence. Peak 2 provided ANA(C)NSV as the major product, identifying it as equivalent to peak 3 of Figure 3.14. Peak 3 was aligned with peak 3 of Figure 3.17, which had the sequence beginning with TGT associated with Cys 364, and was not persued again. Peaks 6 and 7 were aligned with peak 4 of Figure 3.15, associated ;with Cys 12 and Cys 344, and were not sequenced. Peak 5, 8 and 9 seemed less significant and were not processed further.

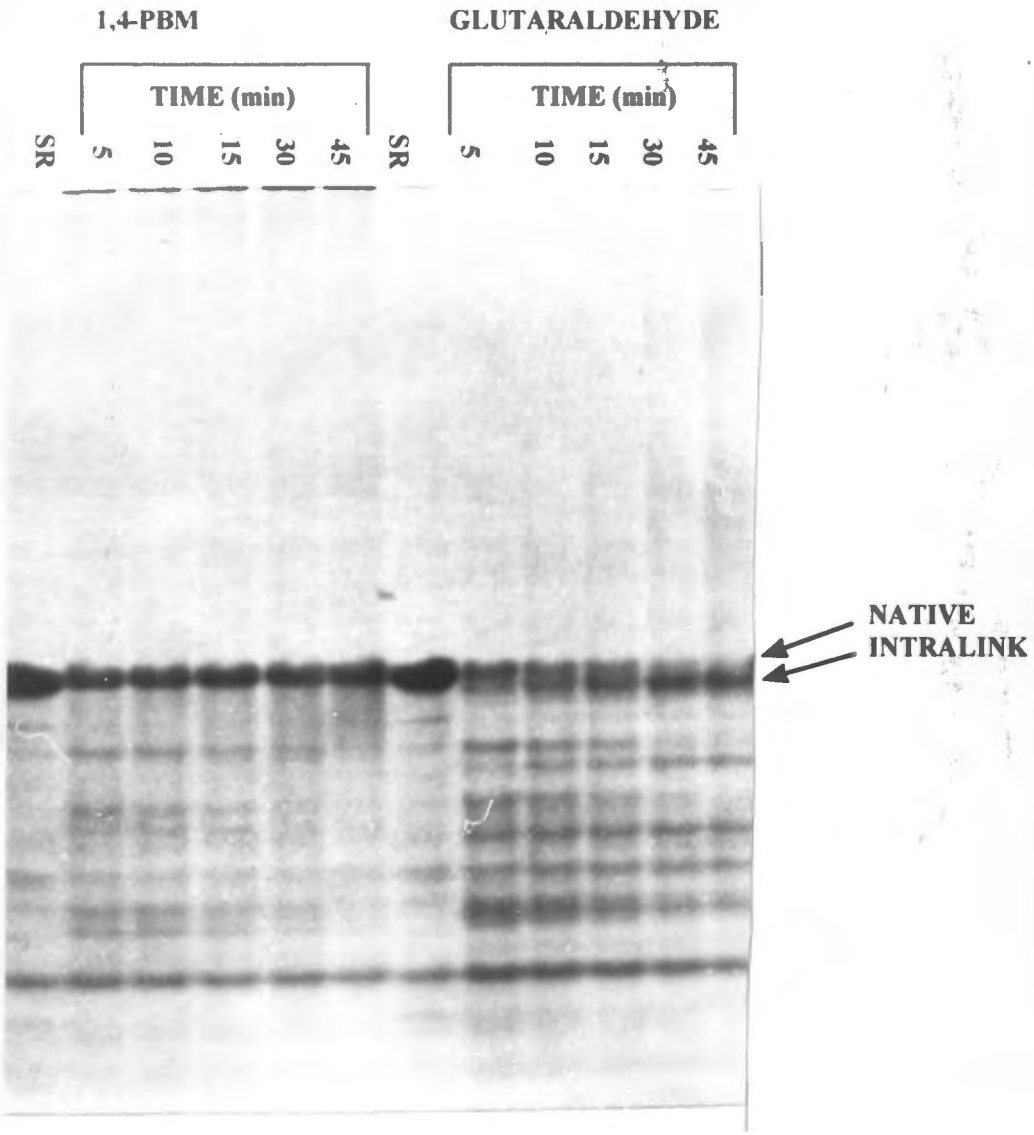

Figure 3.12 Reaction of glutaraldehyde and 1,4-phenylenebismaleimide with sarcoplasmic reticulum vesicles on an acid (pH 2.0) gel. Sarcoplasmic reticulum vesicles (0.5 and 0.4 mg of protein/ml) were reacted at 25 °C with 300 μM glutaraldehyde in 10 mM KCl, 50 μM $CaCl_2$, 0.2 M sucrose, 30 mM MOPS/TMAH, pH 8.1 and 25 μM 1,4-phenylenebismaleimide in 60 mM KCl, 20% (v/v) glycerol, 10 mM CHES/TMAH, pH 8.5 at the times indicated respectively.

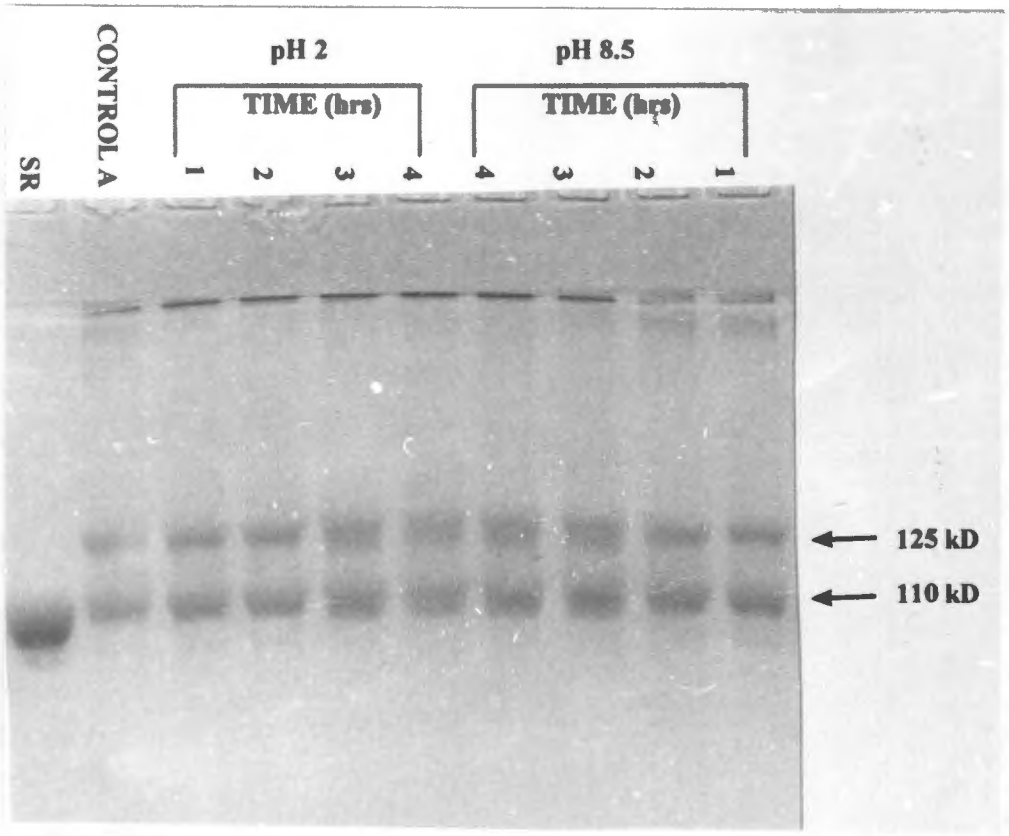

Figure 3.13 Stability of the intramolecular crosslink at pH 2.0. Sarcoplasmic reticulum vesicles were crosslinked with 25 μM 1,4-phenylenebismaleimide for 30 min at 25 °C in 60 mM KCl, 20% (v/v) glycerol, 10 mM CHES/TMAH, pH 8.5, 0.2% (w/v) Triton X-100, 5 mM EGTA, 10 μM thapsigargin (control A). The reaction was stopped with β-mercaptoethanol and then the vesilces incubated at 25 °C for the times indicated in either 50 mM KH_2PO_4/H_3PO_4, pH 2.0 or 50 mM CHES/TMAH, pH 8.5.

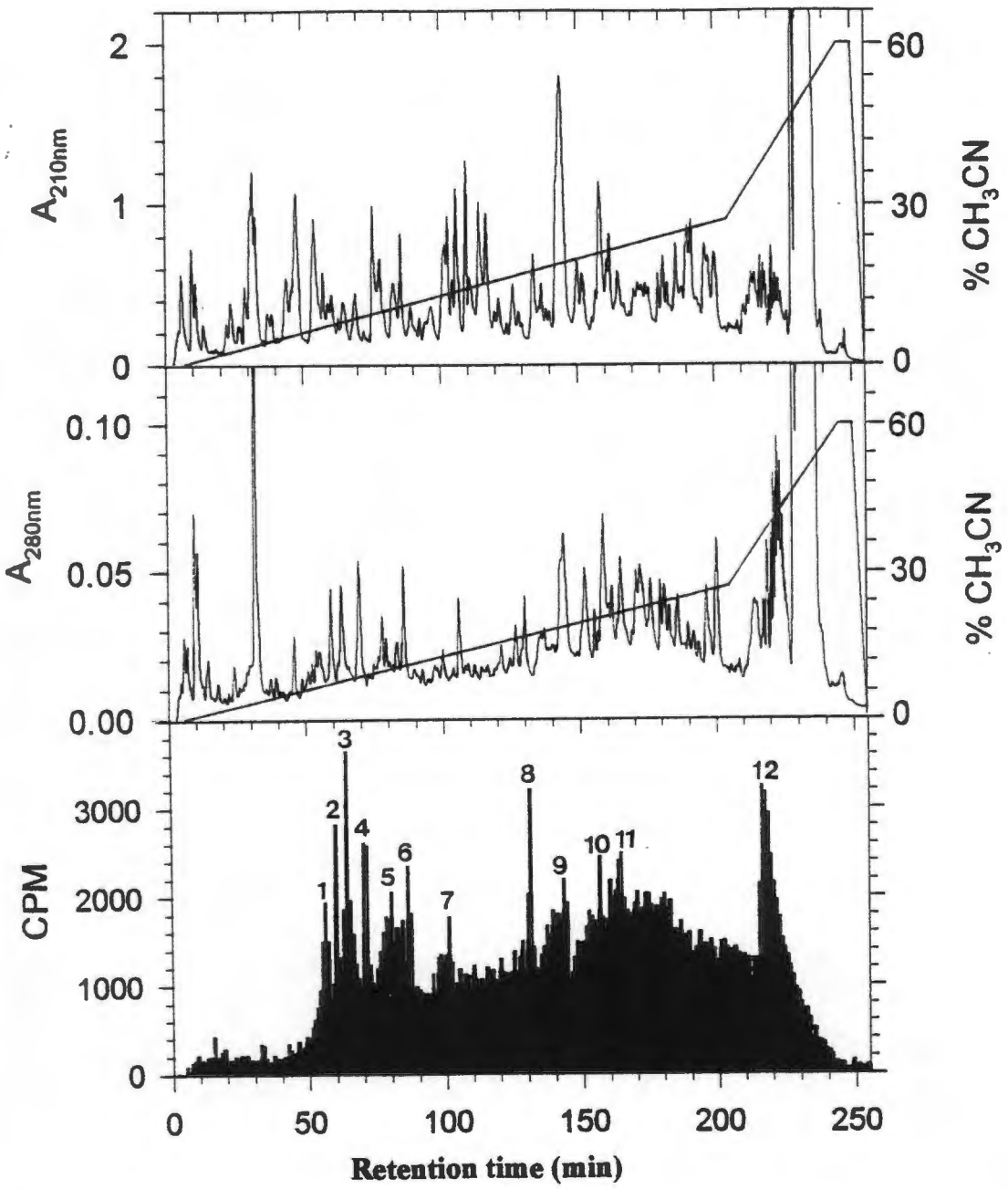

Figure 3.14 HPLC of soluble trypsin digestion products of solubilised sarcoplasmic reticulum vesicles reacted with crude [^{14}C]1,4-phenylenebismaleimide. Sarcoplasmic reticulum vesicles (10 mg) protein were reacted with 25 μM 1,4-phenylenebismaleimide at 25 °C for 30 min in 60 mM KCl, 20% (v/v) glycerol, 10 mM CHES/TMAH, pH 8.5, 0.2% (w/v) Triton X-100, 5 mM EGTA, 10 μM thapsigargin. The reactants were passed through a Sephadex PD-10 column to remove unreacted phenylenebismaleimide while eluting with 25 mM NH_4HCO_3, pH 7.5. Trypsin (4% w/w of sarcoplasmic reticulum protein) digestion continued for 3 h at 35 °C. The digestion products were passed through a C18 cartridge and the retained peptides were eluted with 10 mM KPi/60% (v/v) acetonitrile. The soluble peptides eluate volume was reduced to half with N_2 gas. Then subjected to HPLC on a vydac C4 column with solvent A as 10 mM KPi, pH 5.5 and solvent B 10 mM KPi/60% (v/v) acetonitrile. The elution was measured at 210 and 280 nm. Fractions were collected at 1 min intervals and assayed for radioactivity.

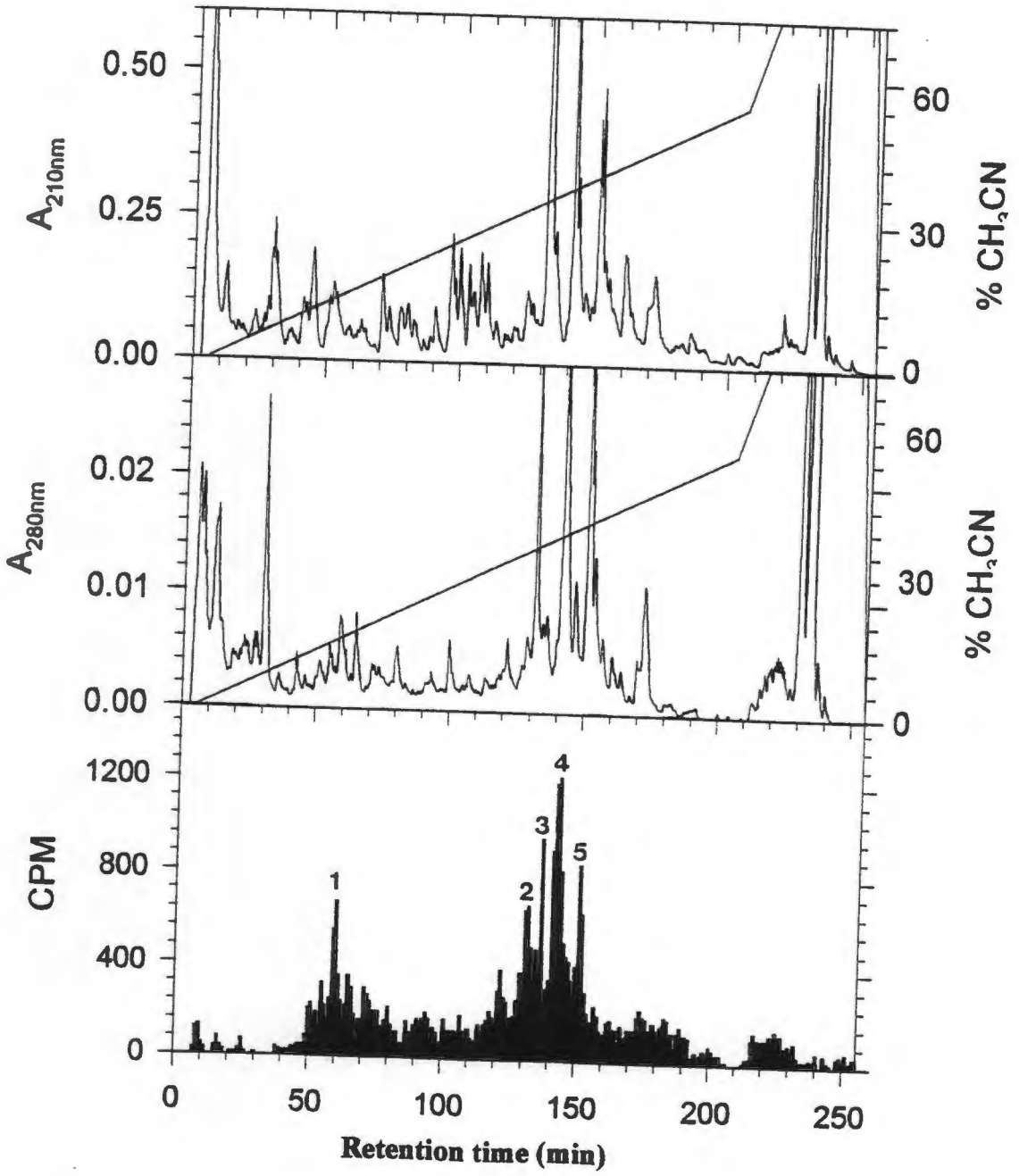

Figure 3.15 HPLC of soluble trypsin digestion products of solubilised sarcoplasmic reticulum vesicles reacted with silica gel column purified [^{14}C]1,4-phenylenebismaleimide. Sarcoplasmic reticulum vesicles (2 mg) protein were reacted with 25 μM 1,4-phenylenebismaleimide at 25 °C for 45 min in 60 mM KCl, 20% (v/v) glycerol, 10 mM CHES/TMAH, pH 8.5, 0.2% (w/v) Triton X-100, 5 mM EGTA, 10 μM thapsigargin. The reactants were passed through a Sephadex PD-10 column to remove unreacted phenylenebismaleimide while eluting with 25 mM NH_4HCO_3, pH 7.5. Trypsin (4% w/w of sarcoplasmic reticulum protein) digestion continued for 3 h at 35 °C. The digestion products were passed through a C18 cartridge and the retained peptides were eluted with 10 mM KPi/60% (v/v) acetonitrile. The soluble peptides eluate volume was reduced to half with N_2 gas. Then subjected to HPLC on a vydac C4 column with solvent A as 10 mM KPi, pH 5.5 and solvent B 10 mM KPi/60% (v/v) acetonitrile. The elution was measured at 210 and 280 nm. Fractions were collected at 1 min intervals and assayed for radioactivity.

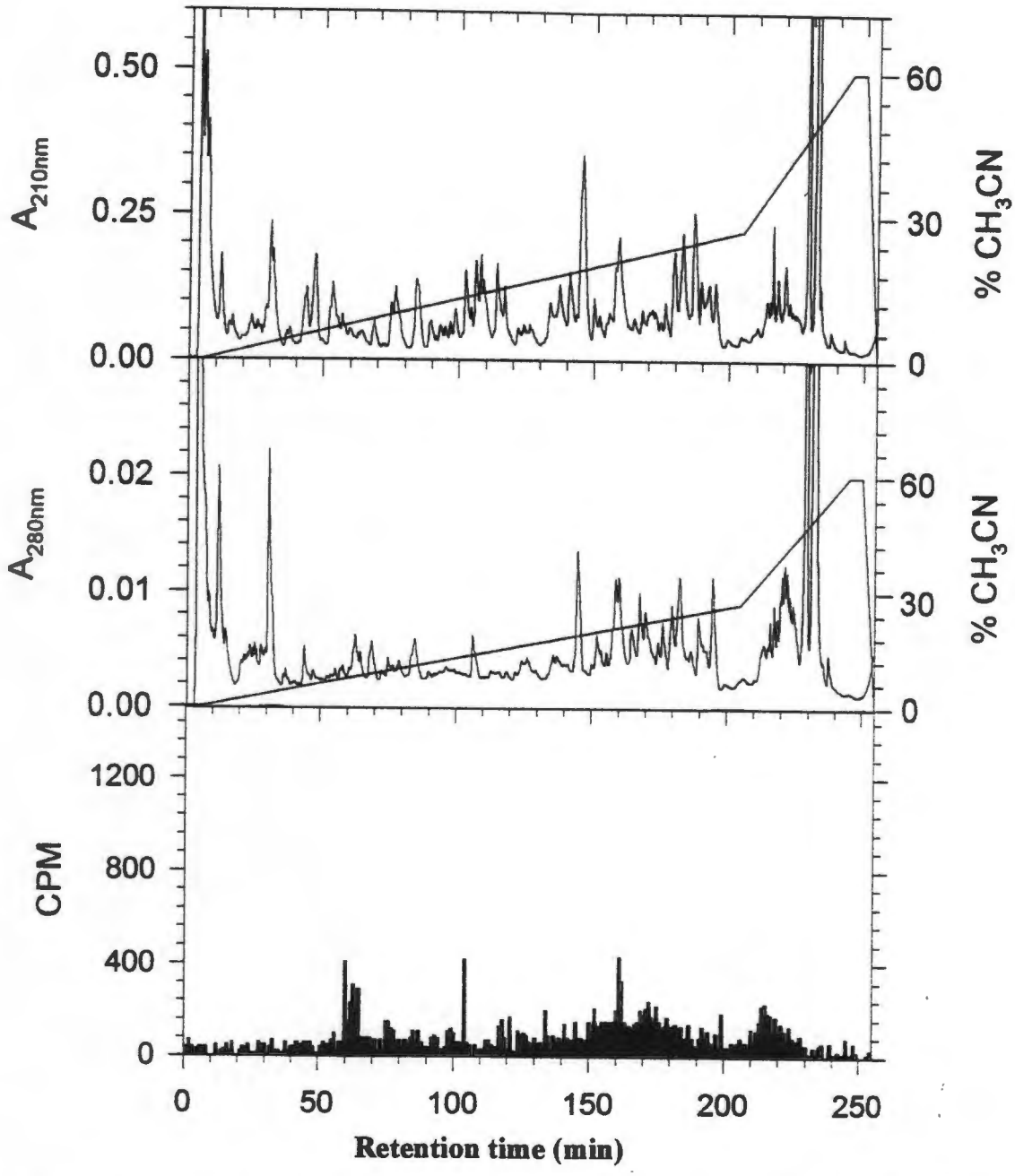

Figure 3.16 HPLC of soluble trypsin digestion products of solubilised sarcoplasmic reticulum vesicles reacted with silica gel column purified [^{14}C]1,4-phenylenebismaleimide in the presence of AMPPCP. Sarcoplasmic reticulum vesicles (2 mg) protein were reacted with 25 μM 1,4-phenylenebismaleimide at 25 °C for 45 min in 60 mM KCl, 20% (v/v) glycerol, 10 mM CHES/TMAH, pH 8.5, 0.2% (w/v) Triton X-100, 5 mM EGTA, 10 μM thapsigargin and 1 mM AMPPCP. The reactants were passed through a Sephadex PD-10 column to remove unreacted phenylenebismaleimide while eluting with 25 mM NH_4HCO_3, pH 7.5. Trypsin (4% w/w of sarcoplasmic reticulum protein) digestion continued for 3 h at 35 °C. The digestion products were passed through a C18 cartridge and the retained peptides were eluted with 10 mM KPi/60% (v/v) acetonitrile. The soluble peptides eluate volume was reduced to half with N_2 gas. Then subjected to HPLC on a vydac C4 column with solvent A as 10 mM KPi, pH 5.5 and solvent B 10 mM KPi/60% (v/v) acetonitrile. The elution was measured at 210 and 280 nm. Fractions were collected at 1 min intervals and assayed for radioactivity.

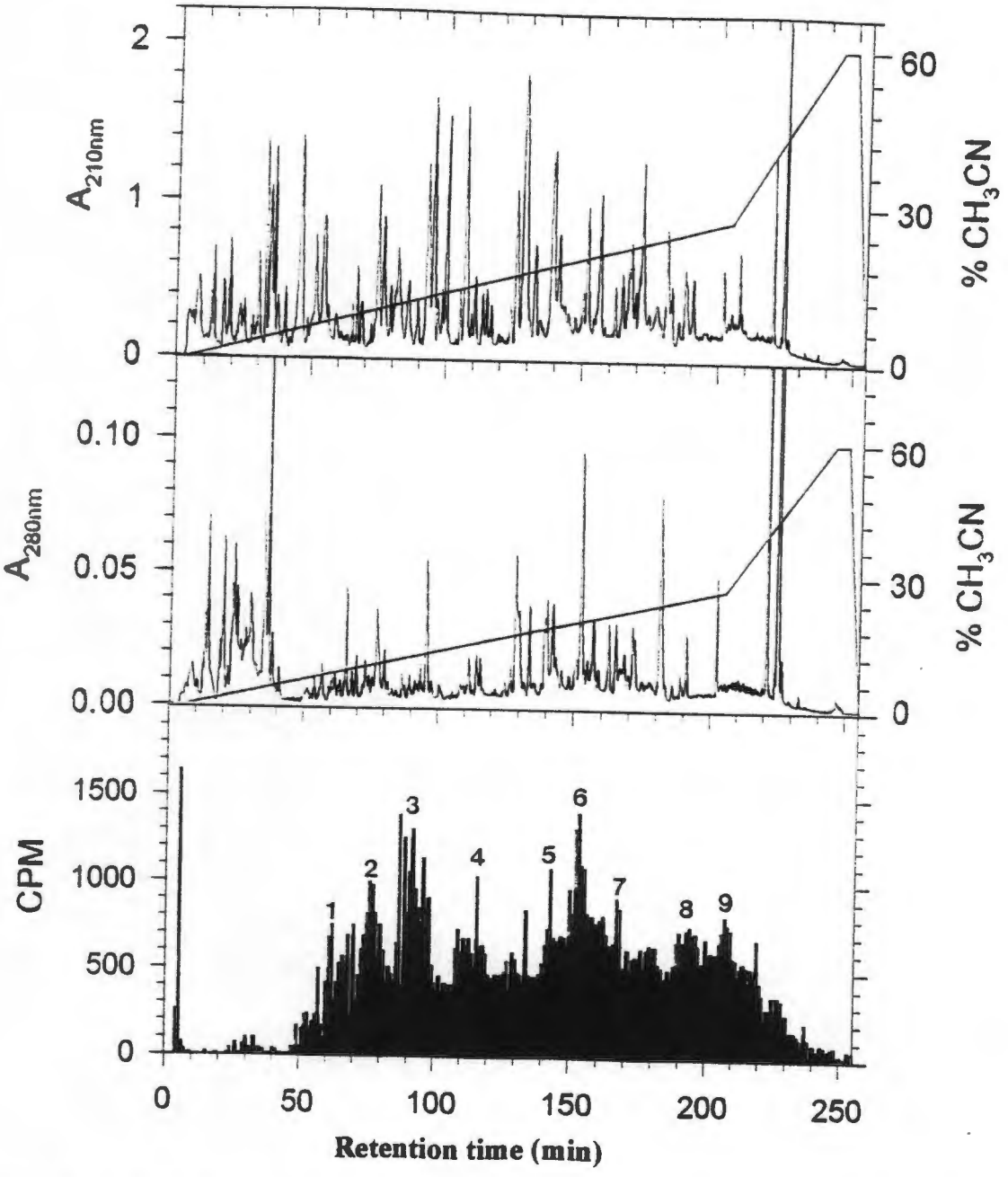

Figure 3.17 HPLC of soluble trypsin digestion products of solubilised sarcoplasmic reticulum vesicles reacted with silica gel column purified [^{14}C]1,4-phenylenebismaleimide. Sarcoplasmic reticulum vesicles (10 mg) protein were reacted with 25 μM 1,4-phenylenebismaleimide at 25 °C for 45 min in 60 mM KCl, 20% (v/v) glycerol, 10 mM EPPS/TMAH, pH 7.8, 0.2% (w/v) Triton X-100, 5 mM EGTA, 10 μM thapsigargin. The reactants were passed through two Sephadex PD-10 column to remove unreacted phenylenebismaleimide while eluting with 25 mM NH_4HCO_3, pH 7.5. Trypsin (4% w/w of sarcoplasmic reticulum protein) digestion continued for 30 min at 35 °C. The digestion products were passed through a C18 cartridge and the retained peptides were eluted with 10 mM KPi/60% (v/v) acetonitrile. The soluble peptides eluate volume was reduced to half with N_2 gas. Then subjected to HPLC on a vydac C4 column with solvent A as 10 mM KPi, pH 5.5 and solvent B 10 mM KPi/60% (v/v) acetonitrile. The elution was measured at 210 and 280 nm. Fractions were collected at 1 min intervals and assayed for radioactivity.

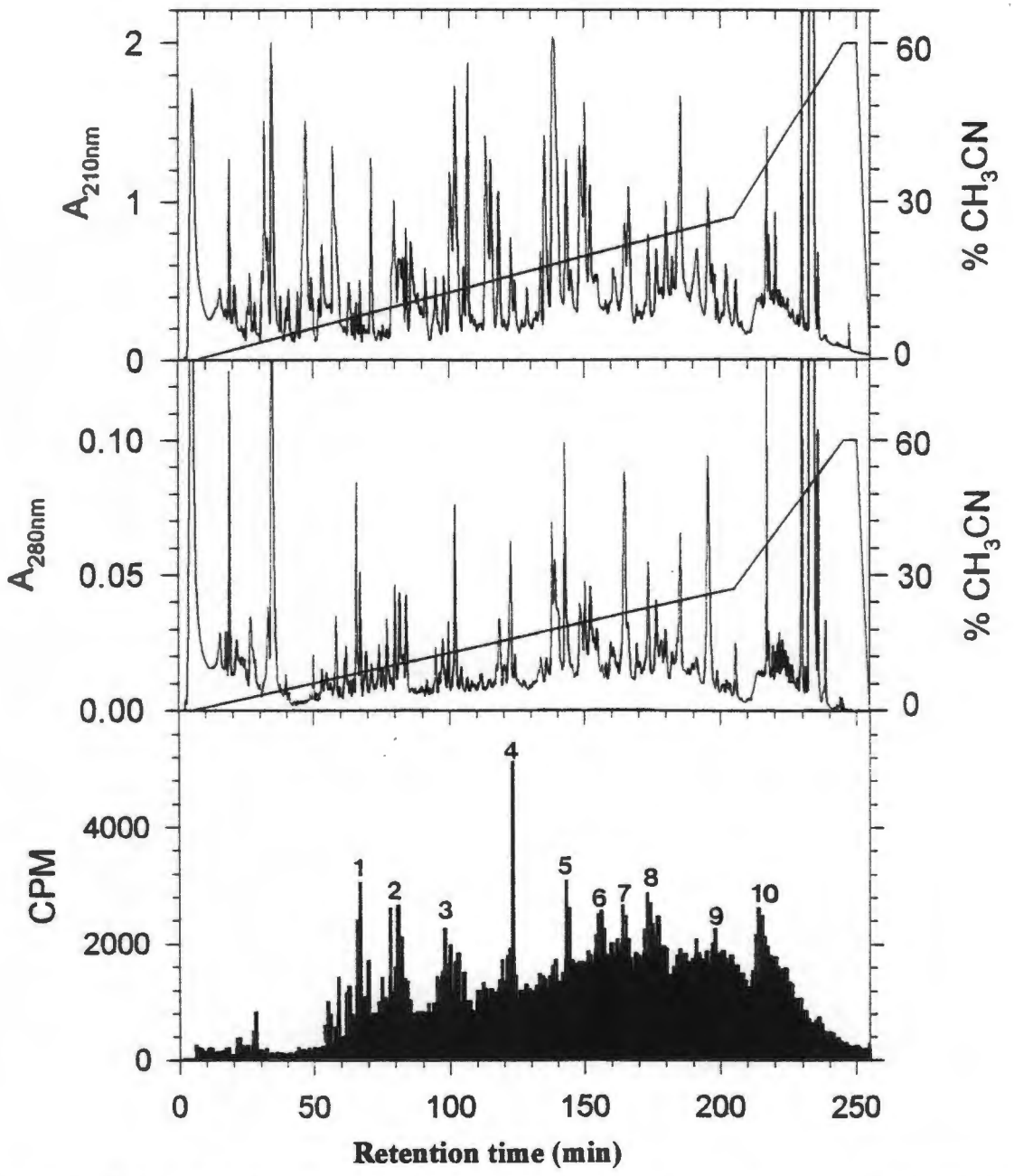

Figure 3.18 HPLC of soluble trypsin digestion products of solubilised sarcoplasmic reticulum vesicles reacted with silica gel column purified [^{14}C]1,4-phenylenebismaleimide. Sarcoplasmic reticulum vesicles (10 mg) protein were reacted with 25 μM 1,4-phenylenebismaleimide at 25 °C for 45 min in 60 mM KCl, 20% (v/v) glycerol, 10 mM EPPS/TMAH, pH 8.1, 0.2% (w/v) Triton X-100, 5 mM EGTA, 10 μM thapsigargin. The reactants were passed through two Sephadex PD-10 column to remove unreacted phenylenebismaleimide while eluting with 25 mM NH_4HCO_3, pH 7.5. Trypsin (4% w/w of sarcoplasmic reticulum protein) digestion continued for 30 min at 35 °C. The digestion products were passed through a C18 cartridge and the retained peptides were eluted with 10 mM KPi/60% (v/v) acetonitrile. The soluble peptides eluate volume was reduced to half with N_2 gas. Then subjected to HPLC on a vydac C4 column with solvent A as 10 mM KPi, pH 5.5 and solvent B 10 mM KPi/60% (v/v) acetonitrile. The elution was measured at 210 and 280 nm. Fractions were collected at 1 min intervals and assayed for radioactivity.

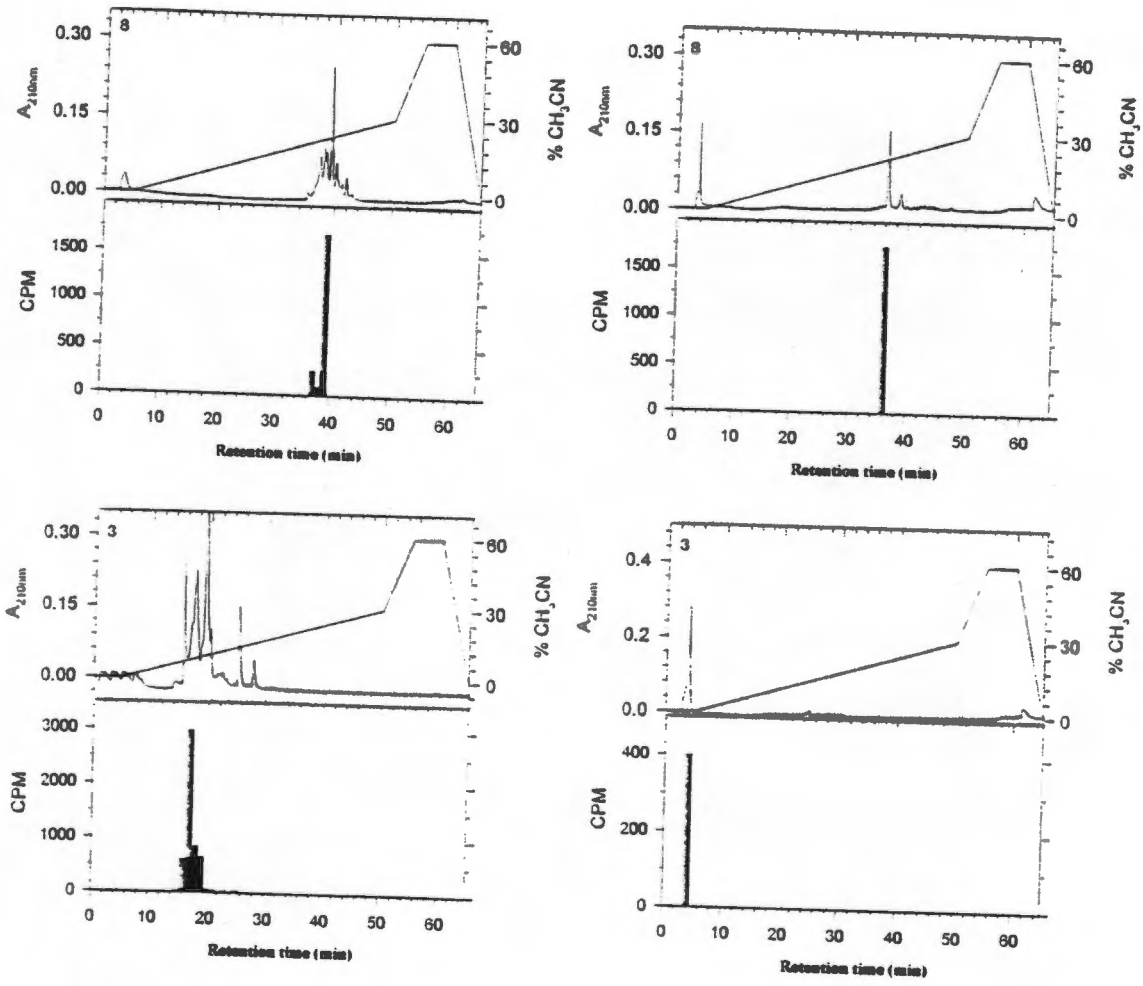

Figure 3.19 Purification of radiocative peaks 3 and 8 (see Figure 3.14) peptides by HPLC. Fractions were pooled and reinjected onto a vydac C18 column with solvent A as 1 mM KPi, pH 5.5 and solvent B 1 mM KPi/60% (v/v) acetonitrile. Fractions were collected at 1 min intervals and assayed for radioactivity. Further purification was onto a C18 column with KPi concentration reduced to 0.1 mM

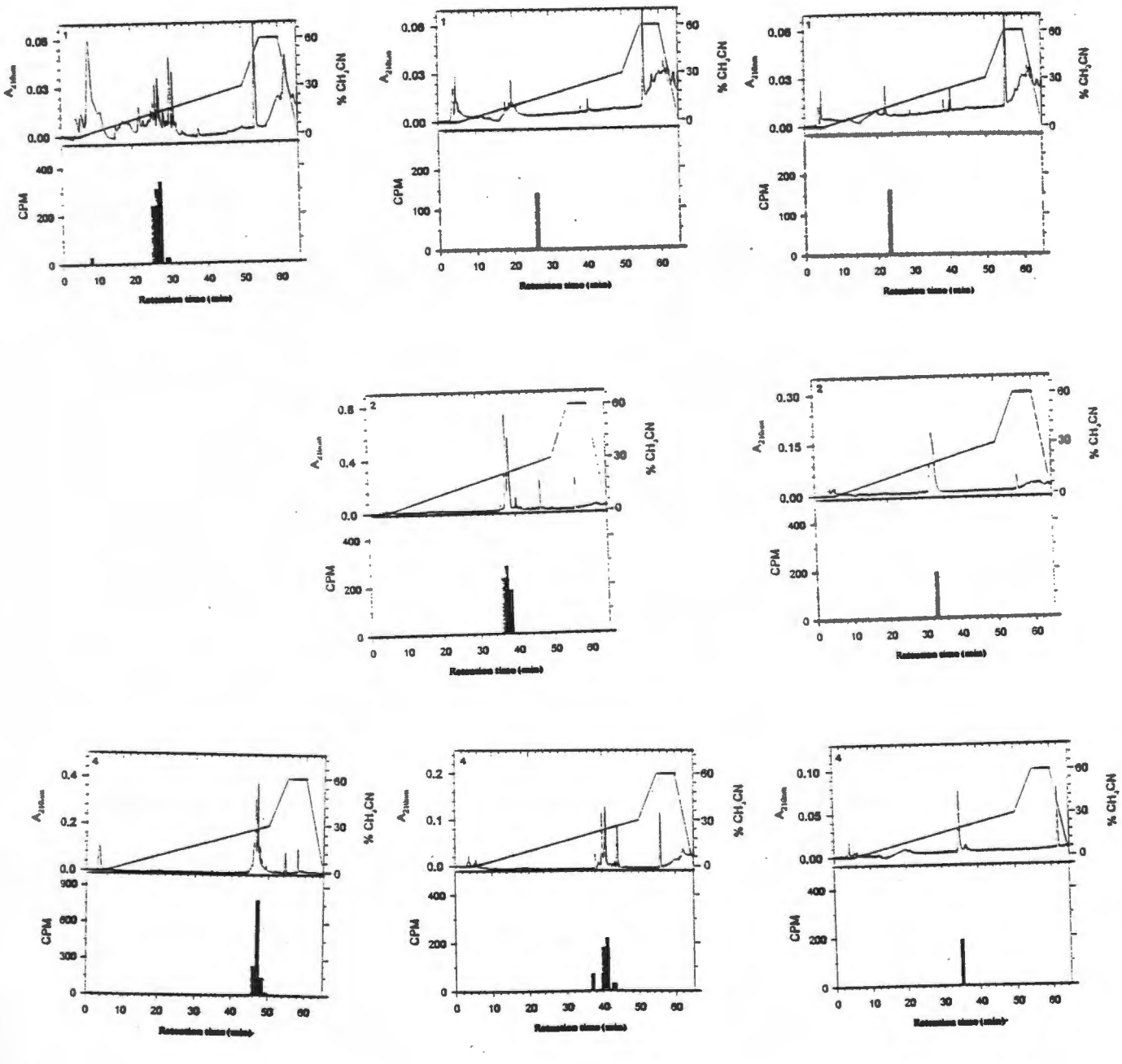

Figure 3.20 Purification of radiocative peaks 1, 2 and 4 (see Figure 3.15) peptides by HPLC. Fractions at 91-93 min were pooled and reinjected onto a vydac C18 column with solvent A as 1 mM KPi, pH 5.5 and solvent B 1 mM KPi/60% (v/v) acetonitrile. Fractions were collected at 1 min intervals and assayed for radioactivity. Further purification was onto a C18 column with KPi concentration reduced to 0.1 mM

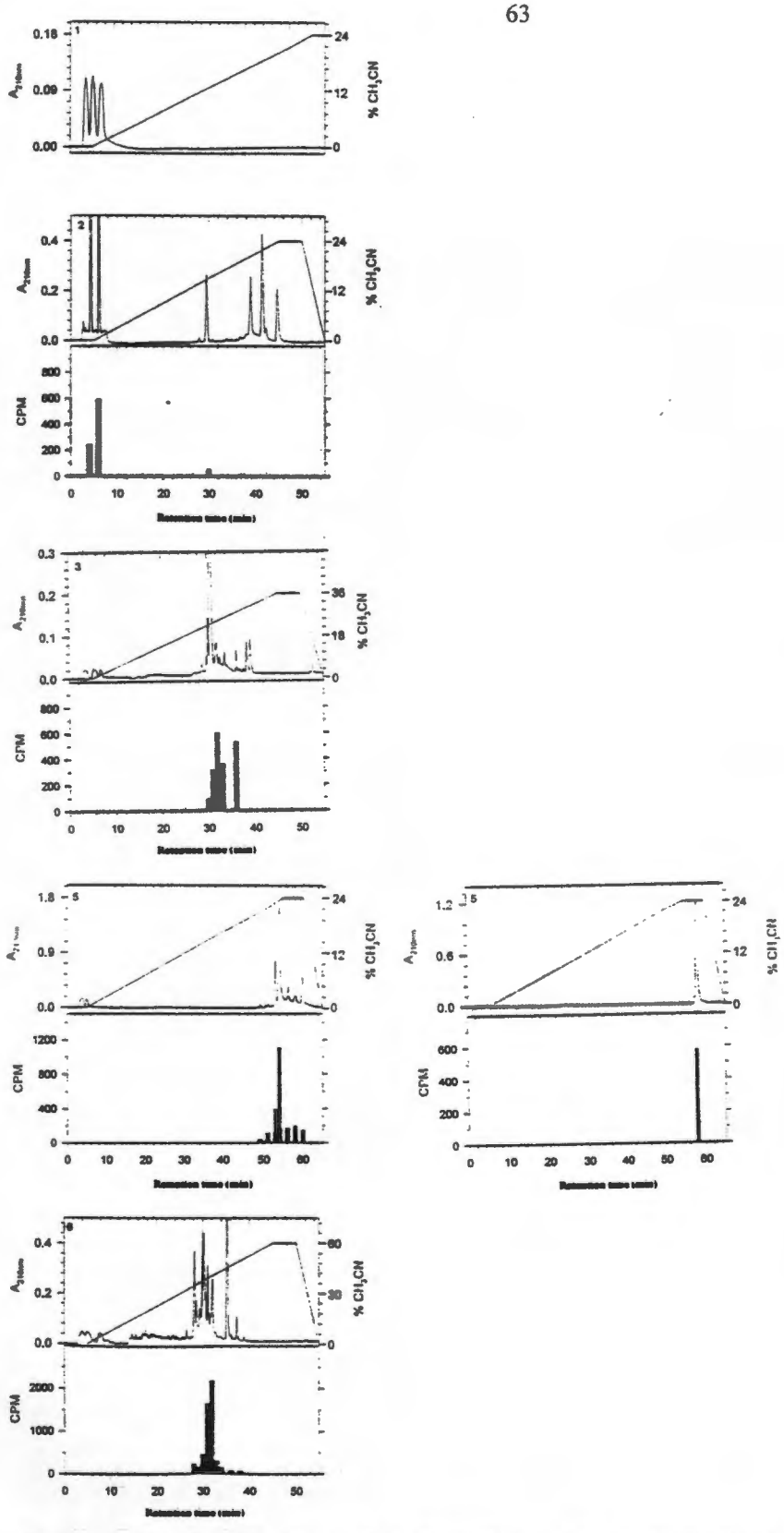

Figure 3.21. Purification of radiocative peaks 1, 2, 3, 5, and 6 (see Figure 3.17) peptides by HPLC. Fractions at 152-155 min were pooled and reinjected onto a vydac C18 column with solvent A as 1 mM KPi, pH 5.5 and solvent B 1 mM KPi/60% (v/v) acetonitrile. Fractions were collected at 1 min intervals and assayed for radioactivity. Further purification was onto a C18 column with KPi concentration reduced to 0.1 mM

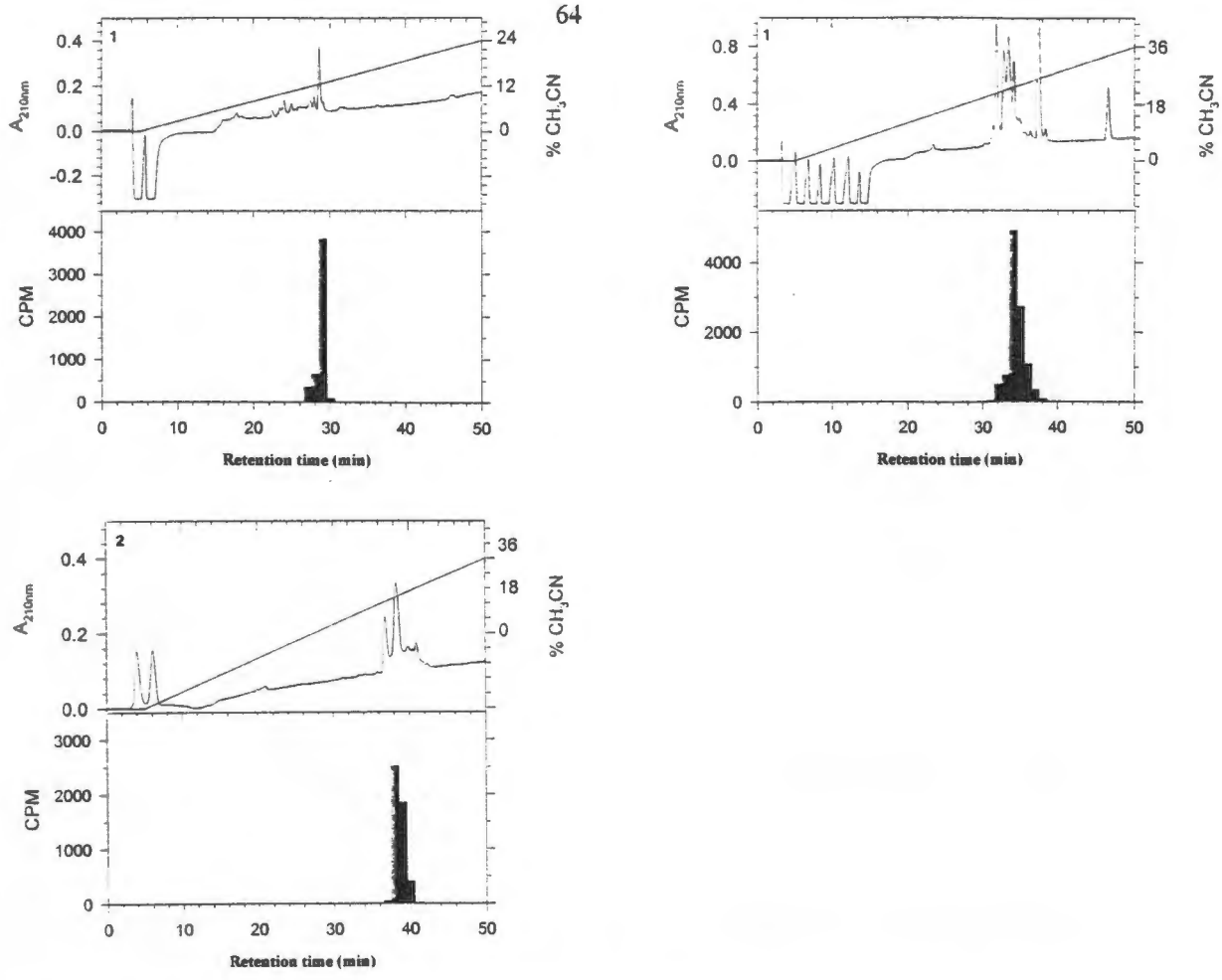

Figure 3.22. Purification of radioactive peaks 1 and 2 (see Figure 3.17) peptides by HPLC. Fractions at 152-155 min were pooled and reinjected onto a vydac C18 column with solvent A as 0.1 % Triflouroacetic acid and solvent B 0.1 % Triflouroacetic acid/60% (v/v) acetonitrile. Fractions were collected at 1 min intervals and assayed for radioactivity. Further purification was onto a C18 column with KPi concentration reduced to 0.1 mM

Table 3.1 Edman degradations of peptides labelled with [^{14}C]1,4-phenylenebismaleimide.

	Amino acid residues (picomoles)								
Cycle No.	**Fig. 3.14 Peak 3**	**Fig. 3.15 Peak 1**	**Fig. 3.15 Peak 2**	**Fig. 3.15 Peak 4**	**Fig. 3.17 Peak 2**	**Fig. 3.17 Peak 3**	**Fig. 3.17 Peak 5**	**Fig. 3.17 Peak 6**	**Fig. 3.18 Peak 2**
1	A (9)	X/ A (20)	I (77)	S (35)/ S (35)	S (152)	S (117)	T (3)	S (86)/ G (85)	A (83)
2	N (1)	A (11)/ X	V (87)	T (10)/ L (18)	M (165)	T (14)	G (11)	L (123)/ V (39)	N (59)
3	A (11)	X/ X	E (80)	E (55)/ P (13)	S (151)	E (118)	T (4)	P (66)/ Y (77)	A (79)
4	X	R (1)/ F (7)	Y (146)	E (42)/ S (6)	V (71)	E (234)	L (11)	S (76)/ E (62)	X
5	N (3)	/ A (8)	L (141)	X/ V (6)	Y (126)	X	T (6)	V (44)/ K (56)	N (55)
6	S (1)	/ R (4)	Q (125)	L (38)/ X	X	L (416)	T (3)	E (61)/ V (40)	S (18)
7	V (2)		S (62)	A (39)/ X	S (87)		N (16)	T (15)/ G (39)	V (12)
8	I (4)			Y (38)/ L (12)	P (55)		Q (27)	L (82)/ E (15)	
9	R (2)								

4. DISCUSSION

In this study, the topology of sulphydryl residues at the active site of sarcoplasmic reticulum Ca^{2+}-ATPase was explored using 1,4-phenylenebismaleimide. This bifunctional reagent has a crosslinking span of 13-14 Å and consists of two reactive maleimide moieties which form thiol ethers with sulfhydryl groups (Riordan and Vallee, 1972; Wells and Yount, 1982).

The reaction of 1,4-phenylenebismaleimide with sarcoplasmic reticulum Ca^{2+}-ATPase has been previously shown to form a 125 kD species and intermolecular crosslinks by SDS-PAGE (Yamasaki and Yamamoto, 1989). The former reaction is inhibited and the latter enhanced at neutral pH by the non-hydrolysable ATP analogue, AMPPNP. Formation of a 125 kD species is reminiscent of an intramolecular crosslinked species formed by the reaction of glutaraldehyde with the active site residues, Lys 492 and Arg 678, of SR Ca^{2+}-ATPase to produce an apparent molecular weight change on SDS-PAGE from 110 to 125 kD (Ross and McIntosh, 1987; McIntosh 1992).

Initially, reaction with 1,4-phenylenebismaleimide was optimised for maximum yield of 125 kD species with the least amount, or ideally none, of the interpolypeptide crosslink and derivatization of other sulfhydryls. We then synthesized [^{14}C]1,4-phenylenebismaleimide in an attempt to elucidate the putative intramolecular crosslinked amino acid residues that yield the 125 kD species following protease digestion of derivatised protein, purification of the radiolabelled peptides by HPLC and amino acid sequencing.

4.1 Optimization of the formation of 125 kD species

The reactivity of the sulfhydryl group of the cysteine residues increases with increase in pH, but so also does the reactivity of lysyl and arginyl residues (Friedman, 1973). Specific modification of sulfhydryl groups is best achieved at neutral pH or moderately alkaline conditions. The pH dependence of the formation of the 125 kD species

revealed that low concentrations of 1,4-phenylenebismaleimide could be used if moderately alkaline conditions prevailed, Thus at 25 μM crosslinker there was significant 125 kD species at pH 8.0-8.5. The latter pH is still within the required range for specific sulfhydryl derivatization with maleimides (Friedman, 1973). Reaction with lysyl residues occurs at pH 10 or above.

The formation of significant amounts of the 125 kD species at pH 7.0 and 1 mM crosslinker formed by Yamasaki and Yamamoto (1989) also suggests that only sulfhydryl residues are implicated in the putative intramolecular crosslink. However, as this issue was of some importance we used iodoacetamide to verify the involvement of sulfhydryls. Haloacetamides are known to react specifically with sulfhydryl groups between pH 6 and 8.5, and the reaction specificity extends on either side of this range depending on the location in the three dimensional structure or/and neighbouring residues effect on the microscopic environment (Means and Feeny, 1971). Prior modification with iodoacetamide inhibited formation of the 125 kD species with 1,4-phenylenebismaleimide. Incomplete inhibition of the putative crosslink may be attributed to incomplete derivatization with iodoacetamide possibly due to alkaline pH-induced hydrolysis of iodoacetamide or too short a reaction time. Taken together these results implicate cysteine residues.

A prominent reaction of 1,4-phenylenebismaleimide with Ca^{2+}-ATPase in intact vesicles is the formation of ATPase dimers. Yamasaki et al, (1990) have determined that Cys 377 and Cys 614 are the residues crosslinked intermolecularly. We attempted to eliminate such crosslinking by solubilizing the Ca^{2+}-ATPase in Triton X-100. This nonionic detergent has been shown previously to reduce ATPase-ATPase interactions and result in an essentially monomeric preparation at 0.3 % concentration (McIntosh and Ross, 1985). We found that 0.2 % Triton X-100 lowered the extent of dimer formation considerably and increased the amount of 125 kD species. Suprisingly, in the presence of Ca^{2+} a 130 kD species, as well as the usual 125 kD species, was produced in detergent. This could represent a second intramolecular crosslink (see later). It appears that Triton X-100 renders a normally unreactive residue(s) reactive or increased the conformational flexibility of the protein. Solubilization of sarcoplasmic

reticulum vesicles with Triton X-100 is known to increase the reactivity of most sulfhydryls in the Ca^{2+}-ATPase (Murphy, 1976).

In the absence Ca^{2+} (due to chelation by EGTA) and presence of Triton X-100 the Ca^{2+}-ATPase was crosslinked to dimers and high order oligomers by 1,4-phenylenebismaleimide. The Ca^{2+}-ATPase is known to be destabilized by nonionic detergent and the removal of Ca^{2+} (Andersen et al., 1982; McIntosh and Ross, 1988). Evidently, the denatured ATPase is readily crosslinked intermolecularly by 1,4-phenylenebismaleimide, as has been found with glutaraldehyde (McIntosh and Ross, 1988).

Thapsigargin, a sesquiterpene lactone is a specific inhibitor of sarco- and endoplasmic reticulum pumps (Wictome et. al., 1992), and stabilizes sarcoplasmic reticulum vesicles against thermal denaturation (Davidson and Berman, 1996) and Triton X-100-induced denaturation of Ca^{2+}-ATPase (Davidson and Varhol, 1995). Thapsigargin binds to Ca^{2+}-ATPase in the proximity of transmembane α-helices TM2 and TM3 anchoring the small (first) cytoplasmic loop (Norregard et. al., 1993). Addition of thapsigargin to the Ca^{2+}-ATPase prior to solubilization in Triton X-100 and EGTA had a pronounced effect on stabilizing the protein and enhancing the formation of the 125 kD species. It is estimated that under these conditions at least 60 % of the ATPases form this species.

4.2 Other characteristics of the reaction of 1,4-phenylenebismaleimide

Formation of the 125 kD species was blocked by AMPPCP binding, in agreement to the results of Yamasaki and Yamamoto (1989), and so was the formation of the 130 kD species. Interestingly, ADP only inhibited the formation of the 125 kD species, suggesting the apparent higher molecular weight form may be the result of an intramolecualr crosslink in proximity to the γ-phosphate of ATP, and the smaller species a crosslink closer to the β-phosphate. AMP had no effect on the formation of either species, compatible with this topography.

Contrary to the results of Yamasaki and Yamamoto (1989), AMPPCP inhibited, rather than increased formation of dimers. This could indicate that different cysteines are involved in dimer formation under our conditions or the conditions change the nucleotide binding effect. In support of our results in detergent, ATP and/or enzyme turnover is known to inhibit ATPase-ATPase interaction in nonionic detergent solutions and promote monomer formation (Andersen and Vilsen, 1985). On the other hand in the intact sarcoplasmic reticulum membrane, AMPPCP has no effect on the formation of tubular crystalline dimers induced by decavanadate (Stokes and Lacapere, 1994).

Quantitation of the 1,4-phenylenebismaleimide reaction kinetics by [^{14}C] labelling and filtration appeared to indicate that the reaction with sarcoplasmic reticulum vesicles resulted in 5 nmol/mg protein of extremely fast reacting SH group(s). The reaction was stopped by a 5000-fold excess β-mercaptoethanol and even though the first sample was at 10 s, it is possible that the quench could take a minute or so to react with all of the maleimide. Nevertheless the time course apparently suggests that there is a very fast reacting set of SH groups. High blanks values were obtained in these experiments and it is possible that some of the labelling may be due to error. Previous studies have indicated that there is a minor contaminant of sarcoplasmic reticulum preparations which has (a) fast reacting cysteine residue(s) (Hidalgo and Thomas, 1977). The reactive residue was identified as Cys 164 of the H subunit of lactate dehydrogenase (Sass et al., 1989). Whether this contaminant can entirely explain the 5 nmoles/mg of protein that we obtained is doubtful. However, pretreatment with NEM to block fast reacting cysteines is often done prior to reacting with other SH probes (Hidalgo and Thomas, 1977; Kawakita et al., 1988; Wawrzynow and Collins, 1993). This fast set was considerably reduced by AMPPCP.

Apart from the fast set, the reaction with sarcoplasmic reticulum vesicles occurred over time course compatible with the formation of the 125 kD species, but the extent of reaction (7 nmoles/mg of protein) was greater than expected for a single

intramolecular crosslink of 10-20 % of ATPases (0.5 nmoles/mg of protein) and evidently other cysteines are targeted.

In Triton X-100, the extent of derivatization is approximately double that of the vesicles and the kinetics are biphasic, with about half of the reaction being complete within 10 min. Although analysis of [^{14}C] peptides by HPLC indicates several derivatized cysteines under these conditions, it is possible that the reaction of 1,4-phenylenebismaleimide with one of the cysteines involved in the intramolecular crosslink occurs fairly quickly and that the reaction with the other , to form the intralink, takes place more slowly (which would not be seen in this experiment). However, it is also possible that the faster set are associated to the reaction with Cys 344 and Cys 364, which are known to be the cysteines targeted by maleimides (Kawakita and Yamashita, 1987) and which are prominently labelled by 1,4-phenylenebismaleimide as our results show. AMPPCP does not change the kinetics nor the extent of reaction, results compatible with either possibility as the nucleotide blocks the crosslink but not necessary reaction with either of the two cysteines involved

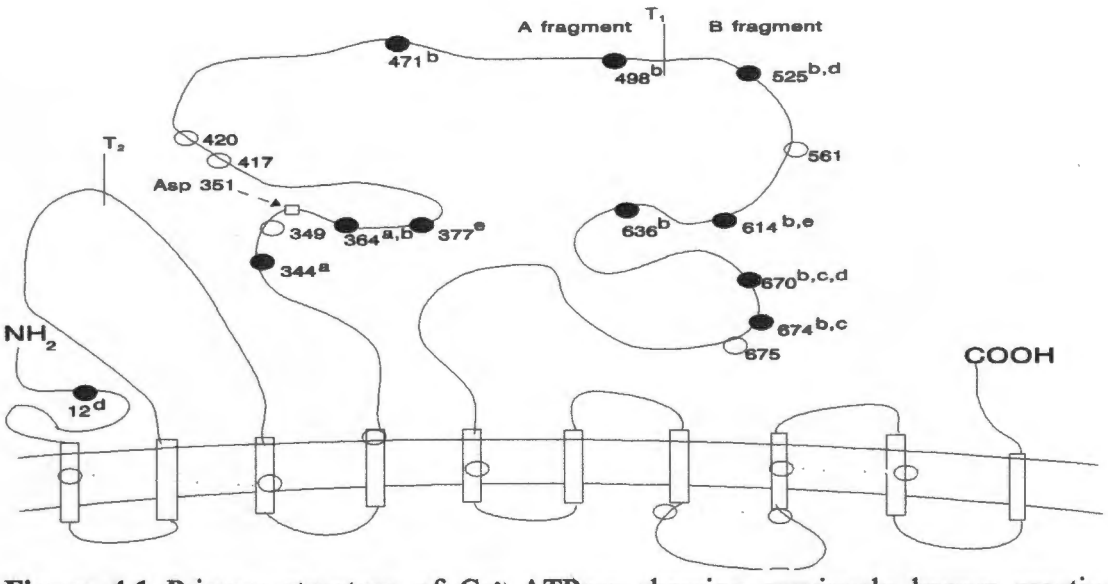

Figure 4.1 Primary structure of Ca^{2+}-ATPase showing previously known reactive sulfhydryls. [a] Kawakita and Yamashita, 1987; [b] Wawrzynow and Collins, 1993; [c] Bishop et al., 1988; [d] Reithmeyer and MacLennan, 1981; [e] Yamasaki et al., 1990)

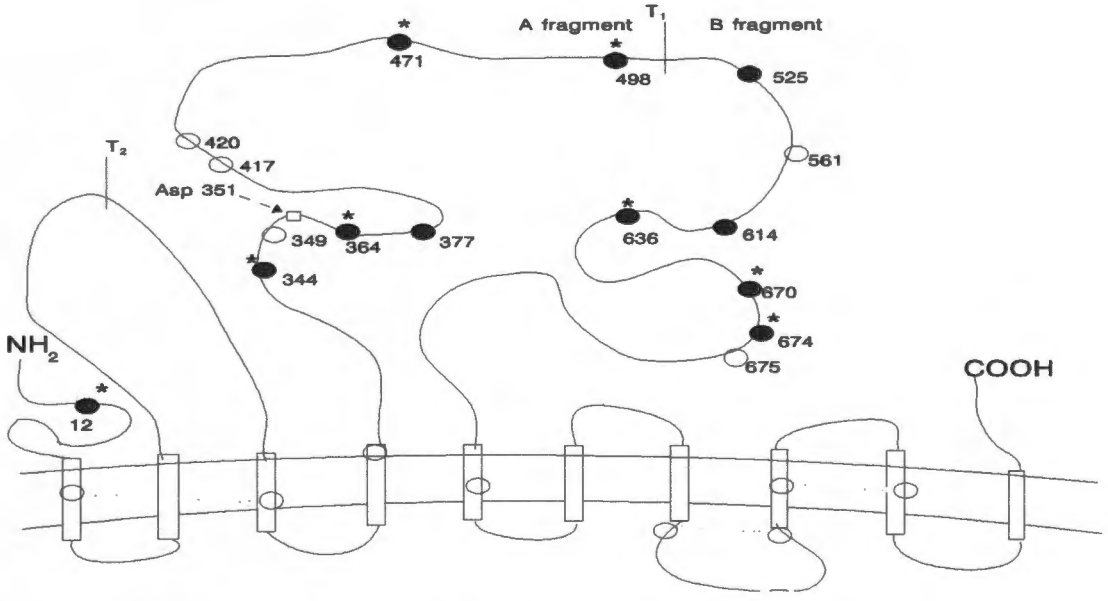

Figure 4.2 Primary structure of Ca^{2+}-ATPase showing previously known reactive sulfhydryls and those reactive to 1,4-phenylenebismaleimide (*).

4.3 Identification of 1,4-phenylenebismaleimide reactive residues and possibilities for residues involved in the putative intramolecular crosslink

Four HPLC peptide profiles of trypsin digests of 1,4-phenylenebismaleimide derivatized Ca^{2+}-ATPase in the absence of nucleotide were presented in the Results section. All were done in 0.2% Triton X-100 and thapsigargin, conditions under which intermolecular crosslink was virtually eliminated and formation of the 125 kD species at pH 8.5 was at least 60 % of the total Ca^{2+}-ATPase present. The first two profiles represented Ca^{2+}-ATPase derivatized at pH 8.5 and digested for 3 h with trypsin (Figures 3.14 and 3.15). The profiles were rather different, but prominent peaks eluted at around 60 min and 150 min. The reason for the different profiles is difficult to explain, but the first one is very similar to the one obtained later at pH 8.1 after 30 min digestion (Figure 3.18), and presumably is the more reliable, even if the profile is more complicated. In the third and fourth profiles the pH of the 1,4-phenylenebismaleimide reaction was lowered to pH 7.8 and 8.1 respectively, and two PD-10 columns were used to remove free crosslinker. It was hoped that the lower pH might provide increased specificity and the shorter digestion time counteract the instability of the maleimide- amino acid adducts.

Cysteine residues that have previously been shown to be reactive with maleimide- and iodocateamide based probes are shown in figure 4.1. Eleven out of the 16 cysteines in the cytoplasmic portion of the Ca^{2+}-ATPase have been labelled. Of these only one, namely Cys 674 has not been labelled by maleimide based reagents.

The cysteine residues implicated in reaction with 1,4-phenylenebismaleimide in this study are shown in Figure 4.2. Most of those previously identified as reactive were labelled with this crosslinker. The exception were the two intermolecularly crosslinked residues, Cys 377 and Cys 614, and residue Cys 525. Unexpectedly the iodoacetamide reactive cysteine Cys 674, was found to be labelled with 1,4-phenylenebismaleimide.

The principal cysteines labelled with 1,4-phenylenebismaleimide appear to be Cys 344, Cys 364, Cys 471 and Cys 498. The former two are the selectively labelled at pH 7.0 with NEM (Kawakita and Yamashita, 1987), and it was not a surprise to find them

well labelled. These two residues reside outside the ATP binding site and catalytic site since their modification with NEM does not affect ATPase activity and is not blocked by AMPPNP (Kawakita and Yamashita, 1987; Kawakita et al., 1988). The latter two are among the cysteines more rapidly labelled by flouresceinmaleimide (Wawrzynow and Collins, 1993) and were also expected. They are located in the linear sequence on either side of Lys 492 and are strong candidates in the formation of the 125 kD species as explained below.

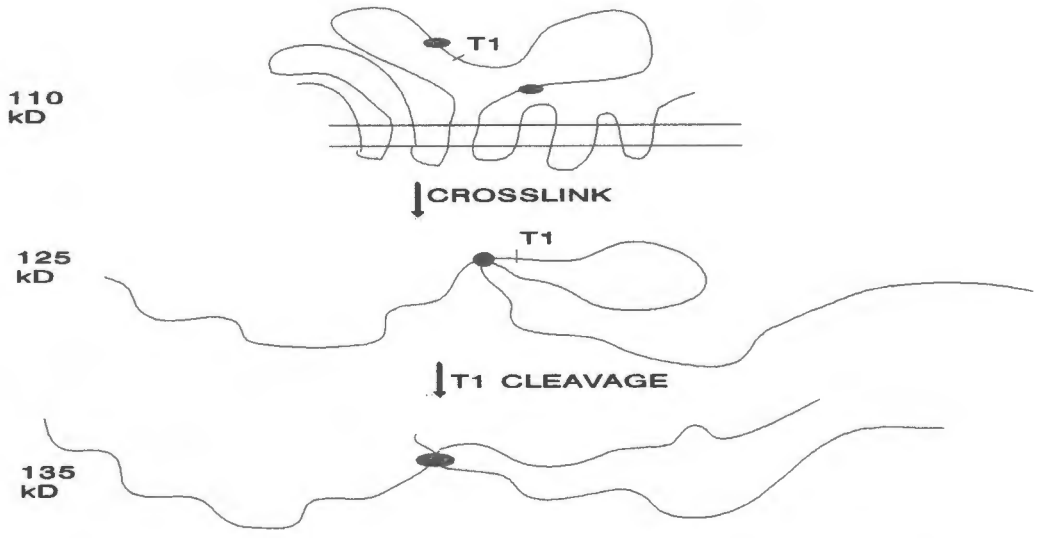

Figure 4.3 Hypothetical crosslink effect between a residue in the A tryptic fragment and a residue in the B tryptic fragment of the Ca^{2+}-ATPase following primary (T1 site) digestion. This primary structure of the polypeptide in the membrane is drawn according to the predictions of MacLennan et al. (1985). The cysteines residues are shown as dots and the change in molecular weight is according to SDS-PAGE (Laemmli, 1970).

T1

^{463}SK|VER|ANA*C*NSVIR|QLMK|K|EFTLEFSR|DR|K|SMSVY*C*SPAK|SSR|AA^{507}

^{625}TGDNK|GTAIAI*C*R|R|IGIFGENEEVADR|AYTGR|EFDDLPLAEQR|EA*C*R|R|A*CC*FA R|VEPSHK|SK|IVEYLQSYDEITAMTGDGVNDAPALK|K^{713}

Figure 4.4 Amino acid sequences in the vicinity of cysteine residues possibly involved in the formation of the 125 kD species. Tryptic sites are indicated by (|), including a primary cleavage site, T1. The underlined sequences indicate the conserved regions.

In considering possible amino acid residues involved in the formation of the putative intramolecular crosslink that produces the 125 kD species it is instructive to examine the amino acid sequence in the vicinity of Lys 492 and Arg 678, residues that are intramolecularly crosslinked by glutaraldehyde, and which also produces a 125 kD species (McIntosh, 1992). Cleavage of the latter crosslinked ATPase at the sensitive T1 cleavage site (Arg 505) changes the apparent molecular weight of the crosslinked enzyme (125 kD) to 135 kD. This is because cleavage changes the shape of the molecule, a linear form with a loop, into one that is Y-shaped (see Figure 4.3). Failure to split the protein into the two previous tryptic fragments A and B, is because the crosslink spans (links) the two. An identical result is obtained with the 1,4-phenylenebismaleimide crosslinked 125 kD species, showing that the putative crosslink is between the A and B fragments suggesting that the residues are close to Lys 492 and Arg 678, because of their similar relationship to the T1 cleavage site. The sequences in question are shown in Figure 4.4. In the A fragment only two cysteines, Cys 471 and Cys 498 are possibilities and in the B fragment, four cysteines can be considered, Cys 636, Cys 670, Cys 674 and Cys 675.

Both of those in the A fragment appear to be reactive to 1,4-phenylenebismaleimide and either is a strong candidate for the putative intramolecular crosslink. Likewise, Cys 670 and Cys 674 were identified in labelled peptides. Unfortunately all four derivatized peptides elute in very similar positions on the HPLC (60-80 min) and an intramolecular crosslink between such peptides is expected to have similar properties. In fact, in the second HPLC profile presented all four peptide were detected and two could have been crosslinked.

Cys 471 has previously been implicated in ATP dependent conformational changes (Kison et al., 1989), and could provide the ATP sensitivity of the intramolecular crosslink. Cys 670 and Cys 674 appear to be outside the ATP binding site as derivatization with iodoacetamide-based probes has no effect on the ATPase activity, but the probes report an ATP dependent conformational changes in the presence of Ca^{2+} (Bishop et al., 1988; Wawrzynow et al., 1993; Suzuki et al., 1994; Mahaney et al., 1995).

The separation of Cys 471 and Cys 498 by 26 residues could provide a simple explanation for the formation of the 130 kD species which found in smaller amount in the presence of Ca^{2+} and Triton X-100. It seems doubtful that different crosslinks between, say Cys 471 and Cys 670 or Cys 674 could produce significant molecular weight changes on SDS-PAGE, but two crosslinks between say Cys 670 and Cys 471 or Cys 498 could produce such a change.

Cys 12 has been demonstrated to be exposed on the cytoplasmic surface of (Reithmeyer and MacLennan, 1981). They show that this residue to be reactive with NEM and this agrees with the model of Toyoshima (1993), see Figure 1.6, in that the amino terminal end is not buried in the 3-D conformation. We also show that this residue is reactive with 1,4-phenylenebismaleimide.

Sarcoplasmic reticulum Ca^{2+}-ATPase was radiolabelled under conditions that would yield approximately 60% intramolecular crosslink yield. Failure to identify the residues involved in the intramolecular crosslink could be attributed to the following factors.

(i) The intramolecular crosslink could be unstable. Under alkaline conditions (pH 9.0) at 25 °C the maleimide rings undergo hydrolysis and conversion to maleic acid (Knight and Offer, 1978). If this same hydrolysis occur with the crosslink it would result in the breakage of the link.

(ii) In the analysis of possible crosslink sites above, cysteine residues were only considered. It is possible that lysine residues may be involved. Reaction of 1,4-phenylenebismaleimide with lysine at pH 9.0 has been reported (Knight and Offer, 1978). This would greatly increase the possibilities for the crosslinked residues.

(iii) From the filtration experiments it was evident that fast reacting cysteines are inhibited by active site nucleotide occupation. Other minor protein components of the preparation also have fast reacting cysteines and previous work has reported that preincubation with micromolar concentrations of N-ethylmaleimide blocks these fast reacting residues (Hidalgo and Thomas, 1977) and this would be pertinent in the

reduction of background counts, and possibly identifying the crosslink peak easier if it was a minor radioactive peak during HPLC analysis.

(iv) The formation of the 125 kD species could be the result of an intramolecular crosslink between several sulfhydryl residues, therefore producing a number of minor peaks instead of a single large peak.

(v) The second peptide could be obscured during sequencing due to overlapping residues; sequencing problems (e.g poor identification of threonines and serines), and blocked and/or derivatized amino acid residues.

5. REFERENCES

Aguilar-Bryan, L., Nichols, C.G., Wechsler, S.W., Clement IV, J.P., Boyd III, A.E., Gonzalez, G., Herrera-Sosa, H., Nguy, K., Bryan, J., and Nelso, D. (1995) Science **268**, 423-426

Albers, R.W. (1969) Annual Rev. Biochem. **36**, 727-756

Amory, A., Foury, F., and Goffeau, A. (1980) J. Biol. Chem. **255**, 9353-9357

Andersen, M.P., Gregory, R.J., Thompson, S., Souza, D.W., Paul, S., Mulligan, R.C., Smith, A.E., and Welsh, M.J. (1991) **253**, 202-205

Andersen, J.P. (1995) J. Biol. Chem. **270**, 908-914

Andersen, J.P., and Vilsen, B. (1995) FEBS Lett. **359**, 101-106

Baba, A., Nakamura, T., and Kawakita, M. (1986) J. Biochem. (Tokyo) **100**, 1137-1147

Bamberg, K., Sachs, G. (1994). **269**, 16909-16919

Bednarska, K. (1993) Folia Histochemica et Cytobiologica. **31**, 147-151

Bednarska, K., and Butowt, R. (1995) Folia Histochemica et Cytobiologica. **33**, 125-132

Bidwai, A.P., Morjana, N.A., and Scarborough, G.A. (1989) J. Biol. Chem. **264**, 11790-11795

Bigelow, D.J., and Inesi, G. (1991) Biochemistry. **30**, 2113-2125

Bishop, J.E., Squire, T.C., Bigelow, D.J., and Inesi, G. (1988) Biochemistry **27**, 5233-5240

Brandl, C.J., Green, N.M., Korczak, B., and MacLennan, D.H. (1986) Cell. **44**, 597-607

Carafoli, E., Garcia-Martin, E., and Guerini, D. (1996) Experientia **52**, 1091-1100

Champeil, P., Guillain, F., Venien, C., and Gingold, M.P. (1985) Biochemistry. **24**, 69-81

Chang, A., and Slayman, C.W. (1990) J. Biol. Chem. **265**, 15531-15536

Chevallier, J., and Butow, R. (1971) Biochemistry **10**, 2733-2737

Chyn, T., and Martonosi, A. (1977) Biochim. Biophys. Acta **468**, 114-126

Clarke, D.M., Loo, T.W., and MacLennan, D.H. (1990) J. Biol. Chem. **265**, 17405-17408

Coan, C., Verjovski-Almeida, S., and Inesi, G. (1972) J. Biol. Chem. **254**, 2968-2974

Coan, C., and Keating, S. (1982) Biochemistry **21**, 3214-3220

Coan, C. (1983) Biochemistry **22**, 5826-5826

Daiho, T., and Kanazawa, T. (1994) J. Biol. Chem. **269**, 11060-11064

Dame, J.B., and Scarborough, G.A. (1981) J. Biol. Chem. **256**, 10724-10730

Davidson, G.A., and Varhol, R.J. (1995) J. Biol. Chem. **270**, 11731-11734

Dufour, J.P., and Goffeau, A. (1978) J. Biol. Chem. **253**, 7026-7032

Dupont, Y. (1980) Euro. J. Biochem. **109**, 231-238

Dupont, Y.(1982) Biochim. Biophys. Acta **688**, 75-87

Dupont, Y., Guillain, F., and Lacapere, J.J. (1989) Methods Enzymol. **157**, 206-219

Epstein, W., Walderhang, M.O., Polarek, J.W., Heese,J.E., Dorns, E., and Daniel, J.M. (1990) Phil. Trans. R. Soc. Lond. **326**, 479-487

Esmann, M. (1985) Biochim Biophys. Acta. **815**, 196-202

Esmann, M. (1994) Biochemistry **33**, 8558-8565

Forbush, B., III (1987) J. Biol. Chem. **262**, 11104-11115

Forge, V., Mintz, E., Canet, D., and Gullain, F. (1993) J. Biol. Chem. **270**, 18271-18276

Forge, V., Mintz, E., Canet, D., and Guillain, F. (1995) J. Biol. Chem. **270**, 18271-18276

Frausto da Silva, J.J.F., and Williams, R.J.P. (1991) in 'The biological chemistry of elements', Clarendon Press, New York

Friedman, M. (1973) in 'The chemistry and biochemistry of the sulfhydryl group in amino acids, peptides and proteins', Pergamon Press, Braunschweig

Froehlich, J.P., and Heller, P.F. (1985) Biochemistry **24**, 126-136

Gambel, A.M., Desrosiers, M.G., and Menick, D.R. (1992) J. Biol. Chem. **268**, 20590-20597

Gambel A.M., and Menick, D.R. (1993) J. Biol. Chem. **267**, 15923-15931

Garcia, C., Ternel, J.A., and Gomez-Fernandez, J.C. (1996) Biochem. J. **318**, 179-186

Goormaghtigh, E., Chadwick, C., and Scarborough, G.A. (1986) J. Biol. Chem. **261**, 7466-7471

Gottesman,M.M., and Pastan, I. (1993) Annual Rev. Biochem. **62**, 385-427

Gutowski-Eckel, Z., Mann, K., and Baumert, H.G. (1993) FEBS Lett. **324**, 314-318

Haywood, S., and Loughram, M. (1985) Liver **5(5)**, 267-275

Heese, J.E., Wieczorek, L., Altendorf, K., Reicin, A.S., Dorus, E., and Epstein. W. (1984) Proc. Natl. Acad. Sci. **81**, 4746-4750

Hennesey, J.P., and Scarborough, G.A (1990) J. Biol. Chem. **265,** 532-537

Hicks, B.W., and Parson, S.M. (1992) J. Neurochem. **58**, 1211-1220

Hidalgo, C., and Thomas, D.D (1977) Biochim Biophys. Res. Commun. **78**, 1175-1182

Higgins, C.F (1995) J.Physiology. **482P**, 313-365

Hinz, H.R., and Kirley, T.L. (1990) J. Biol. Chem. 265, 10260-10265

Horio, M., Gottesman, M.M., and Pastan, I. (1988) Proc. Natl. Acad. Sci. **85**, 3580-3584

Inesi, G. (1985) Annu. Rev. Physiol. **47**, 573-601

Inesi, G. (1987) J. Biol. Chem. **262,** 16338-16342

Karlish,S.J.D., Goldshleger, R., and Jorgensen, P.L (1993) J. Biol. Chem. **268**, 3471-3478

Karlish, S.J.D., Goldshleger, R., and Stein, W.D. (1990) Proc. Natl. Acad. Sci. **87**, 4566-4570

Kawakita, M., and Yamashita, T. (1987) J. Biochem. (Tokyo) **102**, 103-109

Kawakita, M., Yasuoka, K., and Kaziro, Y. (1980) J. Biochem. (Tokyo) **87**, 609-617

Kawakita, M., Yasuoka-Yabe, K., Saito-Nakatsuka, K., Baba, A., and Yamashita, T. (1988) Methods Enzymol. **157**, 251-261

Kirley, T.L., Wang, T., Wallick, E.T., and Lane, L.K. (1985) Biochem. Biophys. Res. Commun. 130, 732-738

Kison, R., Meyer, H.E., and Schoner, W. (1989) Eur. J. Biochem. **181**, 503-511

Knight, P., and Offer, G. (1978) Biochem. J. **175**, 1023-1032

Kosk-Kosicka, D., Kurzmack, M., and Inesi, G. (1983) Biochemistry **22**, 2559-2567

Kraut, J.A., Star, F., Sachs, G., and Reuben, M. (1995) Am. J of Physiology. **268**, F581-F587

Kubo, K., Suzuki, H., and Kanazawa, T. (1990) Biochem. Biophys. Acta. **1040**, 251-259

Kurobe, Y., Nelson, R.W., and Ikemoto, N. (1983) J. Biol. Chem. **258**, 4381-4389

Lacapere, J.-J., Garin, J., Trinnaman, B., and Green, N.M. (1993) Biochemistry **32**, 3414-3421

Laemmli, U.K. (1970) Nature **227**, 680-685

Lee, A.G., Starling, A.P., Ding, J., East, J.M and Witcome, M. (1994) Biochemical Society Trans. **22**, 821-826

Lewis, S.M., and Thomas, D.D (1992) Biochemistry **31**, 7381-7389

Louis, C.F., and Holroyd, J.A. (1978) Biochim. Biophys. Acta. **535**, 222-232

Lutsenko, S., and Kaplan, J.H. (1995) Biochemistry **34**, 15607-15613

MacLennan, D.H., Brandt, C.J., Korczak, B., and Green, N.M. (1985) Nature 316, 696-700

MacLennan, D.H., and Toyofoku, T. (1992) Biochem. Soc. Trans. **20**, 559-562

Mahaney, J.E., Froehlich, J.P., and Thomas, D.D.(1995) Biochemistry **34**, 4864-4879

Maruyama, K., Clark, D.M., Fujii, J., Inesi, G., Loo, T.W., and MacLennan, D.H. (1989) J. Biol. Chem. **264**, 13038-13042

McIntosh, D.B., and Ross, D.C. (1985) Biochemistry **24**, 1244-1251

McIntosh, D.B., and Ross, D.C.(1988) J. Biol. Chem. **263**, 12220-12223

McIntosh, D.B., Ross, D.C., Champeil, P., and Guillain, F. (1991) Proc. Natl. Acad. Sci. **88**, 6437-6441

McIntosh,D.B (1992) J. Biol. Chem. **267**, 22328-22335

McIntosh, D.B., Woolley, D.G., Vilsen, B., and Anderson, J.P. (1996) J. Biol. Chem. **271**, 25778-25789

Means, G.E., and Feeny, R.E. (1971) in 'Chemical modification of proteins', 1st Ed., Holden-Day, New York

Mintz, E., Mata, A.M., Forge, V., Passafiume, M., and Gullain, F. (1995) J. Biol. Chem. **270**, 27160-27164

Mitchinson, L., Wilderspin, A.F., Trinnaman, B.J and Green, N.M. (1982) FEBS Lett. **146**, 87-92

Moller, J.V., Juul, B., and Le Maire, M. (1996) Biochim Biophys. Acta. **1286**, 1-51

Moutin, M.-J., and Dupont, Y. (1991) J. Biol. Chem. **266**, 5580-5586

Murphy, A.J. (1976) Biochemistry **15**, 4492-4496

Murphy, A.J. (1978) J. Biol. Chem. **253**, 385-389

Nakamura, S., Suzuki, H., and Kanazawa, T. (1997) J. Biol. Chem. **272**, 6232-6237

Norby, J.G., and Jensen, J. (1971) Biochim. Biophys. Acta **233**, 104-116

Norby, J.G., and Jensen, J. (1991) in 'The Sodium Pump', P.De Weer and J. Kaplan eds., 173-168, Rockerfeller University Press, New York

Norregard, A., Vilsen, B., and Anderson, J. (1993) FEBS Lett. **336**, 248-254

Odermatt, A., Suter, H., Krapf, R., and Soloiz, M. (1993) J. Biol. Chem. **268**, 12775-12779

Orlowski, S., and Champeil, P. (1991) Biochemistry **30**, 11331-11342

Pardo, J.P., and Slayman, C.W. (1988) J. Biol. Chem. **263**, 18664-18668

Pardo, J.P., and Slayman, C.W. (1989) J. Biol. Chem. **264**, 9373-9379

Pena, A., Cinco, G., Gomez-Poyou, A., and Thena, M. (1969) Biochim. Biophys. Acta. **180**, 1-8

Penefsky, H.S., Pullman, M.E., Datta, A., and Racker, E. (1960) J. Biol. Chem. **235**, 3330-3336

Petithory, J.R., and Jencks, W.P. (1986) Biochemistry **25**, 4493-4497

Petrov, V.V., Pardo, J.P., and Slayman, C.W. (1997) J. Biol. Chem. **272**, 1688-1693

Phung, L.T., Ajlani, G., and Haselkorn, R. (1994) Proc. Natl. Acad. Sci. U.S.A. **91**, 9651-9654

Post, R.L., Kume, S., Tobin, T., Orcutt, B., and Sen, A.K. (1969) J. Gen. Physiol. 54, 306S-326S

Post, R.L., Sen, A.K., and Rosenthal, A.S. (1965) J. Biol. Chem. **240**, 1437-1445

Post, R.L., Hegyvary, C., and Kume, S. (1972) J. Biol. Chem. **247**, 6530-6540

Post, R.L., and Kume, S. (1973) J. Biol. Chem. **248**, 6993-7000

Reithmeyer, A.F., and MacLennan, D.H. (1981) J. Biol. Chem. **256**, 5957-5960

Rephaeli, A., Richards, D., and Karlish, S.J.D (1986) J. Biol. Chem. **261**, 6248-6254

Riordan, J.F., and Vallee, B.L. (1972) Methods Enzymol **25**, 449-459

Robinson, J.D., and Pratap, P.R. (1993) Biochim. Biophys. Acta. **1154**, 83-104

Ross, D.C., and McIntosh, D.B. (1987) J. Biol. Chem. **262**, 2042-2049

Ross, D.C., and McIntosh, D.B. (1987) J. Biol. Chem. **262**, 12977-12983

Ross, D.C., Davidson, G.A., and McIntosh, D.B. (1991) J. Biol. Chem. **266**, 4613-4621

Ross,D.C., and McIntosh, D.B. (1991) J. Biol. Chem. **266**, 4613-4621

Sass, C., Briand, M., Benslimane, S., Renaud, M., and Briand, Y. (1989) J. Biol. Chem. **264**, 4076-4081

Schagger, H., and vonJagow, G., (1991) Ananlytical Biochem. **199**, 223-231

Schulz, G.E., and Schirmer, R.H. (1979) in 'Principles of Protein Structure', Springer-

Verlag, New-York

Siebers, A., and Alkendorf, K. (1988) Euro. J. Biochem. **178**, 131-140

Shani, M., Goldschleger, R., and Karlish, S.J.D (1987) Biochim. Biophys. Acta. **904**, 13-21

Shin, J.M., and Sachs, G. (1996) J. Biol. Chem. **271**, 1904-1908

Shorina, E.A., Mast, N.V., Lopina, O.D., and Rubtsov, A.M. (1997) Biochemistry **36**, 13455-13460

Skou, C.J. (1957) Biochim. Biophys. Acta. **23**, 394-401

Skou, C.J., and Esmann, M. (1983) Biochim. Biophys. Acta. **746**, 101-113

Skriver, E., Kaveus, U., Hebert, H., and Maunsbach, A.B. (1992) J. Ultrastructure. Res. **108**, 176-185

Soloiz, M., Odermatt, A., and Krapf, R. (1994) FEBS Lett. **346**, 44-47

Soloiz, M., and Vulpe, C. (1996) Trends Biochem. Sci. **21**, 237-241

Stokes, D.L., and Lacapere, J.-J. (1994) J. Biol. Chem. **269**, 11606-11613

Stokes, D.L., Taylor W.R., and Green, N.M. (1994) FEBS Lett. **346**, 32-38

Subrahmanyeswara-Rao, V., Hennesey, J.P., and Scarborough, G.A. (1991) J. Biol. Chem. **265**, 14740-14746

Suzuki, H., Nakamura, S., and Kanazawa, T. (1994) Biochemistry **33**, 8240-8246

Takakuwa, Y., and Kanazawa, T. (1979) Biochem. Biophys. Res. Commun. **88**, 1209-1216

Takisawa, H., and Makinose, M. (1981) Nature **290**, 271-273

Taylor, W.R., and Green, N.M. (1989) Euro. J. Biochem. **179**, 241-248

Thoenges, D., and Schoner, W. (1997) J. Biol. Chem. **272**, 16315-16321

Tosten, D.C. (1955) in 'Electrolytes in Biological Systems', p123, American Physiol. Society, Washington

Toyoshima, C., Sesabe, H and Stokes, D.L. (1993) Nature **362**, 469-471

Vasilets, L.A., and Schwarz, W. (1993) Biochim. Biophys. Acta. **1154**, 201-222

Vilsen, B., Andersen, B., Petersen, J., and Jorgensen, P.L. (1987) J. Biol. Chem. **262**, 10511-10517

Vilsen, B., Andersen, J.P., MacLennan, D.H. (1991) J. Biol. Chem. **266**, 16157-16164

Wakabayashi, S., and Shigekawa, M. (1990) Biochemistry **29**, 7309-7318

Wawrzynow, A., Collins, J.H., and Coan, C. (1993) Biochemistry **32**, 10803-10811

Wawrzynow, A., and Collins, J.H. (1993) Biochim. Biophys. Acta. **1203**, 60-70

Wells, J.A., and Yount, R.G. (1982) Methods Enzymol. **85**, 93-116

Wictome, M., Henderson, I., Lee, A.G., and East, J.M. (1992) Biochem. J. **283**, 525-529

Wingo, C.S., and Smolka, A.J. (1995) Am. J. Physiol. **269** (1 Pt 2), F1-F16

Yamada, S., and Ikemoto, N. (1980) J. Biol. Chem. **253**, 6801-6807

Yamasaki, K., and Yamamoto, T. (1989) J. Biochem. **106**, 1114-1120

Yamasaki, K., Sano, N., Ohe, M., and Yamamoto, T. (1990) J. Biochem. **108**, 918-925

Yamasaki, K., Daiho, T., and Kanazawa, T. (1994) J. Biol. Chem. **269**, 4129-4134

Zarain-Herzberg, A., MacLennan, D.H., and Periasamy, M. (1990) J. Biol. Chem. **265**, 4670-4677

6. APPENDIX

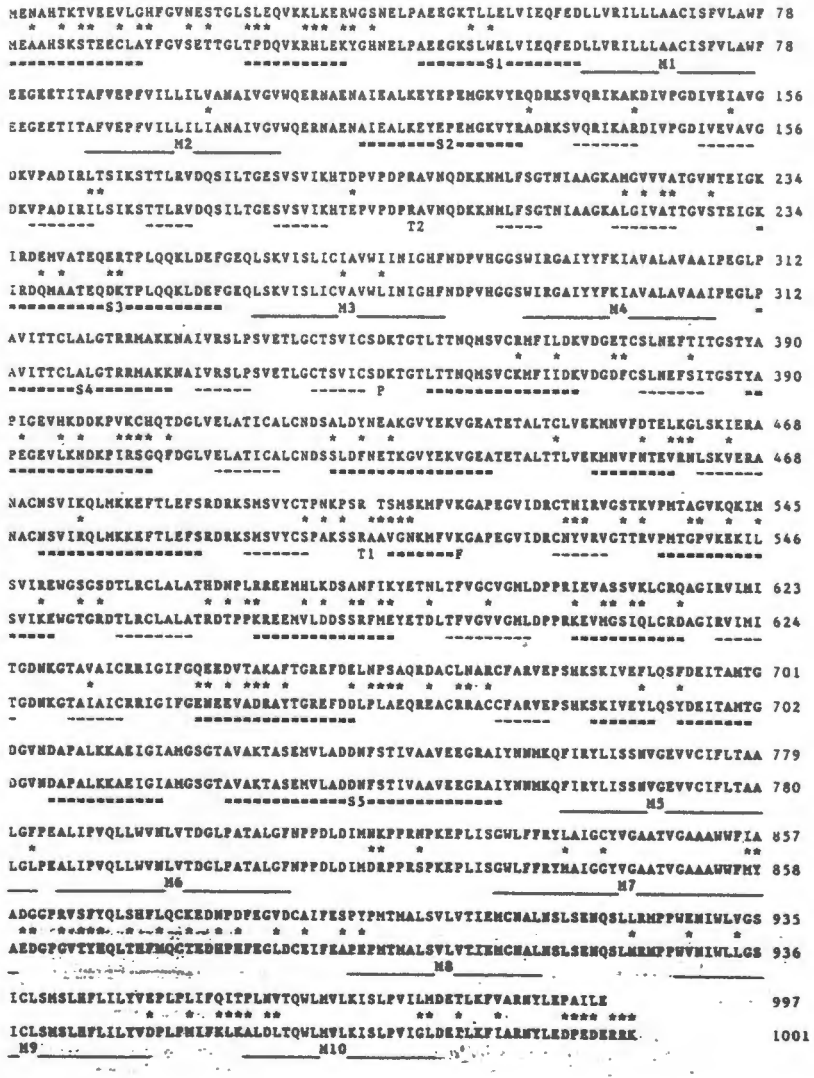

Figure 6.1. Sequence homologies between the Fast Twitch and Slow Twitch skeletal muscle forms of the Ca^{2+}-ATPase. The amino acid sequence of Sarcoplasmic reticulum Ca^{2+}-ATPase of rabbit skeletal muscle is shown below the Slow Twitch Ca^{2+}-ATPase. Asterisks indicate non-homologous amino acids; M1-M10, membrane spanning regions; S1-S5, stalk sections; T1, T2, major tryptic cleavage sites; P, phosphorylation site; F, FITC binding site; (= = =), regions of predicted alpha-helices; (- - - -), regions of predicted beta strands (Brandl et al., 1986).